Ph.D. DISSERTATION

Three-dimensional display systems using half mirror with lens function

렌즈 기능의 반거울을 이용한 3차원 디스플레이 시스템

BY

Jisoo Hong

AUGUST 2012

DEPARTMENT OF ELECTRICAL ENGINEERING AND
COMPUTER SCIENCE
COLLEGE OF ENGINEERING
SEOUL NATIONAL UNIVERSITY

Abstract

This dissertation proposes a new optical component, the half mirror with lens function, and studies about its application to three-dimensional display systems. Half mirror with lens function is a half mirror which provides a lens function by the reflective optic implementation. As an optical combiner, the definition of half mirror with lens function touts the advantageous features of see-through imaging and easy alignment of the optical system. Three viable fabrication methods, each of which has its pros and cons, are proposed to realize the half mirror with lens function. And the comparison of the characteristics of prototypes implemented by the three methods is also given as a reference in determining which one will be the most appropriate for the given application.

The usefulness of the half mirror with lens function is studied in two different aspects: one is the source of inspiration in retrieving new concept of the three-dimensional display system; the other is providing a new way to resolve the existing problems of the conventional three-dimensional display system. The study is conducted by providing various types of three-dimensional display system based on the integral imaging principle.

Two new types of three-dimensional display systems, which are inspired by adopting the half mirror with lens function, are presented considering the applications for the augmented reality. See-through and bidirectional integral imaging is a totally new concept that displays an autostereoscopic three-dimensional image, which is based on the integral imaging principle, around a see-through image without any mechanical motion. It is only realizable using the array of half mirrors with lens function which eventually has the surface structure

of concave mirror array. Using the analysis of the imaging principle of the projection-type integral imaging, the half mirrors with lens function with 10% of reflectance were implemented showing natural overlay of three-dimensional image onto the real world scene.

See-through head mounted display, which can address a correct accommodation, is also presented with the convex side of the half mirror with lens function utilizing the principle of integral floating. The analysis is given which demonstrates that the pixel pitch of the display device imposes the restriction to the imaging distance of the integrated image. The use of convex mirror effectively reduces the pixel pitch of the display device enabling the farther imaging of integrated image without physical improvement of the system.

The half mirror with lens function can also be useful in resolving the long-known problem of integral imaging, implementation of three-dimensional/two-dimensional convertible feature. Especially, there was no adequate solution for the projection-type integral imaging because the conventional methods incorporate the active devices with the size comparable to the screen. The adoption of half mirror with lens function provides the way to implement three-dimensional/two-dimensional convertible feature with the passive optical component. The proposed system is the first proposal to the three-dimensional/two-dimensional convertible projection-type integral imaging.

A number of methods have been investigated for the three-dimensional/two-dimensional convertible integral imaging of *focused mode* configuration while only one method exists for the *real/virtual mode* integral imaging. The half mirror with lens function provides the new method to realize the three-dimensional/two-dimensional convertible feature for the *real/virtual mode* integral imaging. The proposed system also touts various advantageous features such as the wider viewing angle and the shorter optical path difference in creating multiple central

depth planes for the depth enhancement.

Though the usefulness of the half mirror with lens function is investigated only focusing on the three-dimensional display, it is expected that the half mirror with lens function will also be useful for various optical applications.

Keywords: Three-dimensional display, half mirror with lens function, augmented reality, see-through, integral imaging, head mounted display, three-dimensional/two-dimensional conversion, projection-type integral imaging
Student Number: 2008-30889

Contents

List of Figures

List of Tables

Chapter 1

Introduction

1.1 Historical review of three-dimensional displays

Three-dimensional (3D) display has a long history, starting from the first suggestion of a stereoscope by Wheatstone in the mid-19th century [1] through active inventions of various autostereoscopic technologies in the late 19th and early 20th centuries, an era of holography in the 1960s and 1970s, and the adoption of digital devices today [2–4].

The first concept of the parallax barrier had been patented in 1903 by Ives [5] (although the first different-view concept was demonstrated by French painter Bois-Clair in 1692) and Lippmann proposed the integral imaging (InIm) in 1908 [6]. Lenticular lens was proposed and patented by Hess in 1915 to simplify the concept of integral imaging to the one-dimensional case [7]. In the early 1960's, the invention of laser had paved the way of using the holography, which was first proposed by Gabor in 1948 [8], for the display of 3D image. The demonstration of the first holographic 3D display by Leith and Upatnieks at a

1964 meeting of the Optical Society had shown the possibility of displaying a perfect 3D image that replicates the original object in the level of wave optics [9]. However, the early hologram, which depended on the holographic materials, had a severe limitation in its usage because it always demanded coherent light source in recording and reconstruction processes. Although most of the basic ideas were proposed more than tens of years ago or even 100 years ago, none of them are without critical issues that are obstacles to catching a mass market.

Since the late 1990s, development in digital devices has led to widespread use of flat panel displays (FPDs), especially those based on liquid crystal (LC) technology. It was a catalyst for research on implementing commercially acceptable 3D displays again. From Fig. 1.2, recent research trends in 3D display can be inferred. It is interesting to see that research on autostereoscopic displays, including parallax barriers, integral imaging, and lenticular lenses, has grown continuously, starting from around the year 2000, when LC displays (LCDs) became popular. In particular, the parallax barrier, which is more suitable for implementation with LCDs, shows a steeper increase compared with other autostereoscopic technologies. Despite increasing research interest and demand from the market, up until a few years ago, it was a major opinion that 3D display was still far from mass commercialization.

The past few years will be marked as a "historic" period in 3D display technology because, for the first time, several major manufacturers in the display industry have started to supply successful commercial products based on stereoscopy to the mass market. Stereoscopy is a technology that has a history of more than 170 years and there have been no notable breakthroughs other than research and inventions conducted in its early decades. The only difference in the circumstance is that a value chain of the industry started to work with 3D films, which became common and popular in ordinary theaters after the success

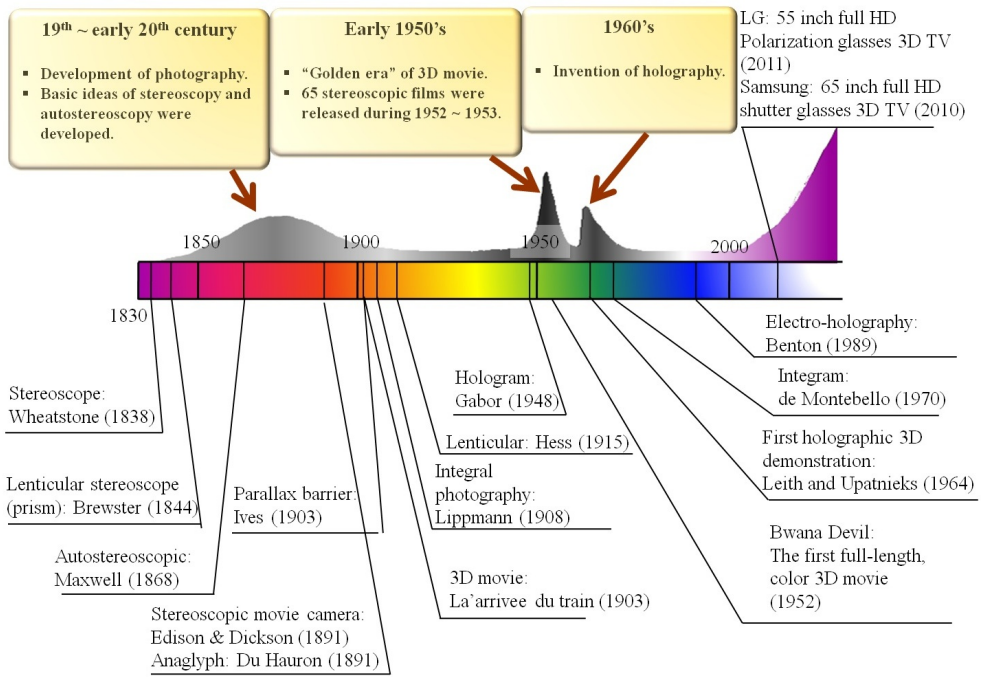

Figure 1.1 Brief history of 3D display. Before year 2000, there were historically three waves when the interest on 3D display had been highly increased. The period and key issues related with those three waves are summarized in three boxes at top of the figure.

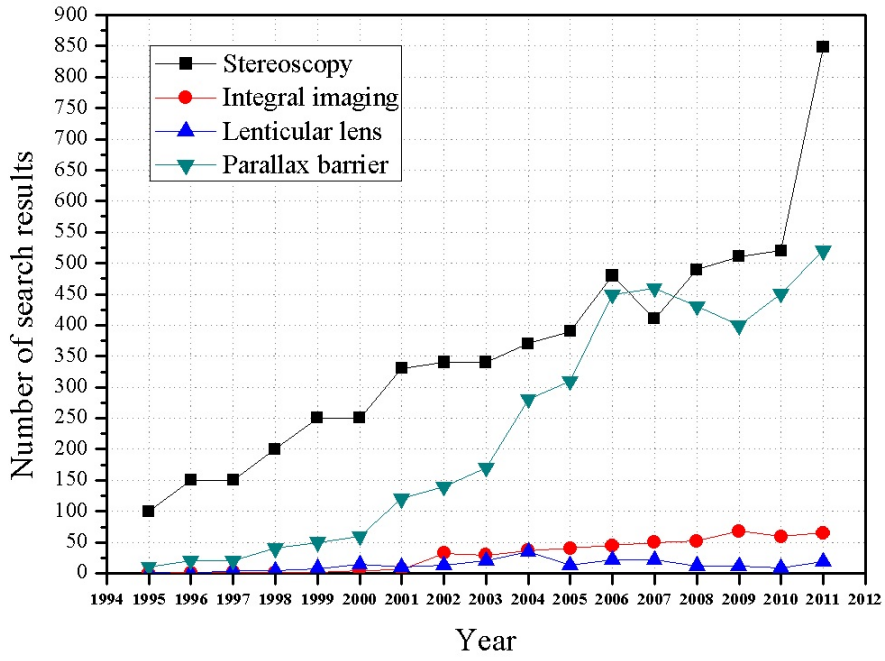

Figure 1.2 Number of search results from Google Scholar. Searching was restricted only to titles of papers. Queries for each technology were "stereoscopy or stereoscopic," "integral imaging," "lenticular lens," and "parallax barrier."

of the monumental movie "Avatar."

Commercialization revealed new issues of stereoscopy in the aspect of products and 3D has again become a very active research topic. The current research trends in the field of 3D display are very interesting: old-fashioned technologies, such as stereoscopy and science fiction movie-like fancy technologies, are active and popular research topics together. This phenomenon comes from a larger time lag of commercialization to the latest technologies compared with other industries.

1.2 Motivation

The setup of value chain between movie industry, TV industry, and broadcasting industry is the foundation of today's success of 3D industry. In the background that makes this value chain to work, there is a hierarchical structure of the required technologies which are necessary for the success of 3D industry.

Figure 1.3 is a diagram describing this hierarchical structure. There should be proper recording devices which can be easily handled and output the recorded images as digital data, and the recorded data should be calibrated and converted to appropriate image source by the post-processing technique. There should exist standards that supports backward compatibility to 2D displays as well as 3D displays. 3D displays should provide 3D images with an acceptable visual quality and it should provide a proper way to support 2D contents. Because a number of factors are related in providing 3D information to human visual system, the investigation on the human factor is inevitable especially considering the safety issue. Because of recent advances in electronics and computer science, the hierarchical structure for stereoscopy finally has been completed from bottom to top.

Going one step further to the end of road map of display, the next step is the commercialization of autostereoscopic displays. However, to achieve a sufficient visual quality using autostereoscopy or holography, outrageous level of resolution and pixel pitch of display device is required.

Regarding the impressive quality of recent holographic stereogram, it is evident that a certain level of pixel pitch can make the multi-view display provide 3D images of the hologram-level. The holographic stereogram by silver halide emulsion with the 8 nm grain size shows similar quality to traditional analog holography [10]. It seems that the pixel pitch of 8 nm is sufficient to

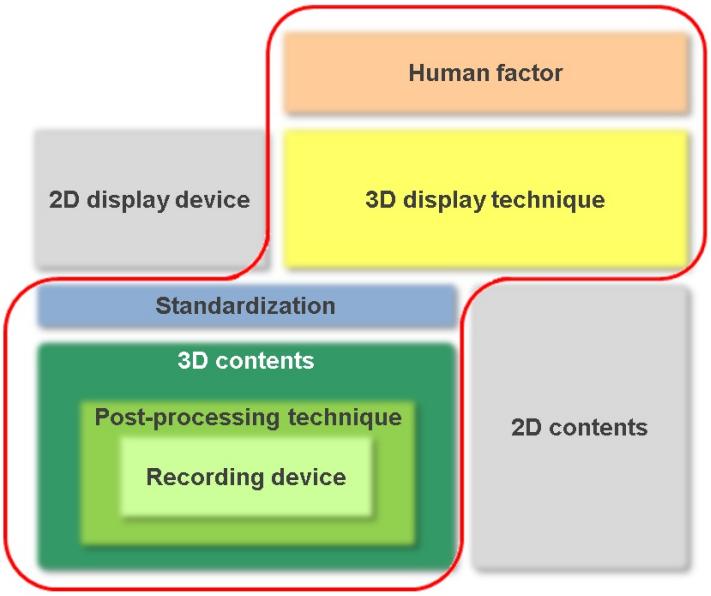

Figure 1.3 Hierarchical structure of technologies related to 3D industry

generate hologram-like multi-view 3D images. Or, the actual requirement might be easier than 8 nm.

Actually, reducing the pixel pitch to the minimum requirement is a quantum jump from current status of spatial light modulator (SLM). The minimum pixel pitch of the state of the art SLM products based on LC can be found from SLM used in the projector JVC 8K4K D-ILA, and it is around 5 μm [11]. However, the size is still far from the ordinary grain size of the analog holographic material. If 8 nm is really the goal, today's best should be improved by about 6 hundredfold.

Because of physical limitations, it seems that today's techniques will not be able to match the requirement of 3D display; e.g., the cell gap of LC cannot be smaller than micrometers; the electron mobility gives restriction to circuit design for smaller pixel pitch [12]. Hence we need to find out a totally new technique to overcome expected improvement.

Hence, there are a number of researches designing the optical system, that can effectively reduce pixel pitch or increase number of pixels by time or spatial multiplexing methods, to relieve the required specifications of display devices. For example, recently, the research group of Hitachi has built an integral imaging system assembling 95 projectors, achieving SXGA image resolution with 25 ray sampling rate [13]. The system can show the same performance as the system supposed to have a tenth part of pixel pitch. The multiplexing will much relieve the target pixel pitch of display device. Increasing complexity and volume of the system, as the number of multiplexing increases, is the issue to be resolved in this approach.

Hence, in the holography society, there are still movements to improve the performance of holographic material instead of waiting for the advance of SLMs though the improvement is not so fast. As a result of such efforts, the time taken refreshing holographic 3D image displayed by photorefractive polymer

has reached 2 seconds recently [14]. Along with the advance in the performance of SLM, development of the new fundamental resource is also necessary for the breakthrough of existing bottlenecks.

1.3 Scope and organization

This dissertation conducts investigations on the various types of 3D display systems based on the half mirror with lens function. Figure 1.4 briefly shows the organization of topics which will be discussed throughout the dissertation. The half mirror with lens function, which is proposed as a new useful optical element, is a cornerstone of this dissertation.

The adoption of new optical element spawned the ideas to develop new types of 3D display systems - see-through 3D displays - which are applicable for augmented reality (AR) displays. It can also be used for dealing with unresolved issues in implementing 3D display systems. In this dissertation, two unresolved problems related to three-dimensional/two-dimensional (3D/2D) convertible InIm are resolved in new ways based on the half mirror with lens function.

Hence, the usefulness of the newly proposed half mirror with lens function is verified in the viewpoint of inspiring totally new concepts of 3D display systems as well as resolving the existing issues in conventional systems.

Chapter 2 provides the motivation and concept of the half mirror with lens function. Because the half mirror with lens function is a newly proposed optical component, the viable fabrication method should be provided to use the concept in real implementation. Hence, three fabrication methods are provided to implement the half mirror with lens function and they are verified by the prototype implementations. However, because each method has its pros and cons, none of them can be considered as superior to others. With the implemented prototypes, the characteristics of those fabrication methods are compared and summarized as a reference for further applications.

Chapter 3 provides two new 3D display systems which are inspired by the

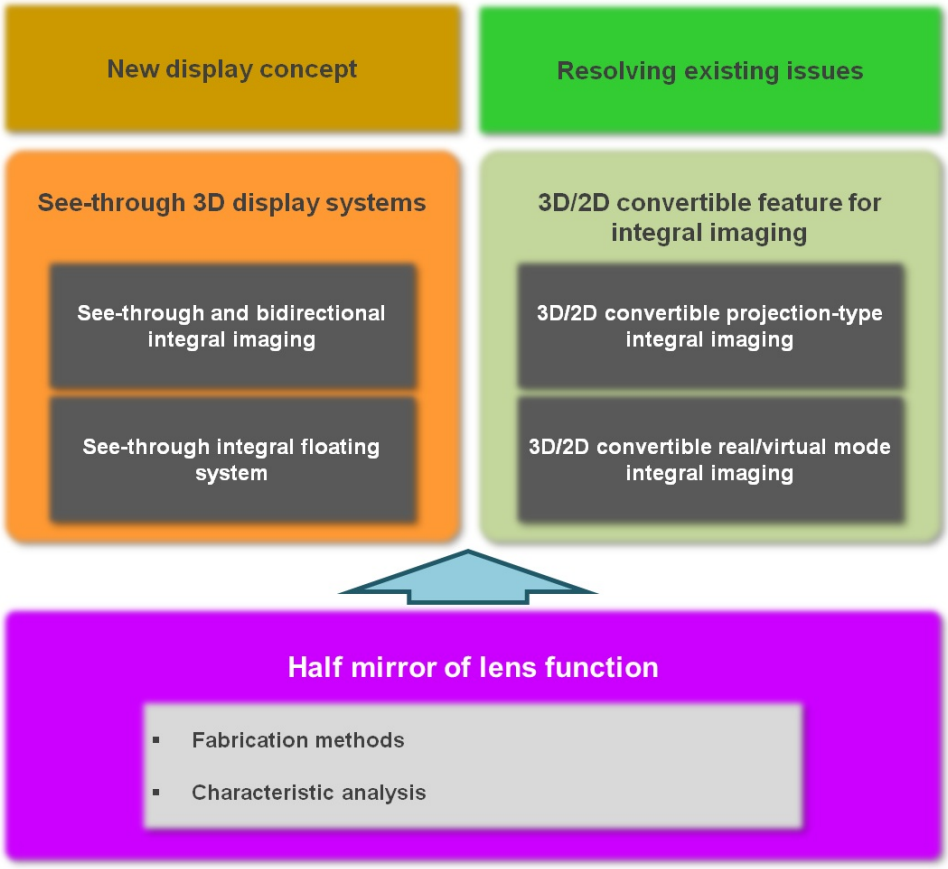

Figure 1.4 Scope and organization of this dissertation.

adoption of the half mirror with lens function. One of them is a see-through and bidirectional InIm system that approaches to the ultimate 3D display in new direction. The proposed display system partially realizes the requirements of the ultimate 3D displays: See-through imaging of 360-degree viewable 3D image. Though the displayed 3D image is not fully 360-degree viewable, it is meaningful that the projection devices of present status can provide a 3D image in a certain angle without any mechanical motion unlike most of existing techniques dealing with this issue. The other one is the optical see-through head mount display which can address the accommodation of virtual 3D image to the location of far distant real world scene. Usually the far distant imaging of 3D image requires the spatial or time multiplexing methods to induce the overperformance of display devices. The proposed method is capable of displaying 3D image at sufficiently far distance without any multiplexing technique which might be obstacle in implementing the head mount display.

Chapter 4 provides the ways resolving the issues related to 3D/2D convertible feature of InIm by the adoption of the half mirror with lens function. One of issues dealt with in this chapter is to realize the 3D/2D convertible feature for the projection-type InIm. What makes difficult to resolve this issue is that it requires discarding the large active devices in the implementation. By using the half mirror with lens function, which is a passive optical element, instead of usually incorporated active devices, a method to implement the 3D/2D convertible projection-type InIm has been developed. The other issue is to implement 3D/2D convertible feature for *real/virtual mode* configuration (to be discussed in Sec. 3.2) of InIm. Unlike the case of *focused mode*, there was only one method considering the 3D/2D convertible InIm for *real/virtual mode*. The adoption of the half mirror with lens function shows another possibility to resolve the issue.

Finally concluding remarks to this dissertation is made in Chapter 5.

Chapter 2

New optical component: half mirror with lens function

2.1 Motivation

A half mirror (or transreflective plate) is an easy and intuitive way in combining two optical images from different image sources to create new functionality or utilize a spatial multiplexing technique. Recent attractive applications can be found from the field of augmented reality (AR) which overlays various artificial data onto the real experiences. Especially for the visual information, most of the AR displays developed so far adopt the half mirror or similar optical component to combine the artificial data onto the real world scene. Surely the artificial visual information is preferred to be a 3D image rather than 2D image to provide more realistic experiences.

Figure 2.1 shows the typical optical setup of the AR display that incorporates the half mirror as an optical combiner that overlays 3D image onto the real world scene. The display system for 3D image was illustrated to be

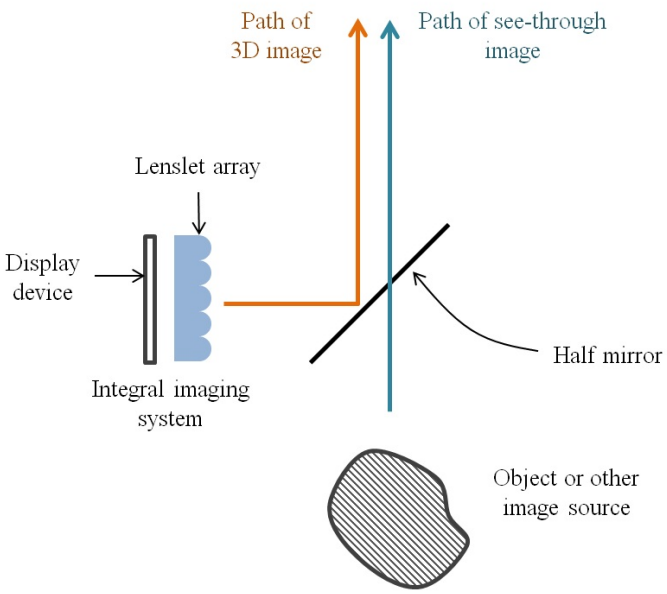

Figure 2.1 Typical configuration of AR display where the half mirror is adopted.

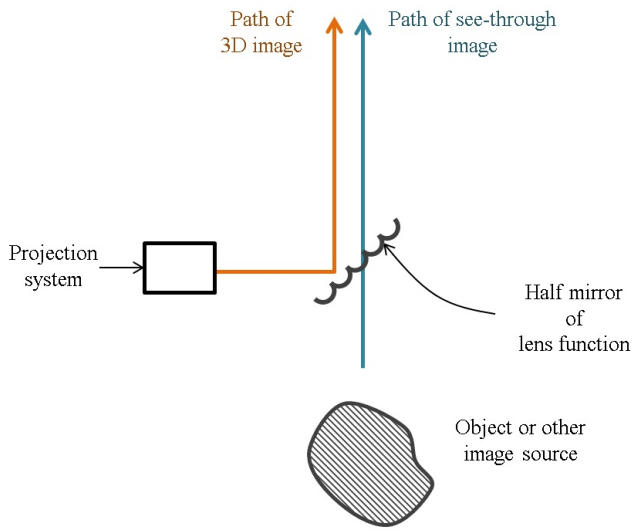

Figure 2.2 Conceptual demonstration of optical system adopting the half mirror with lens function.

integral imaging system which will be discussed throughout this dissertation. Or the setup can also be used for combining two different types of images to alternatively provide one of them. In this case, the transmitted image is also an artificial image displayed by other image source. 3D/2D convertible feature, which will be mainly discussed in the Chapter 4, can be a good example of such application. However, the optical setup adopting the half mirror usually suffers from the problems such as the bulky implementation and alignment.

The motivation of this work is to merge the functionalities of the half mirror and the lenslet array into one optical component. To achieve the objective, the new optical component, the half mirror with lens function (HMLF) is proposed. The HMLF is defined as an (ideally) infinitesimally thin transreflective sheet whose shape is a concave mirrors. And, for the implementation of InIm, a 2D

array of HMLF can be used as shown in Fig. 2.2.

Because the concave mirror is the direct alternative to the convex lens, the concave mirror array can implement the optical function of the lenslet array. Hence, when the shape of the HMLF array is properly designed, the optical function of the lenslet array can be merged by the reflection. On the other hand, for the transmitted image, the infinitesimally thin condition of the HMLF ideally does not affect the optical path at all. Hence, the HMLF array can be considered to be an optical combiner that provides a function of the lenslet array to the reflected image while the transmitted image is bypassed.

Actually, for the reflection-type InIm, it had been revealed that if the projector and the target 3D image are sufficiently far from the surface of concave mirror array compared with the focal length of each concave mirror, the displayed 3D image is simply scaled in lateral and longitudinal directions [15]. Hence the 3D image can be easily compensated without changing the shape of HMLF array from the simple concave mirror array even though the projector projects the image obliquely. However, when the criteria - far projector and 3D image - is not satisfied, the distortion relation becomes complicated hence the HMLF array may require modification in the shape.

By incorporating the HMLF array, the entire optical setup is expected to have some advantages.

1) By using the reflective optical component, it is possible to take various advantageous features stemming from the reflection-type implementation of the integral imaging such as wide-viewing angle and optical ortho-pseudo conversion.

2) The entire system becomes less bulky because the lenslet array can be eliminated from the setup. Moreover, the optical function of the lenslet array

can be implemented inside the area of the optical combiner.

For the first advantage, the detailed features of the reflection-type InIm is listed in the report by Jang *et al.* [16]. They will be partly discussed in the following chapters. For the second advantage, the reduced number of the optical component is especially useful for the bidirectional imaging setup which will be discussed in Sec. 3.2.

In the following sections, three viable fabrication methods for implementing the HMLF will be provided. And the characteristics of the HMLF implemented by proposed methods will be compared and discussed.

2.2 Fabrication methods of the half mirror with lens function

As defined before, the HMLF is supposed to have an infinitesimally thin structure not to affect transmitted light while maintaining a concave mirror shape to support an optical function of lens. Because such structure is very unstable and practically difficult to implement, it is more realistic to implement HMLF inside a transparent plate which can be a supporting structure. Though the transmitted light is slightly altered by refractions occurring at frontal and back surfaces of transparent plate, it is usually acceptable especially for the imaging purpose. Hence, in this section, the objective of proposed fabrication methods is to implement the HMLF embedded inside a transparent plate. Because the usage of the HMLF is mainly for optical component of InIm throughout this dissertation, HMLF will be discussed in this section.

In the fabrication methods presented in this section, the implemented HMLF is commonly composed of three layers; base layer, transreflective layer, and cover layer.

The base layer is the singlet lens or lenslet array whose one side is required to be flat. The shape of the base layer - the side which is not flat - determines the shape of the HMLF. The thin transreflective layer, which is usually formed by evaporation as will be discussed below, covers the surface of the base layer following its shape. It serves as an actual HMLF component in the entire structure. The cover layer covers the transreflective layer making the entire structure to be a transparent plate. Because the thin and uniform transreflective layer is usually implemented by a high temperature process such as thermal evaporation, the glass or the poly(methyl methacrylate) (PMMA), which can endure high temperature, is preferred as a material for the base layer. Ideally, the ma-

terial of the cover layer should have the same refractive index as the base layer not to make any refraction at the interface between the base layer and the cover layer.

The difficulty of fabricating the HMLF exists in providing the proper cover layer, which is supposed to be a perfect negative mold of the base layer, as the air gap at the interface can cause the unexpected artifact especially when the shape of base layer is complicated. Hence, three fabrication methods presented below mainly differ in the method implementing the cover layer. They are "fluid filling method", "soft lithography method", and "negative mask method" where the names represent the cover layer methods.

The first fabrication method to be presented is the fluid filling method. Figure 2.3 shows the outline of the fabrication process for implementing the HMLF array structure embedded inside the transparent plate by the fluid filling method. The fabrication process is illustrated with HMLF array considering the usages of Sec. 3.2 and Sec. 4.3.

At first, the lenslet array whose surface shape is equal to the target concave mirror array should be prepared for the base layer. Then the thin and uniform transreflective layer is formed on the base layer. Usually two types of layer are widely adopted to provide transreflective characteristic; thin metallic film and dielectric mirror. The most suitable way to form the thin metallic layer is usually the thermal evaporation to acquire acceptable uniformity. The ratio between transmittance and reflectance can be determined by controlling the thickness of metallic layer. The other type, dielectric mirror can be obtained by the coating of a number of thin dielectric layers on the surface of the base layer by the thermal evaporation. For the case of dielectric mirror, the ratio between transmittance and reflectance of the dielectric mirror layer can be designed by changing material and thickness of each dielectric layer.

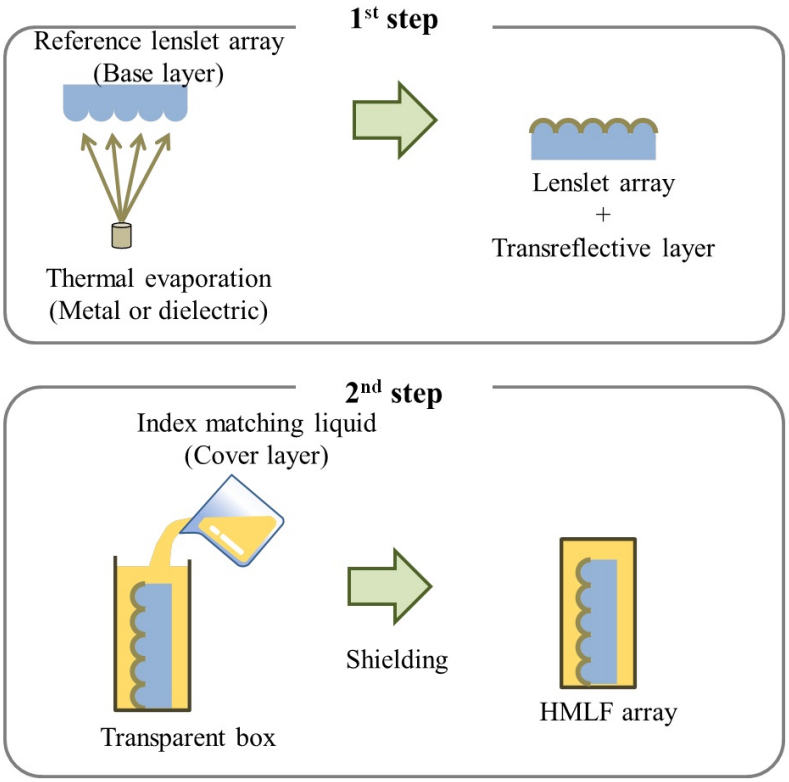

Figure 2.3 Fabrication process of the fluid filling method.

Because both types of layers are evaporated as thin film, the shape follows nearly the same as the surface of the base layer, resulting in HMLF array. Though the thickness of the transreflective layer is not infinitesimal, there is practically no effect to the optical path of the transmitted light by metallic film or dielectric mirror, especially for the imaging purpose. It is known that the transreflective characteristic of the dielectric mirror is better than the metallic mirror because of absorption of metallic layer. However, the dielectric mirror generally has significant angle and wavelength dependance unlike the metallic mirror. Which type of transreflective layer would be selected should be determined considering the application.

The next step is to cancel out the refraction at surface of the base layer by making the entire external shape of the structure be a transparent plate. For the achievement of such objective by fluid filling method, a transparent fluid that has the same refractive index with the target material should be adopted. Suppliers of the index matching liquid such as Cargille Laboratories [17] provides a list of index matching liquids for many representative materials and even the customization is possible if necessary. Hence, if the index matching liquid was properly selected, the transparent sample becomes invisible by immersing it to the index matching liquid. That is, the refraction on the surface of the immersed sample is cancelled out. By using the proper index matching liquid, the base layer can be perfectly immersed without air gap so the base layer can be invisible easily.

For the immersion process, the transparent box whose material is the same with the base layer should be prepared. Then the base layer with the transreflective layer, which is the result of the first step, is put inside the box and then the index matching liquid is injected until it fully immerses the base layer.

The second fabrication method to be presented is the soft lithography

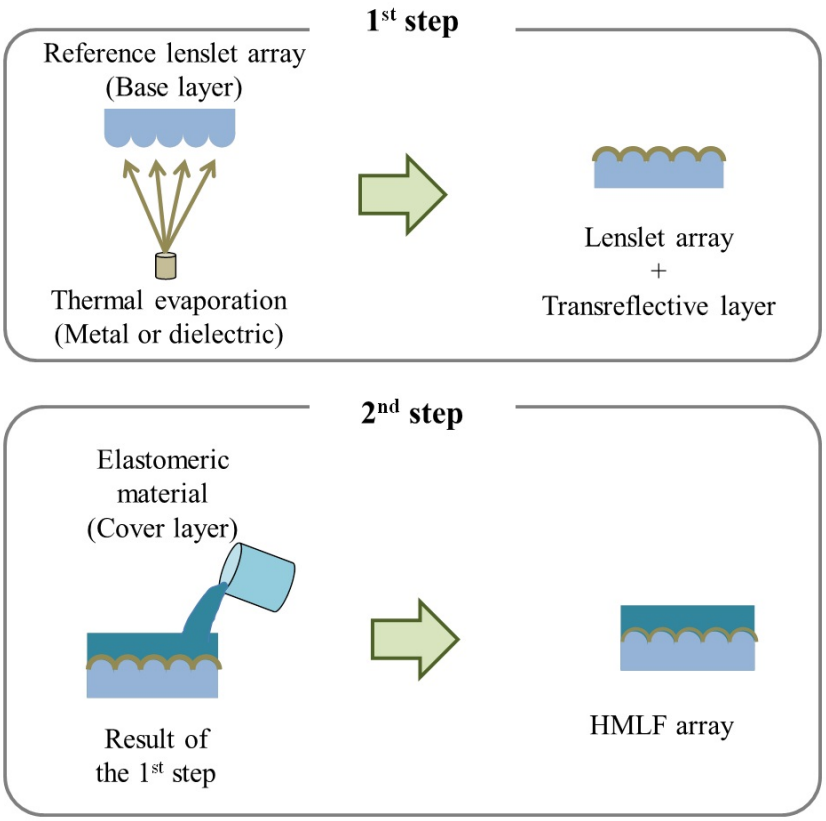

Figure 2.4 Fabrication process of the soft lithography method.

method. Detailed procedures of the soft lithography method are schematized in Fig. 2.4. Again, the HMLF array is represented as a target structure considering the usage of Sec. 4.2. Fabrication is also composed of two steps: one is to form the thin transreflective layer and the other is to cover the transreflective layer with transparent material. As a result, the structure will be a stack of three layers: base layer, thin transreflective layer and the cover layer.

The first step is the same as presented in the fluid filling method: preparing the base layer, evaporating thin metallic layer or dielectric mirror.

As the second step, the result of the first step is covered by the transparent material to adjust the outline of the entire structure to be the transparent plate. The most facile and inexpensive way for constructing transparent cover may be the adopting of soft lithography technique. Following the usual process of the soft lithography, the elastomeric material is poured on the result of the first step. Then the vacuuming in the vacuum chamber is done for the elimination of air to increase the clearance of the elastomeric material. Usually the hardening of the elastomeric material is done by baking. Because the objective of the normal soft lithography is to replicate the reference structure, the hardened elastomeric material is separated from the reference structure in the normal process. However, in creating the HMLF structure, the process of the soft lithography method is completed without separation of the elastomeric material. Usually the polydimethylsiloxane (PDMS) is used for the elastomeric material, and the PDMS will be tested for the soft lithography method in this dissertation.

The third fabrication method is the negative mask method. The most intuitive way to cancel the refraction at the surface of the base layer is to cover the base layer with the corresponding negative mask made of the same material. However the negative mask method is not appropriate for the small-quantity

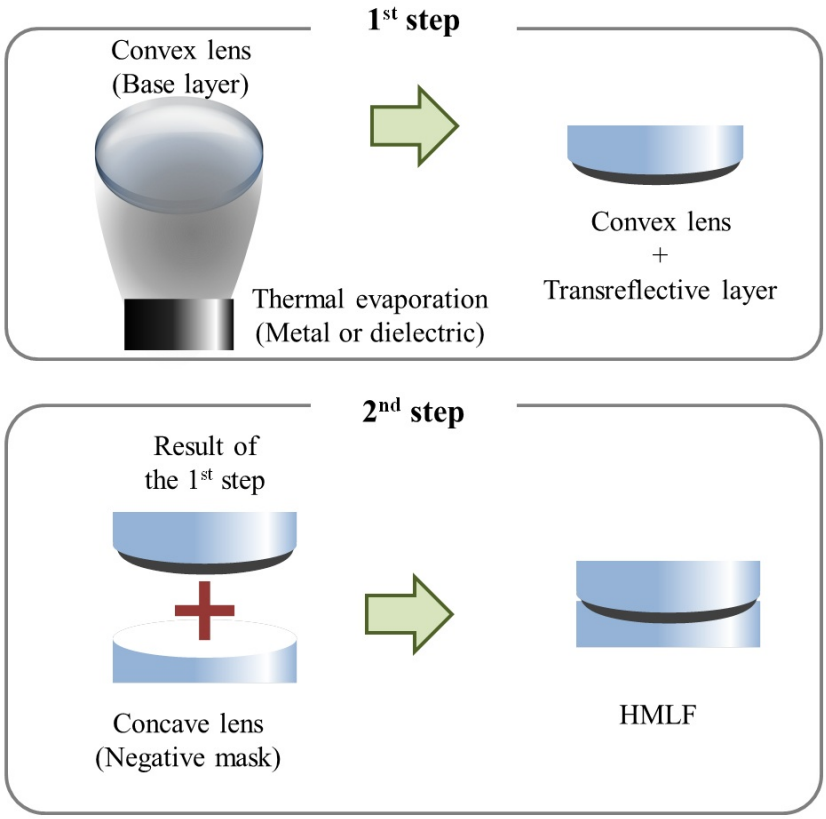

Figure 2.5 Fabrication process of the negative mask method.

production because of the high expense in preparing mold. Moreover, the negative mask should be prepared in very high precision because the air gap at the interface between the base layer and the negative mask can affect the optical path of the transmitted light. Hence, this method is generally useful for the case of single HMLF with relatively large aperture which corresponds to the optical function of the singlet lens.

A fabrication process is shown in Fig. 2.5. The target shape is illustrated as a single HMLF considering the application shown in Sec. 3.3. The preparation process of the base layer covered with transreflective layer is same as the first and second methods. For the cover layer, the optic which has the same refractive index as the base layer and the shape of the negative mask to the base layer should be produced separately unlike two methods above. Then the prepared optic is simply placed on the result of the first step to fill in the surface of the base layer.

2.3 Characteristic of the half mirror with lens function

The implemented HMLF or its array have different characteristic according to the adopted fabrication method. The optical characteristic of the HMLF can be assessed in two aspects: transparency (or see-through characteristic) and reflectance. In the viewpoint of the transparency, it is preferred that the structure does not alter the optical path of the transmitted light.

Largely three factors can affect the optical path of the transmitted light in the real implementation. One factor is that the thickness of the transreflective layer is finite unlike the definition of the HMLF. However, most of optical applications accept the precision provided by usual techniques creating transreflective layer. Another factor is that the HMLF implemented by the proposed methods includes the additional transparent material wrapping up the transreflective layer to protect the thin and carefully designed structure. Hence the transmitted light undergoes the unexpected refractions at the surfaces of the transparent material. This can be a problem for the application where the high precision is required, however it is usually acceptable for the imaging application. Hence this will not be considered as an issue in this dissertation, though the pellicle-type implementation should be investigated for further usages. The last factor is that, because the base and cover layers are created separately, the interface between the base and cover layers can cause an unexpected refraction. This can be a severe problem especially for the complicated structure of HMLF array. Hence, the see-through characteristic will be investigated according to the fabrication methods.

To compare the see-through characteristic, the prototypes of HMLF or its array have been implemented by the fluid filling, soft lithography, and negative

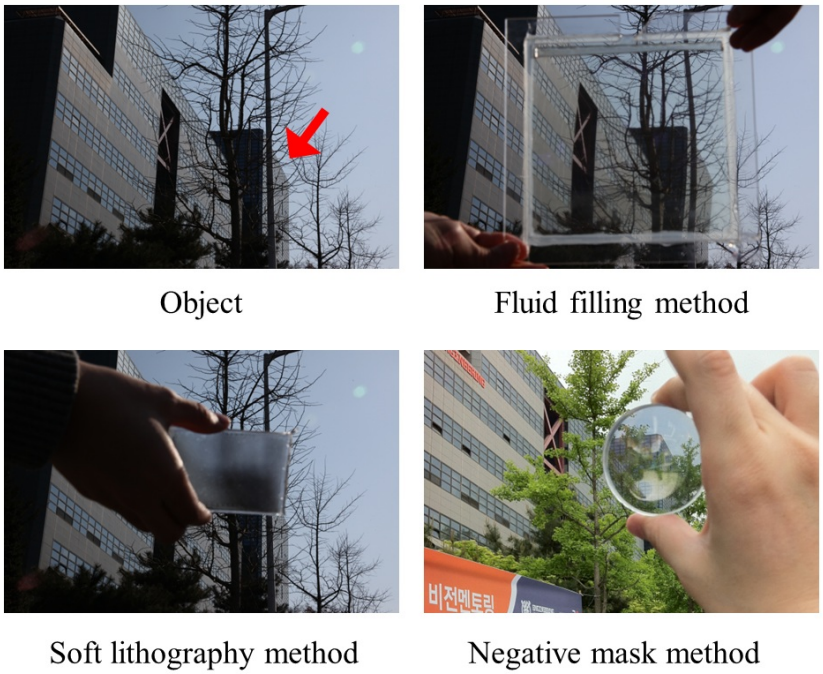

Figure 2.6 Comparison of the see-through characteristic among the fabrication methods. Object is the natural outdoor scene. The building indicated by the red arrow is about 150 m far from the camera.

Table 2.1 Specifications of the implemented prototypes

Fabrication method	Base layer		Transreflective layer
Fluid filling method	Lenslet array	Focal length: 3 mm	Dielectric mirror layer (Reflectance: 10 %)
		Lenslet pitch: 1 mm	
		Material: PMMA	
Soft lithography method	Lenslet array	Focal length: 3 mm	Thin metallic layer (Reflectance: 70 %)
		Lenslet pitch: 1 mm	
		Material: PMMA	
Negative mask method	Singlet lens	Focal length: 100 mm	Thin metallic layer (Reflectance: 50 %)
		Lens pitch: 5 mm	
		Material: BK7	

mask fabrication methods following the specifications listed in Table. 2.1. For the soft lithography method, PDMS was adopted for the elastomeric material.

Figure 2.6 shows the comparison of see-through characteristic for the far-distant object. Because the base and cover layers have the same refractive index in the fluid filling and negative mask fabrication methods, the prototypes by the fluid filling and negative mask methods show a satisfactory see-through characteristic (especially for imaging purpose) even for the object at very far distance. The negative molding method also shows a good see-through characteristic for the far distant object when the target structure is HMLF as the implemented prototype. Because the PDMS is usually not acceptable for the base layer considering the high temperature process required for forming the transreflective layer, the soft lithography method results in the prototype which has different refractive index for the base and cover layer when PDMS is adopted for the elastomeric material. Hence the see-through characteristic is not achievable as shown in Fig. 2.6 and the soft lithography method with PDMS is not adequate for the imaging of far distant object.

In the viewpoint of the see-through characteristic, the investigation of Fig. 2.6 implies that the fluid filling method can be considered as the best method while the soft lithography method with PDMS is useless. The negative mask method is useful when HMLF is the target structure. However, the implemented structure by fluid filling method is quite unstable because of using fluid for the cover layer. And the negative mask method is not acceptable considering expense required for preparing the cover layer especially for the small quantity production. On the other hand, the prototype implemented by soft lithography method has advantages in that viewpoint; the fabrication process is inexpensive and the implemented prototype is stable.

Though the refractive indexes of base and cover layers are not perfectly

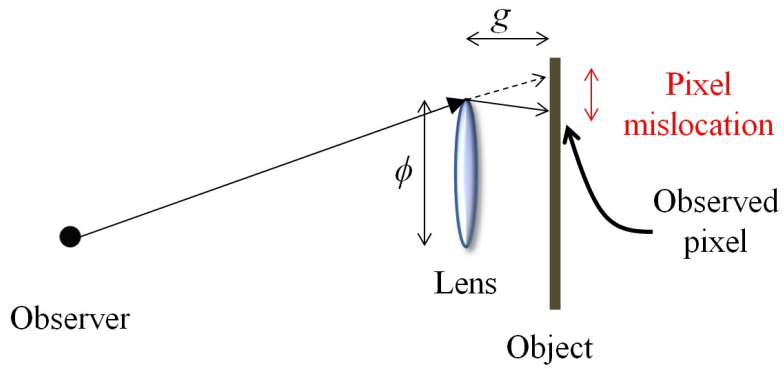

Figure 2.7 Distortion in observation of image occurred by the introduction of lens

matched, the combination of PDMS and base layer material - usually glass or PMMA - considerably reduces the refraction at the interface between base and cover layer. Hence, if the usage is limited for the see-through imaging of the object just behind the structure as discussed in Sec. 4.2, the soft lithography method with PDMS will be the useful one for implementing the HMLF or its array.

The lens affects the see-through characteristic by magnifying the image of the object. Hence each pixel of the object is shifted from its original position in the observed image through the lens. The largest shift occurs at the edge of the lens as shown in Fig. 2.7. In Fig. 2.7, the situation where the observer, which is modeled as a pinhole camera, stare at the upper edge of the lens is illustrated. The observer should observe the point on the object pointed by the dashed arrow if there is no lens. However, the refraction by the lens makes the actual observed pixel come from different position. This kind of shift induces the pixel mislocation and it can be easily calculated as $\phi g^2/2f$ where g is the gap between lens and the object, ϕ is the pitch of the lens, and f is the focal

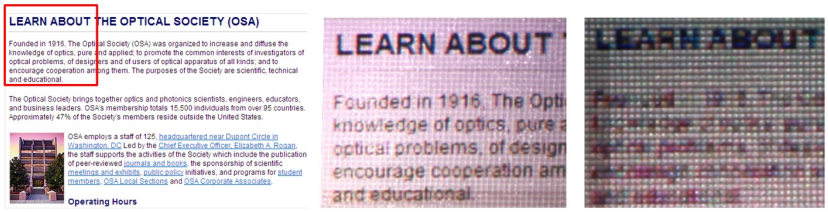

Original image Soft lithography method Base lenslet array

(a)

Original image Soft lithography method Base lenslet array

(b)

Figure 2.8 Comparison of the 2D images shown through the HMLF array and the base layer. (a) Highly textured image is used as the test object. Part of the image indicated as the red square box in the original image is magnified to show the details of the result. (b) A landscape image is used for the comparison of a natural image.

length of the lens. The PDMS cover layer reduces the index difference at the surface of the lens and it makes the focal length of the lens be enlarged to $f_0(n-1)/\delta n$, where f_o is the focal length of the lens, n is the refractive index of the lens, and δn is the index difference between lens and cover layer.

To show the feasibility of soft lithography method with PDMS, the see-through characteristics of the prototype by the soft lithography method and the base layer itself were compared when the object was located just behind the structure as shown in Fig. 2.8. From the relationships described above, the focal length of each lenslet is enlarged to 25 mm by PDMS cover and the pixel

mislocation is reduced to 0.18 mm. Figure 2.8 shows that the PDMS cover layer is a viable option in implementing see-through characteristic for the case where the object is located at just behind the HMLF array. As a reference, the quality of 2D images shown through the HMLF array and the base lenslet array are compared in Fig. 2.8.

The difference clearly appears for the highly textured image such as the text image compared in Fig. 2.8(a). The shape of each character is clearly recognizable only through the HMLF array fabricated by the soft lithography method. As shown in Fig. 2.8(b), even the quality of the natural image where the low spatial frequency is dominant is noticeably degraded by the base lenslet array. Therefore the cover layer made of PDMS is enough to provide the high quality image for the object loacted just behind the structure. According to the application, the soft lithography method with PDMS can also be a candidate fabrication method considering other advantages of adopting it.

Other than the methods forming cover layer, there are also options in creating the transreflective layer. In this dissertation, thin metallic layer and dielectric mirror are investigated in the viewpoint of the reflectance. The reflectance of the HMLF can be controlled during the fabrication step forming the transreflective layer. As described, the reflectance of metallic layer can be controlled by simply controlling the thickness of the layer while the dielectric mirror requires a complicated design of multiple layers. Generally, it is considered to be difficult to design the dielectric mirror appropriate for the imaging purpose because of the angle and wavelength dependencies. Figure 3.9 shows one example of optical characteristic of the dielectric mirror designed for the imaging purpose.

For both cases of transreflective layer, the reflectance has the tradeoff relationship with the transmittance of the structure. Hence the reflectance should be determined considering the application. For example, the reflectance has

been determined to be 10% for the implementation in Sec. 3.2 and 50% in Sec. 4.3. Usually the thin metallic layer is sufficient for the imaging applications, however the performance of dielectric mirror will also be presented in Sec. 3.2.

2.4 Summary and discussion

The HMLF is a new optical structure which can be applied to the 3D displays base on the InIm implemented incorporating the optical combination concept. The functionality of the HMLF can be understood as combining the half mirror (or transreflective plate) with the lens function at the reflection-side. The HMLF can inspire new 3D display applications as well as simplify the system by combining two optical elements into one component.

However, the actual implementation, which can realize the definition of proposed HMLF, cannot be easily achieved. In this chapter, three fabrication methods, which can implement the concept of HMLF, have been demonstrated, and they were verified and investigated by implemented prototype of each method. However each method has its disadvantages and the fabrication method should be continuously developed to find out better way realizing the HMLF with less problems. For now, the proposed three methods are only available ones to implement the HMLF and one of them should be selected in configuring a certain optical system. To make the choice easier, the characteristics of the methods for the cover layer are compared in Table 2.2. The transreflective layer can also be prepared by the thin metallic layer or the dielectric mirror, and the characteristics of them are compared in Table 2.3. In the following chapters, the novel 3D diplay devices, which provide new functionalities or resolve the existing problems by adopting the HMLF, are demonstrated. They present the way choosing appropriate fabrication method and the usefulness of the HMLF.

Table 2.2 Pros and cons of the cover layer

	Pros	Cons
Fluid filling method	• Easy to implement • Good index matching	• Unstable structure • Depending on the index matching liquid
Soft lithography method	• Easy to implement • Stable structure	• Depending on the elastomeric material
Negative mask method	• Good index matching • Stable structure	• Not adequate for complicated structure • Economically inefficient for small quantity production

Table 2.3 Pros and cons of the transreflective layer

	Pros	Cons
Thin metallic layer	• Low wavelength dependency • Low angle dependency	• Large absorption
Dielectric mirror	• Low absorption	• Wavelength dependency • Angle dependency

Chapter 3

See-through three-dimensional displays using half mirror with lens function

3.1 Introduction

Augmented reality (AR) is a technology that combines the artificial sensory input with the physical real world. The artificial sensory input can cover all of the five senses, but the visual information will be the most important and impressive input in realizing AR. In that viewpoint, one of the most important issues in AR is how to merge the artificial image with the real world more naturally. So far, there have been many technological developments in overlaying the image onto the real world [18], but it is still in progress because the guidelines for AR display are not satisfactorily achieved yet.

Eitoku *et al.* suggested 4 requirements for AR display to be achieved [19]: (1) Virtual information coexists with the real world; (2) Supports collaborative work; (3) Does not burden the users with special apparatus; (4) Supports the

need to naturally display 3D images. Especially, it is difficult to implement AR display that satisfies the conditions (3) and (4) together.

See-through head mount display (HMD) is one of the AR display candidates and it shows natural overlaying of the real world and virtual image [20, 21]. Display of 3D image is also supported by the stereoscopy. However it enforces the users to wear a special apparatus so the users can feel inconvenience and should carry such bulky devices. Besides, about the 3D images, the stereoscopic 3D image can cause the accommodation mismatch so it may be the source of nausea in using AR application. Recent development in the handheld devices led to the widespread of AR applications in the market by implementing AR display with the overlay of virtual image onto video of the real world captured in real-time [22, 23]. However the 3D information of the real world is lost in this way, so it cannot realize the seamless overlay.

The projection-based system can also be a good candidate for AR display because the users need not to wear anything while it provides the large-sized image easily. However the main concern of the projection-based system is the demand on the special screen that shows see-through property and good screen characteristic simultaneously. The earlier report on this type of system used the transreflective screen to combine the real and virtual images [24]. However the support for 3D image was not considered in the implementation. Recent report by Takaki *et al.* also used the transreflective screen to combine the super multi-view image with the real world [25]. Though the quality of 3D image is pretty good, it is difficult to provide the 3D image to the group of people surrounding the system hence the system cannot support the collaborative work.

Considering the collaborative work, the 3D image should be observable from all directions and the interactivity should be supported. Jones *et al.* reported impressive work on 360-dgree viewable 3D display [26]. However the fast me-

chanical motion is needed and the tracking technique is necessary for the expression of vertical parallax. Moreover, fast spinning screen makes it difficult to provide interactivity to displayed 3D image. Holographic optical element (HOE) can also be a candidate for the AR display, however it is difficult to record large sized HOE [27].

The efforts to satisfy the conditions listed above are still in progress and there is long way to go. The conditions required for AR display can also be interpreted in more technical descriptions in the viewpoint of 3D display: (1) Free space imaging without any noticeable frame; (2) Supports interaction with 3D image; (3) Autostereoscopic 3D image; (4) Volumetric 360-degree viewable 3D image of high visual quality. Considering these descriptions, the ultimate 3D display can be summarized as one sentence - *Free space (or see-through) imaging of volumetric and 360-degree viewable 3D image supporting interaction.* It reminds the scene of holographic telecommunication from the famous movie "*Star Wars*" which is considered as a representation of ultimate 3D display. It is interesting to see that the conditions required to develop the satisfactory AR display are eventually related to realizing the ultimate 3D display system. Despite of choosing any way, at the end of the development of display, there will be an objective of the ultimate 3D display. Hence, the efforts to implement AR display resolving the listed issues are connected to the way approaching the ultimate 3D display.

In this chapter, two types of novel 3D display systems, which are applicable to AR displays, are developed based on the HMLF. In Sec. 3.2, the new concept of see-through and bidirectional InIm is defined as an effort to partly realize the 360-degree viewable see-through 3D display. In implementing this concept, a 2D array of HMLF is used. From the both sides of the HMLF array, 3D images are provided by the principle of projection-type InIm and each side has

a certain viewing angle. Hence the collaborative work is partially supported though the 3D image, which is not fully 360-degree viewable. In Sec. 3.3, the new see-through HMD system is proposed considering the issue of accommodation mismatch between the real world scene and virtual images. By adopting the principle of integral floating display, the proposed see-through HMD system is capable of displaying 3D image at relatively far distance where the real world scene is usually located. In implementing the concept, the single concave lens is alternated by the HMLF, hence the convex side of HMLF is prepared for the implementation. In following sections, the implementations and characteristics of proposed see-through 3D displays are discussed in detail.

3.2 See-through and bi-directional integral imaging using an array of half mirror with lens function

3.2.1 Introduction

In this section, the new 3D display system, that shows see-through and bidirectional imaging functionalities, is proposed. The bidirectional imaging means that the 3D integrated image is provided in the front and rear sides of the system. Hence the 3D image is viewable all around the system except a certain angle formed at the side of the system. Such area, where the image is not expressed well, will be called the shadow region. Such functionalities make it possible to realize the concept shown in Fig. 3.1. A group of people surrounding the system can share the 3D virtual image which looks like floating in the air. The system is implemented based on the HMLF array which provides the optical function of lenslet array by the reflective-optic alternative. The 3D image is displayed following the principle of InIm by projecting a proper elemental image onto the surface of HMLF array.

InIm is one of autostereoscopic 3D display methods which do not require users to wear any special apparatus in providing 3D images [3, 28]. It is advantageous in that 3D images with both horizontal and vertical parallaxes can be displayed by incoherent light. In the early configuration of InIm developed by Lippmann, recording of 3D information and its reconstruction as a 3D image was implemented by 2D lenslet array of the same specification.

Figure 3.2 shows the basic principle of recording and displaying processes of InIm. In recording 3D information, each lenslet of the lenslet array images different directional view of the real object scene, and it is recorded by a record-

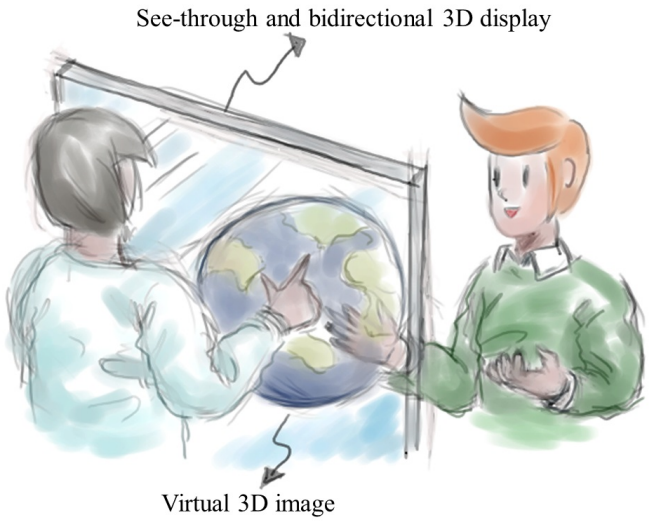

Figure 3.1 Usage scenario of the see-through and bidirectional 3D display system.

ing device such as charge coupled device (CCD). The entire recorded image is called the elemental image and each directional view which is recorded by a corresponding lenslet is named a *cell*, following the expression used by Lippmann [6]. In displaying a 3D image, the recorded elemental image is displayed by a display panel. By using the same lenslet array of the recording process, the displayed elemental image is synthesized to reconstruct 3D images. With the aid of the recent computer vision techniques, the 3D information in the recorded digital data can be extracted and used to compute the elemental image appropriate for lenslet array of arbitrary specification [29, 30]. Hence the lenslet arrays need not be the same in recording and display process. Though it was not explicitly studied in Lippmann's report, recent investigations have revealed that the gap between the lenslet array and the display panel can be adjusted considering which parameter will be prior among the resolution and

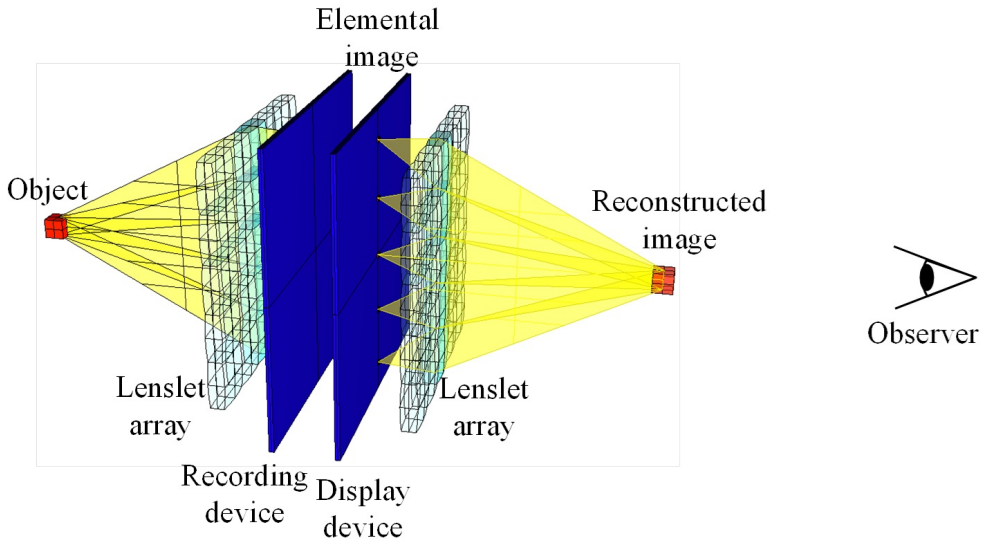

Figure 3.2 A diagram that shows the recording and display processes of InIm scheme.

the expressible longitudinal range of 3D image [31–33] as shown in Fig. 3.3.

The configuration where the resolution is important is called the *real/virtual mode* while the other case is the *focused mode*. In the *real/virtual mod*, the gap between the lenslet array and the display panel is different from the focal length of each lenslet. In this case, there exists a certain plane, which is called the central depth plane, where the focal planes of all the elemental image *cell*s are superposed [34]. Specifically, when the gap between the lenslet array and the elemental image is larger than the focal length of lenslet, the configuration is called *real mode* and the central depth plane is located in front of the lenslet array. In the opposite case, it is called *virtual mode* and the central depth plane is located behind the lenslet array.

The longitudinal expressible range of InIm system configured as *real/virtual mode* is known to be limited to a certain range around the central depth plane because the visual quality of integrated image is degraded as it goes farther from the central depth plane. Hence, it is supposed to design InIm to locate the central depth plane at the center depth of 3D image to be displayed.

When the gap between the lenslet array and the elemental image is the same as the focal length of the lenslet, the configuration is called *focused mode*. In the *focused mode*, the surface of the lenslet array is considered as a central depth plane and the pixel pitch of the displayed 3D image is determined by the pitch of each lenslet. Hence the size of each lenslet is limited to a certain level not to significantly degrade the resolution of the displayed 3D image. On the other hand, in the *real/virtual mode*, the magnification of the elemental image at the central depth plane can be controlled by changing the gap between the lenslet array and the elemental image, and the resolution of displayed 3D image is accordingly controllable. However, the longitudinal expressible range of the *real/virtual mode* is narrower than that of the *focused mode*, which is usually

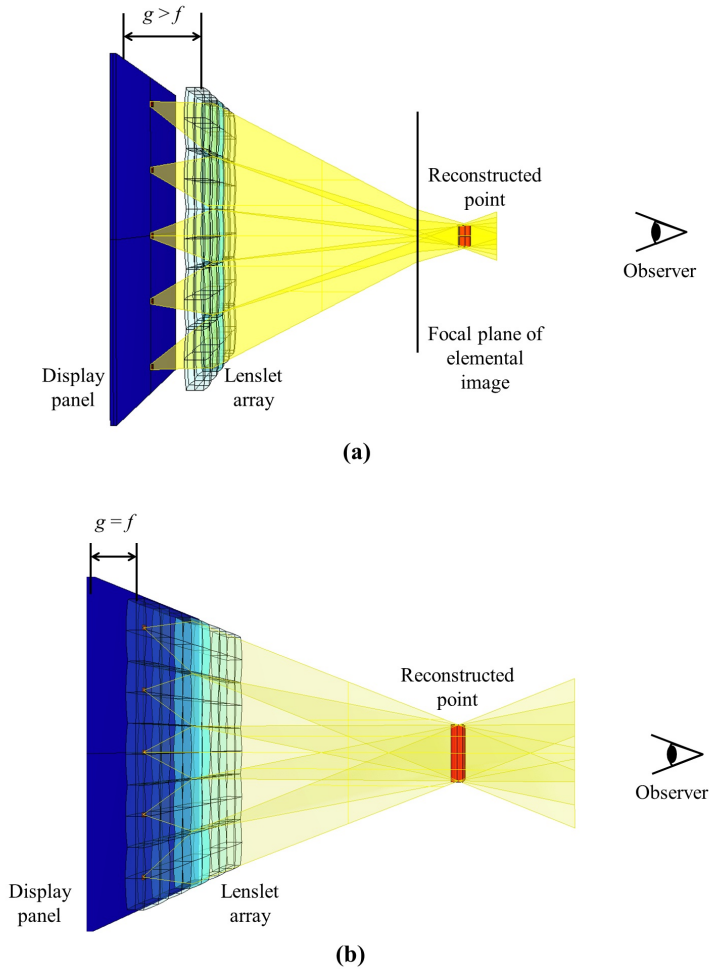

Figure 3.3 A diagram that illustrates the configuration of two modes of InIm: (a) *real/virtual mode* and (b) *focused mode*. g is the gap between the display panel and the lenslet array, f is the focal length of each lenslet of the lenslet array. In the *real/virtual mode*, $g \neq f$ while $g = f$ in the *focused mode*. In the *real/virtual mode*, the focal planes of lenslets are overlapped at the same longitudinal position and that position is called the *central depth plane*.

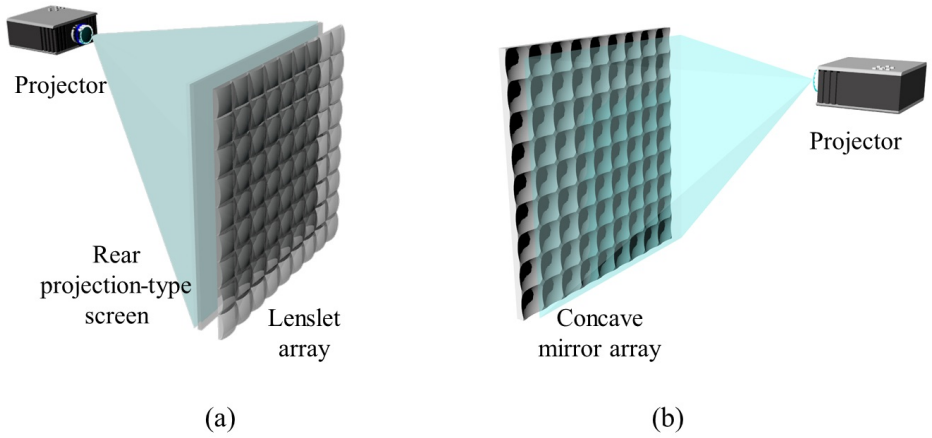

Figure 3.4 Two categories of projection-type InIm. (a) Rear projection-type and (b) frontal projection-type.

considered to be determined by available voxels or diffraction, and it had been analyzed in many reports.

One of the recent notable advances of InIm is that the InIm now can be implemented in the projection-type form. Regarding the development of various types of video technology, the theater always has been the best place to introduce a new video technology and get interest from public. Recent success of commercial product of stereoscopic 3DTV is also based on the prior success of 3D movies in theater. The success in theater encourages producers to create more contents based on the new video technique which might be a necessary condition for the value chain to be set up. Hence it is important to provide a way to implement the projection-type InIm, which can provide a large-sized screen suitable for theater, to expect InIm to come up to the commercial market.

The most intuitive way to implement the projection-type InIm is to replace the display device of the usual InIm setup with the combination of the rear-

projection-screen and the projector as shown in Fig. 3.4(a). However, this kind of setup requires additional space behind the screen and it is usually considered economically inefficient. To reduce the required space in preparing the theater based on InIm, the frontal projection-type setup is generally preferred.

The basic idea of the frontal projection-type InIm is that the refractive optics can be easily replaced with the reflective optics [35]. Because the direct alternative to the convex lens is the concave mirror, InIm can be implemented by using the 2D array of concave mirrors instead of the lenslet array. By incorporating the reflective optics, the display device of typical InIm can be replaced by the projector. Figure 3.4(b) shows a typical configuration of the projection-type InIm. As shown in Fig. 3.4(b), the elemental image is projected by the projector and it is integrated by a concave mirror array.

Later, it has been revealed that the pitch of mirror of the concave mirror array should be sufficiently small in the projection-type InIm configuration to avoid the visual quality degradation coming from the limited exit pupil of the projector [16]. The relationship between the pitch of the mirror and the visibility of the integrated image of the projection-type InIm has been analyzed using the Recognition-By-Component theory [36]. Other than many advantageous features listed in [16], the use of directional image source launched by the projector can avoid the flipping problem which is usual in the normal InIm which incorporates the diffusive image source.

3.2.2 Principle of the proposed scheme

As discussed in the previous chapter, the HMLF array is an optical structure whose external appearance looks like a transparent plate while the thin concave/convex mirror array structure is buried in the middle as shown in Fig.

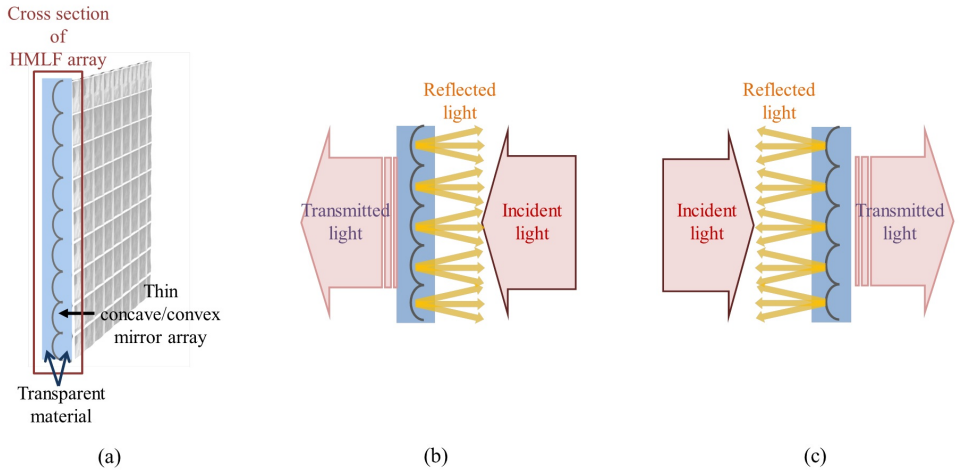

Figure 3.5 Structure and function of HMLF array. (a) Cross sectional view of the HMLF array. (b) Effect on the incident light when the incidental direction is the concave side and (c) the convex side of the HMLF array.

3.5(a). HMLF array affects the optical path of the incident light in unique way as shown in Fig. 3.5(b) and (c).

If the light is incident from the right side of HMLF array as shown in Fig. 3.5(b), a part of incident light will be reflected back by the concave mirror layer inside the transparent plate. Then it will propagate just as it is reflected by the ordinary concave mirror array except the refraction at the surface of the structure. On the other hand, the other part of the incident light will be transmitted through the concave mirror layer because it has the half mirror characteristic. Under the assumption that the concave mirror layer has infinitesimal thickness, there is no change of refractive index through the transmission, so the transmitted light will propagate just as it is passing through the transparent plate. Therefore the incident light is separated into two paths - one is reflected by the concave mirror array and the other is the path without any effect - by HMLF

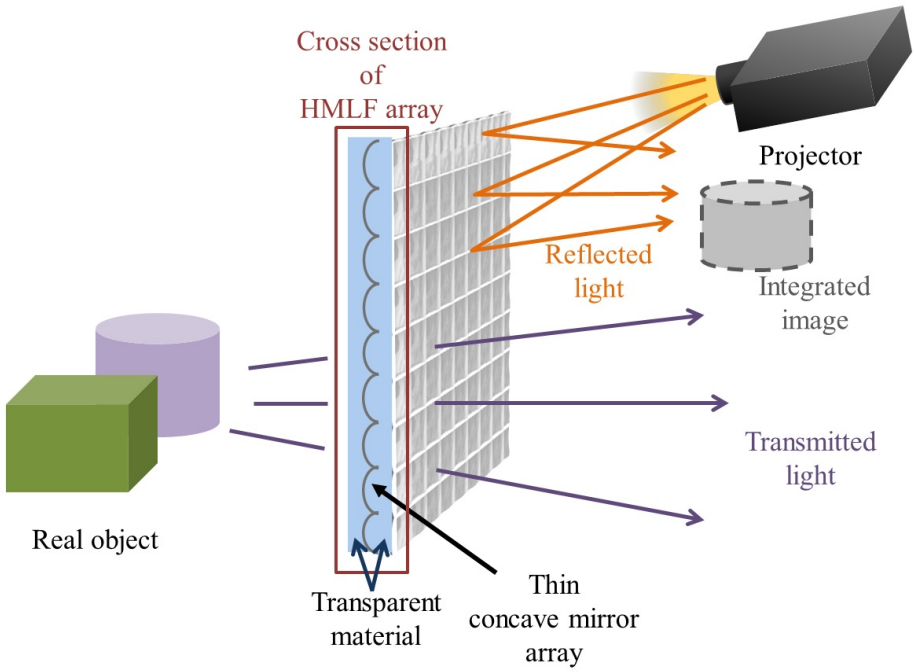

Figure 3.6 Concept of the see-through 3D display system.

array. For the case where the light is incident from the left side as shown in Fig. 3.5(c), the result is much similar but the reflection is made by the convex mirror array.

Figure 3.6 shows the concept of see-through 3D display system. The reflected light of HMLF array can be used for the imaging process of the reflection-type InIm because the concave mirror is the exact counterpart of the convex lens [33, 35]. And the rest of the incident light is transmitted as if it passes through the transparent plate in the ideal case. With the ideal HMLF array structure, it is possible to see the real world through HMLF array while a 3D integrated image is displayed by the reflection inside HMLF array when

a proper elemental image set is projected by an auxiliary projector. This is the basic concept of the see-through integral imaging display system by using HMLF array structure.

However, in such configuration, the reflection of the surroundings by the embedded half mirror inside HMLF array can appear as the halo effect and it can be the cause of the image quality degradation. Such halo effect can be resolved by balancing the reflection/transmission ratio of HMLF array. The reflection/transmission ratio of the incident light is determined by the reflectivity of the embedded half mirror. Hence, if the reflectivity is sufficiently low, the reflection of the surroundings will not be noticeable and HMLF array will appear as the clear window for the observer. However there is a tradeoff relationship because the low reflectivity will result in the low brightness of the 3D integrated image. As discussed later, a certain level of the reflectivity can be found where HMLF array is perceived as a clear window to the observer while the integrated image has the brightness comparable to the image projected to the ordinary screen. Under such condition, HMLF array can implement the see-through 3D display that can be used for AR application.

Up to this point, assumed was to use the concave-side of the embedded half mirror for the display of the integrated image. However, it is known that the 2D convex mirror array can also be used for the reflection-type InIm [16]. The only difference of using convex-side of the mirror array is that the ortho-pseudo conversion occurs. Hence both sides of the embedded half mirror can be used for the display of the 3D integrated image.

Figure 3.7 shows the system configuration of the proposed see-through bidirectional InIm system based on the principle discussed so far. The system is composed of three parts; HMLF array and two projectors. Two projectors are located in front and behind of HMLF array, respectively. Projector 1 projects

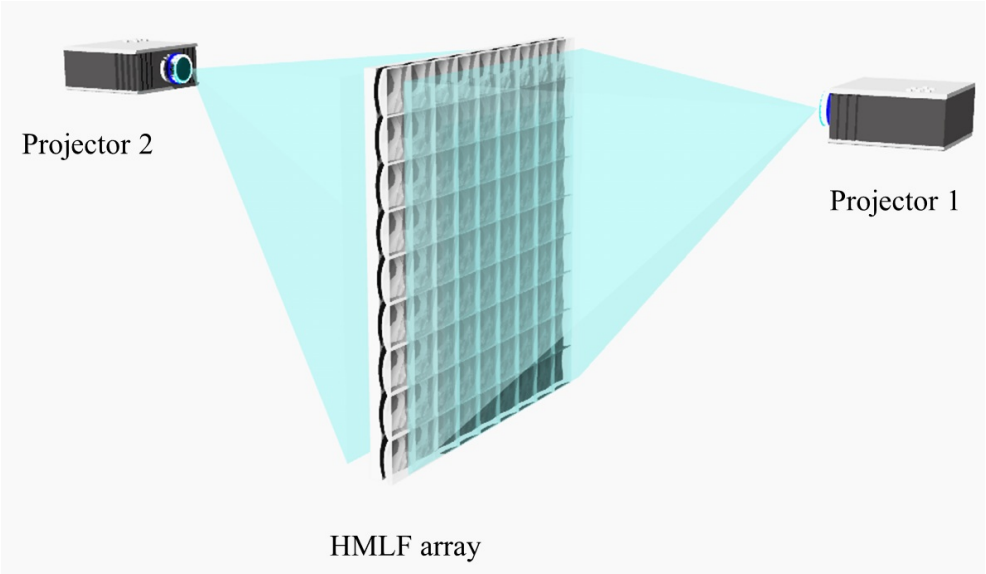

Figure 3.7 Concept of the see-through and bidirectional InIm system.

the elemental image set to the concave side of the embedded half mirror as depicted in Fig. 3.7. The reflected light of the projected elemental image set is integrated to show 3D image from the concave side of HMLF array. Projector 2 projects the elemental image set to the convex side of the embedded half mirror, and the reflected light is integrated to show 3D image from the convex side. However, in this case, the elemental image set should be generated considering ortho-pseudo conversion because the integration by the convex mirror array results in the ortho-pseudo conversion to the 3D image as mentioned above [37,38]. And the transmitted term of each projected elemental image set does not affect the displayed 3D image or see-through property.

Hence the bidirectional imaging of 3D volumetric image is possible by activating both projectors. Because InIm provides the continuous viewing zone, the group of observers surrounding the HMLF array can share the same volumetric

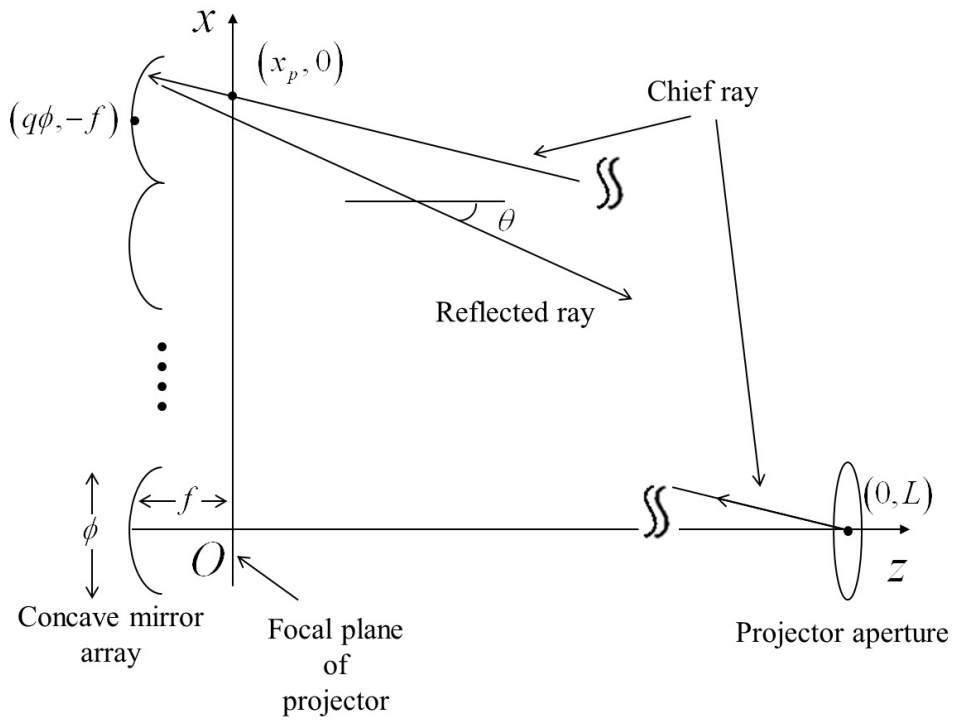

Figure 3.8 Geometry for the ray optic analysis of the reflection-type InIm.

3D image. Besides, the 3D image will look as if floating in the air because of the see-through property of HMLF array. However it is not possible to observe the displayed 3D image from the side of HMLF array because the viewing region of InIm is limited in a certain solid angle. Hence we will investigate how the viewing angle of the projection-type InIm is determined. Without the loss of generality, only the case where one-dimensional (1D) concave mirror array is used will be considered.

Figure 3.8 shows the geometry for the ray optic analysis where the 1D concave mirror array is laid parallel to the x-axis. The 1D concave mirror array is f distant from the x-axis where f is the focal length of each elemental mirror

of the mirror array. Therefore, the coordinate of the center of the mirror array is $(0, -f)$. The projector aperture is located at $(0, L)$ where L is the distance between the projector aperture and the focal plane of the projected image. The pitch of each mirror of the mirror array is ϕ, so the center of the q^{th} elemental mirror from the center elemental mirror is at $(q\phi, -f)$. For the further investigation, only the path of the chief ray of the projector aperture will be traced and the small error will be neglected.

The reflection-type InIm usually uses the focal mode where the projected image is focused at the focal plane of each elemental mirror. Hence the projected image will be focused along the x-axis, and the center of each pixel will be denoted as $(x_p, 0)$. Considering the rays reflected by the q^{th} mirror, the range of x_p should be

$$\frac{(q - 1/2)\,\phi}{(1 + f/L)} < x_p < \frac{(q + 1/2)\,\phi}{(1 + f/L)}. \tag{3.1}$$

And Eq. (3.1) can be approximated as

$$\left(q - \frac{1}{2}\right)\phi\left(1 - \frac{f}{L}\right) < x_p < \left(q + \frac{1}{2}\right)\phi\left(1 - \frac{f}{L}\right) \tag{3.2}$$

because L is sufficiently larger than f in general. Then the chief ray passing through $(x_p, 0)$ will be reflected by the q^{th} elemental mirror. Therefore, if we let θ be the angle between the reflected ray and the z-axis, the range of $\tan\theta$ should be

$$\left[\frac{q}{L} - \frac{1}{2}\left(\frac{1}{f} - \frac{1}{L}\right)\right]\phi < \tan\theta < \left[\frac{q}{L} + \frac{1}{2}\left(\frac{1}{f} - \frac{1}{L}\right)\right]\phi. \tag{3.3}$$

As we can see from Eq. (3.3), the viewing angle of each elemental mirror varies with its location. Hence the direction of reflection by the q^{th} elemental mirror can be represented by the mid value of the range in Eq. (3.3), and it can be calculated as

$$\tan\theta_c = \frac{q}{L}\phi, \tag{3.4}$$

where θ_c is the reflection angle corresponding to that mid value. And Eq. (3.4) is limited by the size of the projected image as

$$-\frac{N_p p}{2L} \leq \tan\theta_c \leq \frac{N_p p}{2L}, \tag{3.5}$$

where N_p is the number of pixels in the projected image and p is the pitch of the pixel. In the viewpoint of the light field, Eq. (3.5) means that the light field exists inside the range satisfying Eq. (3.5), so the viewing angle can be estimated as

$$\theta_{view} = 2\tan^{-1}\left(\frac{N_p p}{2L}\right). \tag{3.6}$$

And this result still holds for the convex mirror case. Hence, by using our proposed system, the bidirectional imaging of 3D image is possible for the total viewing angle of

$$2\theta_{view} = 4\tan^{-1}\left(\frac{N_p p}{2L}\right). \tag{3.7}$$

From Eqs. (3.6) and (3.7), it can be concluded that the viewing angle can be enhanced by increasing N_p and p, while decreasing L. However these parameters are also related to the other quality factors of InIm; so it is not simple to change them. Because the direction of the reflected ray becomes more outward for the outer mirror of the mirror array, only the image inside a certain viewing window is shown to the observer. If we assume that the observer on the z-axis is sufficiently far from the mirror array, we can estimate the boundary of the viewing window by finding the condition where the lower ray of the uppermost mirror and the upper ray of the lowermost mirror become parallel to the z-axis. The size of the viewing window is calculated as

$$w = \left(\frac{L}{f} - 1\right)\phi, \tag{3.8}$$

which can be approximated as

$$w \simeq \frac{L}{f}\phi. \tag{3.9}$$

And the lateral and depth resolution of the integrated image are also related with those parameters. If R_x denotes the lateral resolution and R_z the depth resolution, it is well known that

$$R_x = \frac{1}{\phi} \tag{3.10}$$

and

$$R_z = \frac{f}{p}. \tag{3.11}$$

Combining Eqs. (3.6), (3.9), (3.10) and (3.11), we obtain

$$N_p = 2\tan\left(\frac{\theta_{view}}{2}\right) w R_x R_z. \tag{3.12}$$

Therefore it can be concluded that the various quality factors of the reflection-type InIm have a tradeoff relationship and they can only be enhanced by increasing the number of the pixels of the projected image, N_p. Equation (3.12) is the reflection-type InIm version of the characteristic equation in [39]. From this equation, it can be shown that the viewing window and the viewing angle has the tradeoff relationship. It is known that the reflection-type InIm generally enjoys the wider viewing angle than the normal InIm, however such advantage comes from the sacrifice of the viewing window. By using the recent directional backlight technique [40], it might be possible to easily control the viewing window and viewing angle actively.

3.2.3 Implementation of the prototype

For the implementation of the prototype, the fluid filling method was adopted among three fabrication methods. The 2D lenslet array, which is made of polymethyl methacrylate (PMMA) whose refractive index is 1.4917, was prepared for the base layer. Hence the product #19576 of Cargille Lab. which has the same refractive index with PMMA [17] was selected for the immersion.

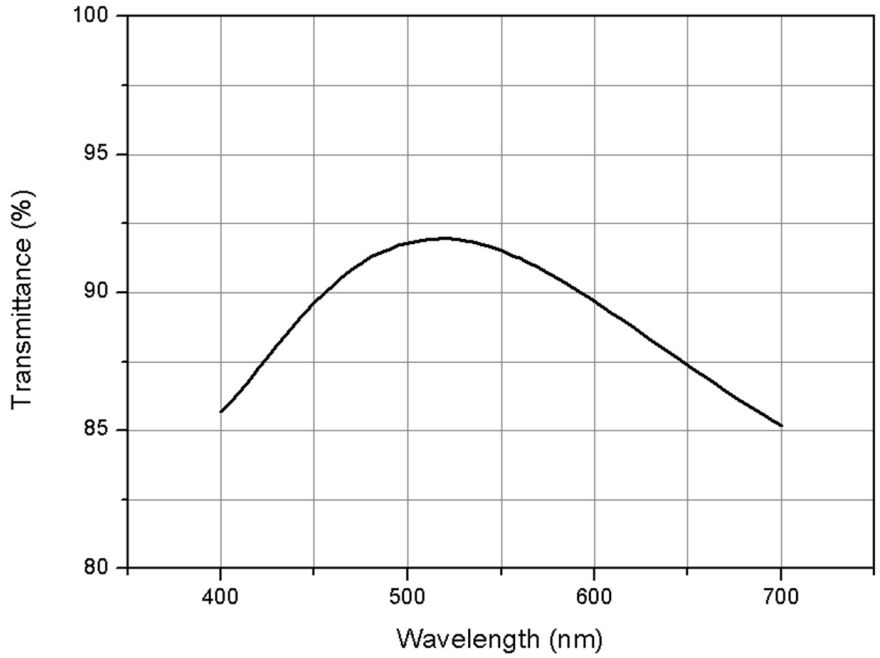

Figure 3.9 Transmittance of HMLF array in the visible range.

For the transreflective layer, the dielectric mirror coating was chosen and the ratio between transmittance and reflectance of the dielectric mirror layer can be designed by changing material and thickness of each dielectric layer. The transmittance for the prototype was determined to be around 90% in the visible range which will be discussed in the following subsection. The dielectric mirror with around 90% of transmittance was coated on the prepared 2D lenslet array and the transmittance according to the wavelength of the incident light is shown in Fig. 3.9.

For the immersion process, the transparent box should be prepared and it is preferred to match the material of the box with the base lenslet array. The transparent box made of PMMA is prepared for the immersion process and

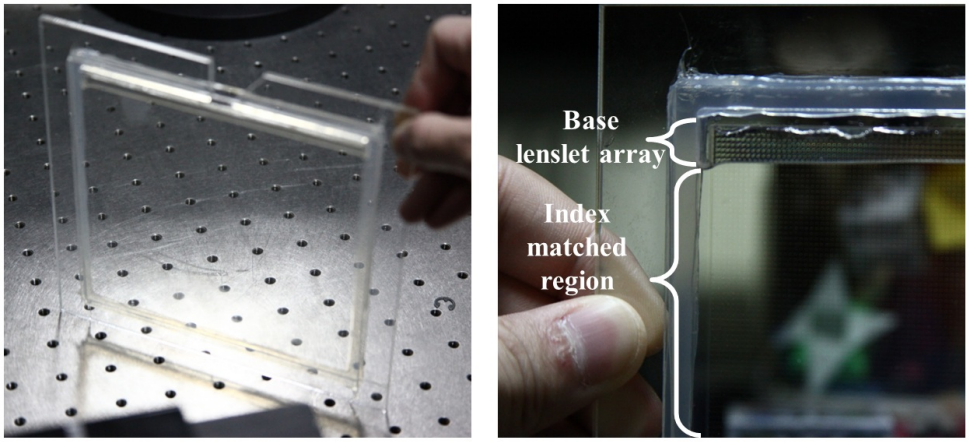

Figure 3.10 (a) Prototype of HMLF array fabricated following the fluid filling method. (b) Comparison between the region of the base lenslet array and the region immersed by index matching liquid.

the surface of the box was treated with the anti-reflective coating to avoid the unnecessary reflection of the projected image. Then the 2D lenslet array with the dielectric mirror coating, which is the result of the first step of fabrication process, is put inside the box and then the index matching liquid is injected until it fully immerses the 2D lenslet array. Figure 3.10 shows the result of the fabrication.

3.2.4 Characteristic of the prototype

As discussed before, the reflectance should be determined at the level where the prototype is perceived as the clear window while it shows sufficient brightness for the integrated image. Therefore, the brightness of the 3D image of the reflection type InIm will be compared with the 2D image on the normal screen

under the condition using the same projector for both cases. The comparison starts considering each pixel of the projected elemental image set with the same geometry as in Fig. 3.8.

For the pixel whose center is located at $(p_i, 0)$, the chief rays from the projector passes through the range on the projected image defined by $[p_i - p/2, p_i + p/2]$, where p is the pixel pitch of the projected image. Then the tangent of the reflected rays in this range will be limited as

$$\frac{q\phi - p_i - p/2}{f} < \tan\theta < \frac{q\phi - p_i + p/2}{f}, \tag{3.13}$$

where θ is the angle between reflected ray and the z-axis. $\tan\theta$ in Eq. (3.13) can be approximated by the first order expansion of Taylor's series around θ_c where θ_c is the reflection angle for the ray passing through the center of the pixel. Therefore, if q^{th} elemental mirror of the mirror array is related to the reflection of the considering pixel,

$$\tan\theta_c = \frac{q\phi - p_i}{f} \tag{3.14}$$

holds and $\tan\theta$ in Eq. (3.13) can be approximated as

$$\tan\theta \simeq \tan\theta_c + \left[\frac{\sqrt{(q\phi - p_i)^2 + f^2}}{f}\right]^2 (\theta - \theta_c)\,. \tag{3.15}$$

If we designate the maximum and minimum values of θ in the range of Eq. (3.13) as $\theta_{\max}$ and $\theta_{\min}$ respectively,

$$\Delta\theta = \theta_{\max} - \theta_{\min} = \frac{fp}{(q\phi - p_i)^2 + f^2} \tag{3.16}$$

can be obtained from Eq. (3.15). And this result also holds for the y-axis of the 2D concave mirror array case because we are considering the rectangular mirror array. Hence the projected ray for one pixel of the elemental image set will be

scattered in the angle defined by Eq. (3.16). If we assume that the intensity of light projected on one pixel is uniform and the ordinary screen scatters the projected image to all directions uniformly, the intensity of the scattered light for the ordinary screen will have the uniform value of $I/2\pi$ over the solid angle, where I is the total power on one pixel of the projected image. For the integrated image, Eq. (3.16) determines the scattering angle and it varies according to the location of pixel. Considering the case where the intensity of the scattered light is weakest, the scattering angle should be maximized and it will be

$$\Delta\theta_{\max} = \frac{p}{f} \tag{3.17}$$

because $|q_x\phi - p_i| < \phi/2$. Hence, the scattered light will approximately have the uniform intensity of

$$\frac{f^2 I}{2\pi p^2} \tag{3.18}$$

over the solid angle if $\Delta\theta_{\max}$ is sufficiently small. However the reflection type InIm shows only one pixel per each elemental mirror to the observer, so the perceived intensity will drop by

$$\left(\frac{p^2}{\phi^2}\right)\left(\frac{f^2 I}{2\pi p^2}\right) = \frac{f^2}{2\pi\phi^2} I, \tag{3.19}$$

considering the normal intensity throughout the entire image. Hence the perceived normal intensity of the integrated image is $f^2\pi^2/\phi^2$ times larger than the ordinary screen. In my prototype, this can be calculated as 6.7 referring to Table 3.1. The transmittance for my prototype was determined to be around 90% in the visible range and the perceived brightness of the integrated image will be about 67% of the ordinary screen. It was empirically concluded that this level of transmittance shows good see-through property while the brightness of the image is enough for displaying 3D image. However the transmittance can be adjusted according to the application. The prototype fabricated following

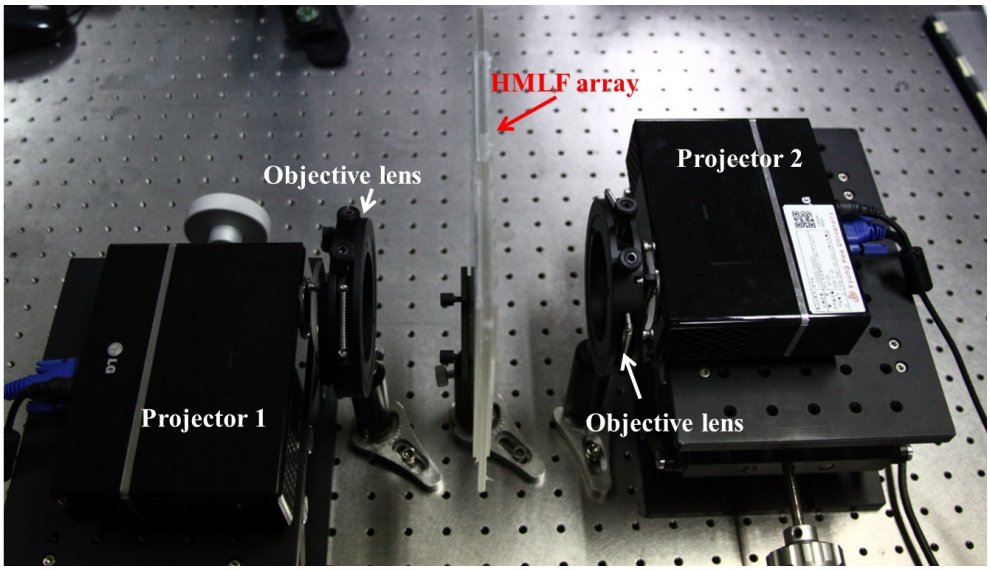

Figure 3.11 System configuration of the experimental setup.

the process described above is expected to have the see-through characteristic for the transmitted light. It is determined by how the refractive index between the lenslet array and the index matching liquid was matched well.

3.2.5 Experimental results

The preliminary experiments were performed to show the feasibility of the proposed scheme. Figure 3.11 shows the camera captured image of the experimental setup. The configuration is composed of two projectors, two objective lenses and the prototype of HMLF array. The projectors are the product of LG Electronics whose model name is HS102. The resolution of the projector is 800 $\times$ 600.

The pixel pitch of the projector affects the depth expression of the integrated image as shown in Eq. (3.11). However the ordinary projector does not

Table 3.1 Specifications of the implemented prototype system.

	Two-dimensional lenslet array	
Base lenslet array	Lenslet pitch	1 mm
	Focal length	3.3 mm
	Refractive index	1.4917 (PMMA)
	Total size	150 mm × 150 mm
Projector	Resolution	800 × 600
	Pixel pitch	133 μm
Objective lens	Focal length	175 mm

support sufficiently small pixel pitch for the reflection-type InIm, so an auxiliary objective lens was attached in front of the projector aperture to reduce the pixel pitch of the projector. In this configuration, the pixel pitch was reduced to 88 μm, however the operating distance where the integrated image is well focused was shortened to 80 mm as the side effect.

The specifications are summarized in Table 3.1. To utilize the bidirectional imaging functionality, two projectors with attached objective lenses are located in front and behind of the HMLF array respectively as shown in Fig. 3.11. The convex side of HMLF array directs to the projector 2, so the elemental image set for the projector 2 should be generated considering ortho-pseudo conversion as discussed before. To verify the see-through and bidirectional imaging functionality of the proposed system, two numbers “1” and “2” are integrated at 15 mm in front and 15 mm behind of HMLF array from the concave-side view. So the elemental image set for the projector 2 should be prepared to display backside view of these letters. In other words, the left and right of two letters should be

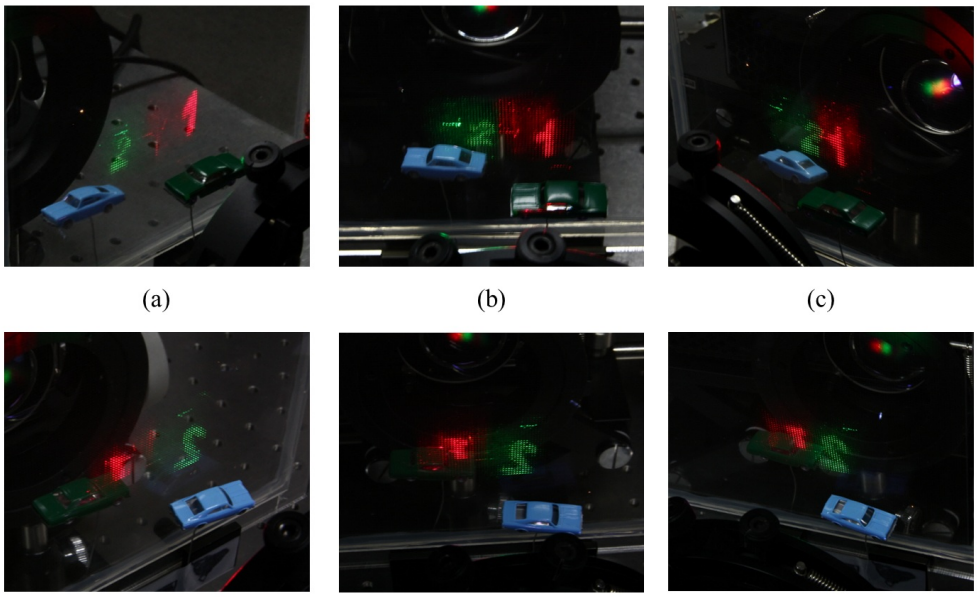

Figure 3.12 Camera captured images of the experimental results. (a)-(c): Frontal side view of the displayed 3D image. (a) Left, (b) center and (c) right views, respectively. (d)-(f): Back side view of the displayed 3D image. (d) Left, (e) center and (f) right views, respectively.

reversed. And, of course, the depths of two letters should also be reversed in display, but the depths should not be reversed in generating elemental image set because of the ortho-pseudo conversion occurring by the convex-side mirror array. Two real objects, green and blue cars, were also located to show the possibility for AR application. The green car and blue car are also located at 15 mm in front and 15 mm behind of HMLF array. So the situation where the green car is labeled by "1" and the blue car is labeled by "2" will be demonstrated by the experiment.

Figure 3.12 shows the camera captured images of the displayed integrated

image from various directions. Because of the see-through property of HMLF array, we can see that the virtual integrated image is naturally combined with two real objects though the object is located behind HMLF array. And two cars and their labels are aligned well regardless of watching direction because labels are 3D images.

Moreover, as shown in Fig. 3.12, it is possible to observe the image from frontal and backside of the system by the bidirectional imaging. Hence the proposed system supports the collaborative work for the group of people surrounding the system [19]. We can see that the bidirectional imaging functionality is enough for the group of people sitting face to face each other. When the observer is around the optic axis of the projector, the halo image appears. The multiple reflection of the transmitted term of the projected image causes such effect and it can degrade the quality of the integrated image. If we can reduce the reflection at the surface of HMLF array, the halo effect can be eliminated.

3.3 See-through integral floating display system for augmented reality

3.3.1 Introduction

HMD has been investigated since the early stages of AR research and it can be categorized into video see-through and optical see-through types [42]. Optical see-through HMD has a relatively shorter history than the video see-through type and some unresolved issues related to the optical see-through HMD still remain. As discussed before, one of these is the accommodation mismatch between the virtual image and the real world scene that arises because the gap between the real world scene and the virtual image is usually so large that the human visual system (HVS) cannot accommodate them both. The other issue is the demand to display 3D images of the overlaid virtual information.

Liu *et al.* proposed an HMD system that adopts a liquid lens for dynamically changing the optical distance of the virtual image [43]. Though their report showed that the accommodation response was successfully addressed, their system cannot display 3D images. The recent super multi-view (SMV) theory provides a way to display 3D images with an accommodation response corresponding to the intended distance. Takaki *et al.* presented an optical see-through system that satisfies the SMV condition of providing a distant 3D image with a precise accommodation response [25]. Though their system successfully provides 3D images with proper accommodation cues, the implementation of SMV has an inherent difficulty in that it demands an excessive number of rays per lateral 3D image pixel. As seen from many reports related to SMV, the SMV system is usually implemented in the form of a highly complicated system with

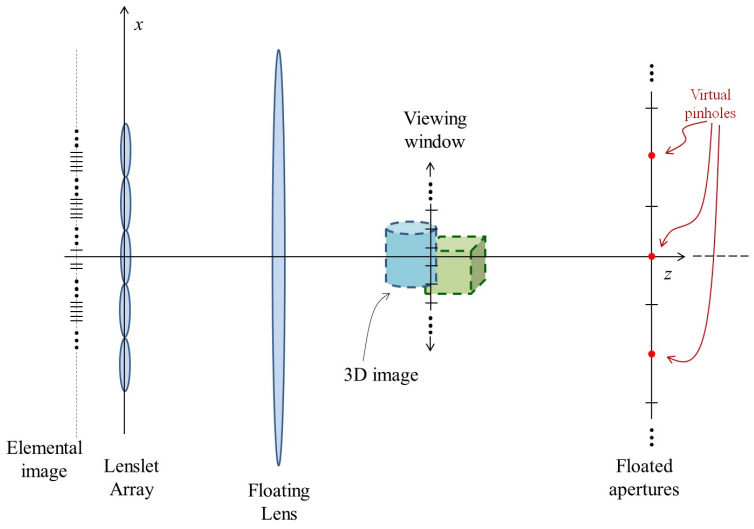

Figure 3.13 Typical configuration of integral floating scheme.

a large volume in order to make use of time or spatial multiplexing [44]. Hence, the SMV feature is not adequate for HMD adoption. The implementation of HMD providing 3D images of an appropriate accommodation cue still remains to be investigated.

In general, the *real/virtual mode* implementation of InIm is thought to be able to express a 3D image around the central depth plane regardless of its location [34]. One might expect that the optical see-through HMD without issues described above can be realized using the *virtual mode* InIm if the longitudinal range of the 3D image is not too large. However, general observations from experiments related to the *real/virtual mode* InIm show that the central depth plane location is restricted to a certain range, which means that a displayed 3D image cannot go farther than a certain distance.

In this section, an integral floating system with a concave floating lens, that can be applied for HMD with a 3D image satisfying an accommodation response

based on the principle of the *virtual mode* InIm, is proposed. Integral floating display is a 3D display technique to display 3D image, combining InIm and a convex floating lens [45–49]. A typical configuration of the integral floating scheme is shown in Fig. 3.13. Integral floating display is known to provide many advantageous features than InIm itself despite of its simple modification to the entire configuration. Usually integral floating display provides a larger viewing angle and depth expression than InIm. Moreover, the appearance of borders from the lenslets of the lenslet array, which is one factor that deteriorates visual quality of InIm scheme, is also eliminated from displayed 3D images.

As shown in Fig. 3.13, a convex floating lens floats the lenslet array of InIm system to the right-hand side of the floating lens. As a result, the lenslet array is imaged as an array of floated apertures in the right-hand side. In the integral floating system, these virtual apertures are considered as appropriate viewing zones for the observer. When the observer is located at a certain aperture location, the observer watches the corresponding *cell* of the elemental image of InIm system through the aperture. And the observed *cell* of the elemental image is changed as the observer moves from one aperture to another. This is the source of the disparity that provides 3D information to the observer. In this imaging principle, the observer's movable range is determined by the size of the floated apertures which can be enhanced by increasing the number of lenslets of the lenslet array maintaining other optical specifications. Hence the viewing angle is usually much larger than InIm where the viewing angle is only determined by the optical specifications.

And, because the observer views only one *cell* of the elemental image at a specific location, the boarders of the lenslet array are not usually observed. However, the cost of advantageous properties obtained without increase in the fundamental resource - the resolution of the display device - appears as draw-

backs in other properties [47]. For example, the size of displayed image is limited inside a certain region which is called viewing window; the motion parallax of the displayed image has discontinuities because of the finite size of the viewing zone; the crosstalk between the viewing zone becomes larger as the observer goes farther from the longitudinal position of the floated apertures.

As investigated in the following subsection, the pixel pitch of display panel that is adopted for the system is mainly related to the upper bound of the distance of central depth plane from the lenslet array when the system is the *virtual mode* InIm. The use of a concave floating lens effectively reduces the pixel pitch of display panel and extends the expressible range of the 3D image. The characteristics of the proposed system is analyzed and verified by experimental results. To impose a see-through characteristic on the proposed scheme, a system adopting a convex side of HMLF is presented. The AR system can be successfully implemented using the proposed HMLF, which has the same optical property as the concave lens.

3.3.2 Limitations on a long distance imaging by integral imaging

The final goal of this study is to design an integral floating system with a see-through characteristic in the form of HMD for the purpose of AR, as shown in Fig. 3.14. Instead of a concave mirror, which is equivalent to the convex floating lens of the conventional integral floating system, the proposed scheme adopts a convex mirror as a floating optic.

This configuration can be interpreted as an effective InIm system with various parameters changed (see Fig. 3.15. Detailed explanation will be provided in subsection 3.3.3). As described before, a significant problem of the HMD-type

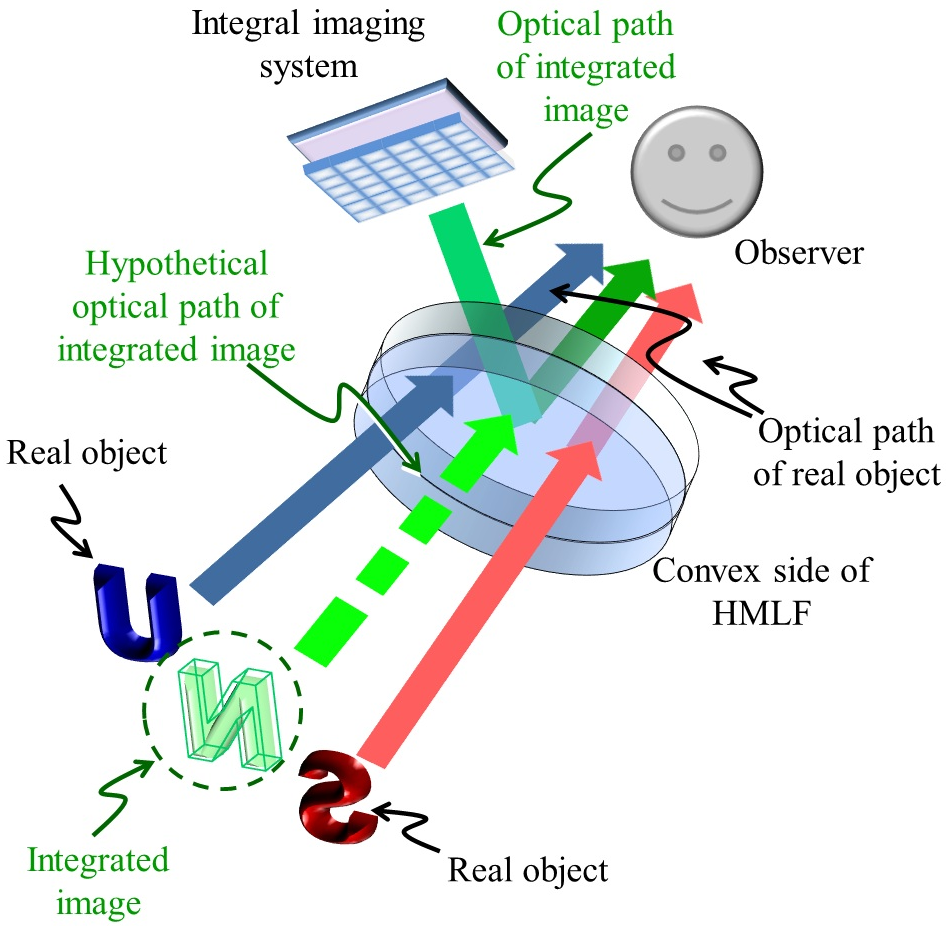

Figure 3.14 Concept of optical see-through head-mounted display based on an integral floating scheme adopting a convex side of HMLF. The integrated image is provided to the observer through the optical path specified as the "optical path of integrated image." The integrated image appears as a virtual image behind the HMLF; therefore, the perceived optical path is a dashed arrow specified as the "hypothetical optical path of integrated image."

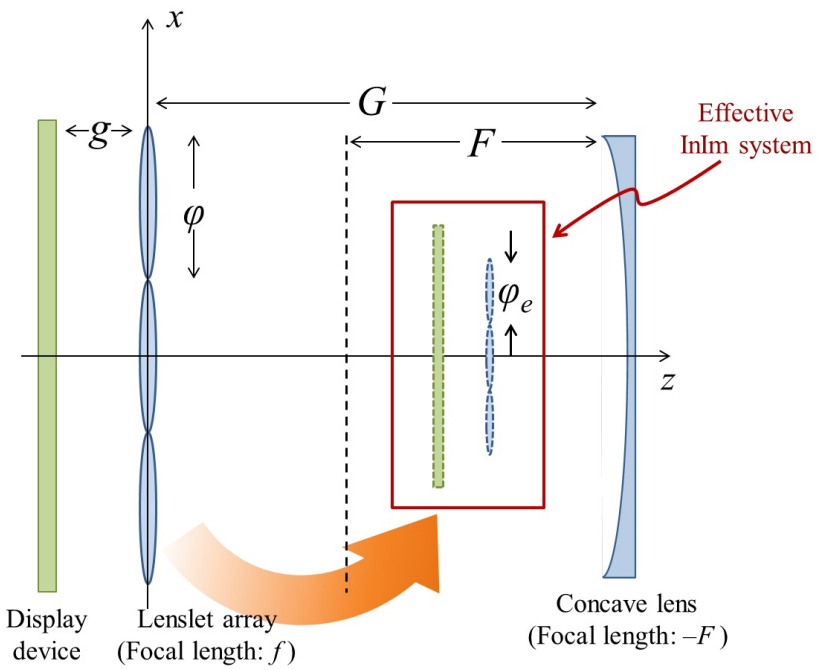

Figure 3.15 Interpretation of an integral floating scheme adopting a concave lens instead of a convex lens. The entire system can be interpreted as an effective InIm system.

AR system is that there is usually a large difference between the accommodation cues of the real world scene and the virtual image. In this subsection, the limitations in long distance imaging by the InIm method and their relations to the system specifications are investigated in terms of three different constraints: the lateral pixel pitch of the integrated image should satisfy a given angular resolution requirement (Eq. (3.21), to be discussed more in the following); the minimum resolvable depth around the central depth plane should be smaller than the depth discrimination of the human visual system (Eq. (3.22), to be discussed); and the central depth plane should be located inside the available voxels (Eq. (3.29), to be discussed). The result of this investigation will be used in designing the proposed system to address the appropriate accommodation response from the displayed integrated images corresponding to a given real world scene.

As discussed in Ref. [39], the resolution (or pixel pitch) of the display device used for implementation of the InIm system is a fundamental resource for three important visual quality factors: the lateral resolution, viewing angle, and marginal depth, of a displayed 3D image. In other words, the visual quality of a displayed 3D image is limited by the pixel pitch of the display device adopted for the InIm system. Under a given pixel pitch, it is only possible to balance the quality factors; one quality factor can be enhanced by degrading other factors. The viewing angle of most InIm systems is not large enough, though it is a very critical quality factor. Therefore, a number of techniques have been developed for enhancing the InIm viewing angle with various additional hardware components [50]. Hence, it is very important to define an appropriate lower bound for the viewing angle and strictly design the system accordingly. For simplicity, we

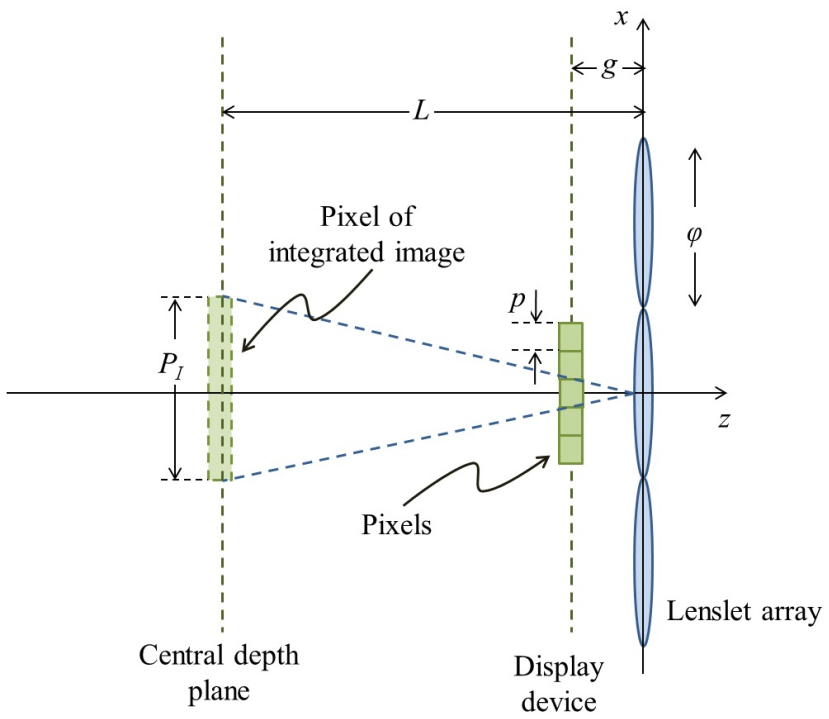

Figure 3.16 Definition of parameters used for analysis in the virtual mode InIm scheme.

define the viewing angle parameter Ω as

$$\Omega = 2\tan^{-1}\left(\frac{\theta}{2}\right), \tag{3.20}$$

where θ is the viewing angle of the system. In our discussion, only the virtual mode of the InIm scheme, in which the central depth plane is located behind the lenslet array, is considered.

Figure 3.16 shows the parameters defined for further discussions. To utilize the virtual mode of the InIm system, the lateral pixel pitch of the integrated image, P_I, should be smaller than the pitch of each lenslet of the lenslet array, ϕ, as described in Ref. [39]. However, this point should be revisited because

a lateral resolution perceived by an observer is assessed by angular resolution (cycles per degree). A more exact restriction on the lateral resolution can be found by considering human visual acuity. The required lateral resolution of the display device, defined as cycles per degree (or lines per degree), is well established in the conventional 2D display device. For a given angular resolution requirement, say m lines per degree (lpd), the lateral pixel pitch of the integrated image, P_I, is limited by the inequality

$$P_I < \frac{\pi}{180}\frac{(L+D)}{m}, \tag{3.21}$$

where D is the distance between the observer and the lenslet array and L is the distance between the central depth plane and the lenslet array, referring to Fig. 3.17; Otherwise, this inequality can be rewritten using the pixel pitch of the display device, p, as

$$\frac{L\Omega}{\phi}p < \frac{\pi}{180}\frac{(L+D)}{m}, \tag{3.22}$$

considering that $\Omega = \phi/g$ and $P_I = pL/g$.

Equation (3.22) can be rewritten by imposing an upper bound on L as

$$L < \frac{D}{\left(\frac{180}{\pi}\frac{mp\Omega}{\phi} - 1\right)}, \tag{3.23}$$

and this inequality is valid only when

$$p > \frac{\pi}{180}\frac{\phi}{m\Omega} = p_{lpd}. \tag{3.24}$$

where p_{lpd} is the required pixel pitch subject to a given angular resolution requirement (i.e., m lpd) for the case where the observer is located at the position of the lenslet array. The perceived angular resolution increases as the observer goes farther from the lenslet array; therefore, if $p \leq p_{lpd}$, the constraints given by Eq. (3.21) will always hold; i.e., Eq. (3.23) is meaningless.

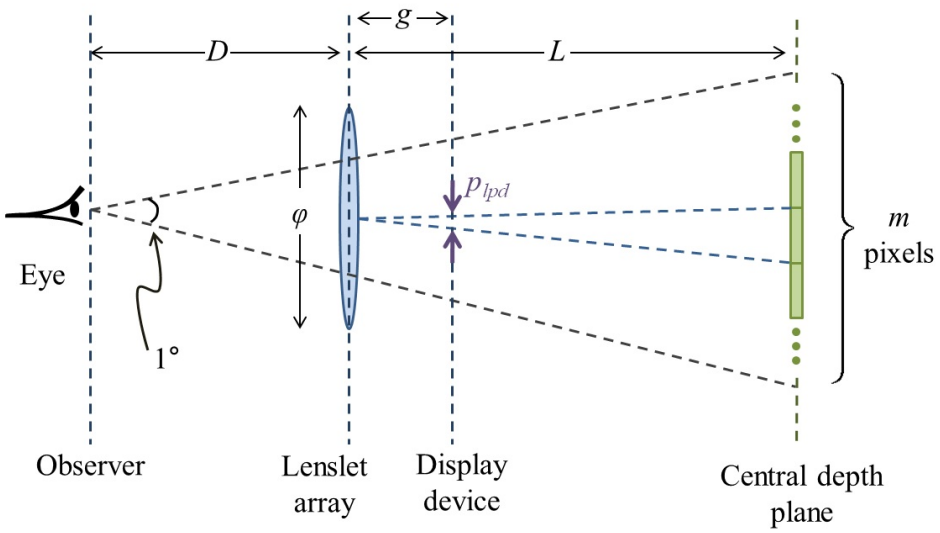

Figure 3.17 Relationship between lenslet pitch and lateral pixel pitch of the integrated image used for enabling virtual mode InIm. Human visual acuity is also depicted as cycles per degree.

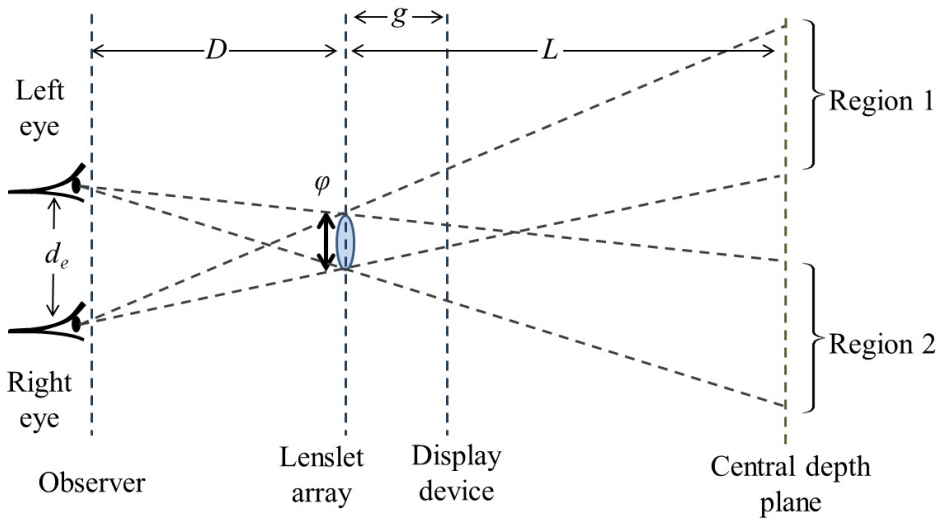

Figure 3.18 Conditions for avoiding crosstalk between the disparity information of left and right eyes. Regions 1 and 2 should be completely separated.

Equation (3.23) shows that the upper bound of L has a dependence on ϕ as well as p. However, a large ϕ value cannot be freely determined to give proper depth information to the observer. To provide an accurate depth cue to the observer, the images shown to the left and right eyes of an observer should be independent of each other and not cause crosstalk in disparity information, as shown in Fig. 3.18. On the basis of Eq. (3.28) in Ref. [51], the size of ϕ should be limited by an inequality

$$\phi < \frac{L}{L+D} d_e, \tag{3.25}$$

where d_e is the distance between the eyes of the observer, to avoid the crosstalk in the disparity information.

From Eq. (3.25), though the upper bound of ϕ varies according to the values of L and D, ϕ cannot be larger than d_e for any case. It is well known that the distance between human eyes is around 65 mm; this means that ϕ cannot be

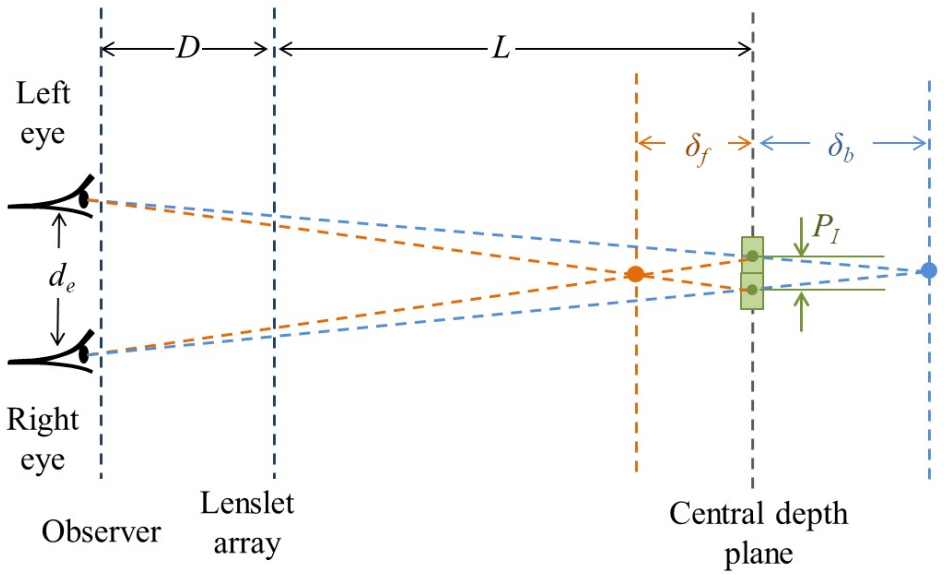

Figure 3.19 Minimum quantization step of the displayed integrated image around the central depth plane.

larger than 65 mm. Hence, the upper bound of L is mainly affected by p under the condition of Eq. (3.25).

The longitudinal quantization step (or depth resolution) of the system should also be taken into account to assess its performance as a 3D display device. Following a similar analysis shown in Ref. [25], the minimum resolvable depth around the central depth plane of the displayed integrated image can be estimated. It can be easily calculated by finding the perceived depth when the left and right eyes of an observer focus on different adjacent pixels on the central depth plane, as shown in Fig. 3.19. Accordingly, the calculated minimum

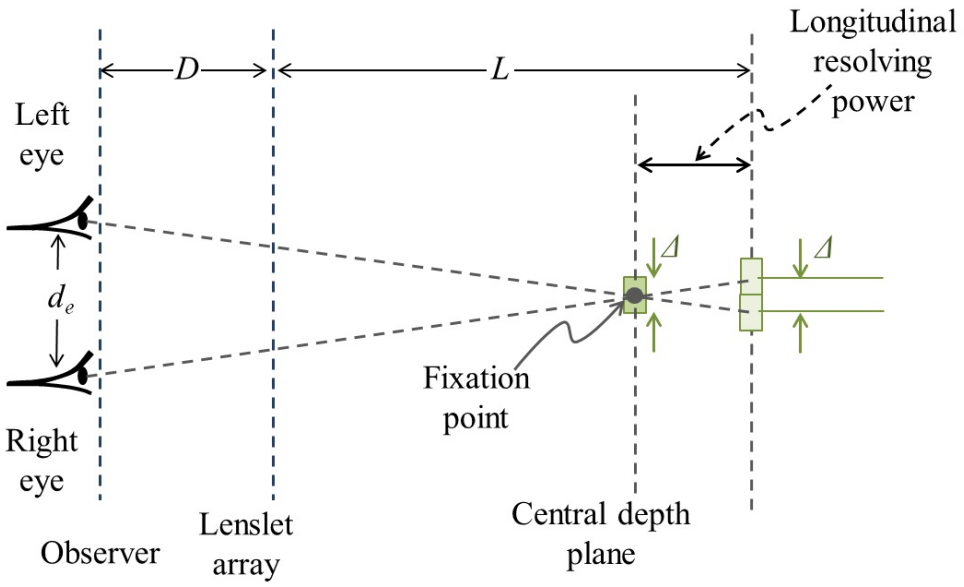

Figure 3.20 Depth discrimination (or longitudinal resolving power) of the human visual system around the central depth plane.

resolvable depths in front of and behind the central depth plane are

$$\begin{aligned} \delta_f &= \frac{P_I(L+D)}{d_e + P_I}, \\ \delta_b &= \frac{P_I(L+D)}{d_e - P_I}, \end{aligned} \tag{3.26}$$

respectively. The system's design is expected to have a longitudinal resolution, determined by Eq. (3.26), which is higher than the depth discrimination of the human visual system. The minimum resolvable longitudinal distance for humans is related to various factors and deducing an accurate expression is difficult. We will consider a relatively loose condition for the longitudinal resolving power of the human visual system based on the perceived disparity.

As shown in Fig. 3.20, the longitudinal resolving power around the central depth plane is determined by the range in which the disparity information is

confused by the restriction in human visual acuity. Hence, δ_b should be restricted by the inequality

$$\delta_b = \frac{P_I(L+D)}{d_e - P_I} < \frac{\pi}{180}\frac{(L+D)^2}{d_e m}. \tag{3.27}$$

From this relationship, the upper bound of L can be calculated as

$$L < \frac{1}{2}\left[\left(\frac{\phi d_e}{p\Omega} - \frac{180}{\pi}d_e m - D\right) + \right. \\ \left. + \sqrt{\left(\frac{\phi d_e}{p\Omega} - \frac{180}{pi}d_e m - D\right)^2 + \frac{4\phi d_e D}{p\Omega}}\right]. \tag{3.28}$$

Of course, the actual upper bound of L should be much smaller than that in Eq. (3.28) because we used the loose requirement. However, Eq. (3.28) can be useful for investigating the tendencies of the upper bound of L according to various parameters.

Other than the limitation related to human depth discrimination, L is also restricted by a finite range of voxels created by the InIm system. It was determined that the locations of the available voxels, which are determined by points where at least two different rays cross, are limited inside a certain range owing to the finite pixel pitch of the display panel [52]. Such a range is bounded by Ng, where N is the number of pixels per lenslet of the lenslet array and g is the gap between the lenslet array and the display panel; i.e., the voxels exist at the farthest $(L+Ng)$ distance from the lenslet array, meaning that the InIm cannot display a 3D image over this distance. However, considering the perceived depth resolution determined by Eq. (3.26), there should be at least one resolvable depth behind the central depth plane because the longitudinal expressible range of InIm is determined around the central depth plane. Hence, to show a 3D image behind the central depth plane, $(L+\delta_b) < (L+Ng)$, i.e.,

$$\delta_b = \frac{P_I(L+D)}{d_e - P_I} < Ng. \tag{3.29}$$

This limitation can be rewritten as

$$L < \frac{d_e \phi^3}{p^2 \Omega^2 D + p\phi(\phi + d_e)\Omega}. \tag{3.30}$$

Combining Eqs. (3.23), (3.28), and (3.30), the limitation becomes

$$L < \min\left(\frac{1}{2}\left[\left(\frac{\phi d_e}{p\Omega} - \frac{180}{\pi} d_e m - D\right) + \sqrt{\left(\frac{\phi d_e}{p\Omega} - \frac{180}{\pi} d_e m - D\right)^2 + \frac{4\phi d_e D}{p\Omega}}\right], \frac{d_e \phi^3}{p^2 \Omega^2 D + p\phi(\phi + d_e)\Omega}, \frac{D}{\left(\frac{180}{\pi}\frac{mp\Omega}{\phi} - 1\right)}\right). \tag{3.31}$$

where min(A,B,C) means the minimum value of A, B, and C.

Figure 3.21 shows the simulation results demonstrating the way in which the upper bound of L is affected by p, Ω, and m. The angular resolution of the displayed image, m, is a subjective parameter that varies according to the acceptable visual quality decision. The widely accepted standard in the 2D display industry claims that 60 lpd is enough to satisfy human visual acuity [53]. However, it is common to regard a much lower visual quality as acceptable for a 3D display system, considering the present status of display devices. A lenslet array with a pitch of 1 mm is often used for the InIm focal mode for research purposes [54]. From a distance of about 600 mm, which corresponds to about 10 lpd, the display quality is such that simple symbols are recognizable. Considering that the goal is to implement HMD, for calculation, D and Ω are set to 100 mm and 0.2, respectively, and the required ϕ is assumed to be 2 mm.

As shown in Fig. 3.21(a), the upper bound for 30 lpd and 60 lpd is mostly ruled by depth discrimination, which is explained by Eq. (3.28). However, the upper bound for 10 lpd is ruled by the existence of voxels when p is smaller than around 18 μm. In Fig. 3.21(a), the upper bounds determined by the depth

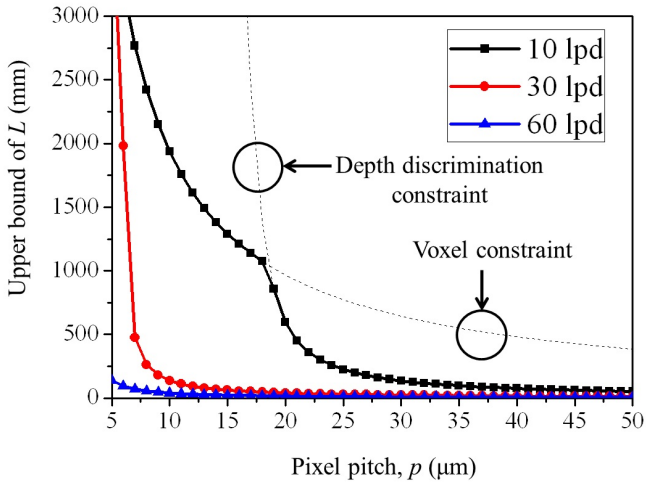

(a)

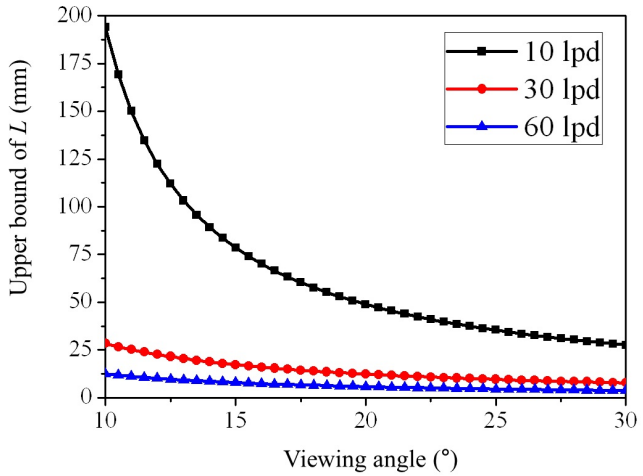

(b)

Figure 3.21 Results of a numerical simulation showing the dependence of the upper bound of L on p, ϕ, and m. (a) Upper bound according to p and m. (b) Upper bound according to θ and m.

discrimination and voxel constraints are illustrated as dashed lines respectively. Considering an angular resolution of 10 lpd, we can see that the 3D image can be displayed at 1000 mm behind the lenslet array for $p < 18\mu$m. However, an angular resolution of 30 lpd requires p to be smaller than 6 μm, which nearly approaches the current best spatial light modulator based on liquid crystals [11] and 60 lpd requires a much smaller pixel pitch, even for displaying 3D images at a distance of 1000 mm.

Hence, it can be said that displaying 3D images of 60 lpd at farther than 1000 mm still needs further development. Figure 3.21(b) shows the dependence of the upper bound on the viewing angle of the system. As expected, the viewing angle has a tradeoff relationship with the upper bound of the central depth plane. The viewing angle used for Fig. 3.21(a) corresponds to approximately 11.4°. Hence, a greatly reduced pixel pitch is required for enlarging the viewing angle.

3.3.3 Integral floating display using a convex mirror

Integral floating display is a 3D display technique that combines an InIm scheme and a floating technique. Previous research has demonstrated that an integral floating system can show more advantageous features than an InIm system, owing to an additional convex lens [46, 47]. The additional convex lens results in a wider viewing angle and a larger depth expression in the integral floating system. Moreover, the appearance of borders from the lenslets of the lenslet array can also be eliminated.

Adopting a concave lens instead of a convex lens for the floating scheme is more beneficial for displaying a long distance 3D image. As conceptually depicted in Fig. 3.15, the concave floating lens images the lenslet array and the elemental image with a magnification factor less than one; i.e., the lateral

size is reduced; this is unlike in the conventional integral floating system with a convex floating lens. The entire system can be interpreted as an InIm system composed of the effective lenslet array and elemental images that are images of the actual lenslet array and elemental images transformed by the concave floating lens. With a simple calculation, the effective parameters of the effective lenslet array and elemental image are

$$p_e = \frac{1}{G/F + g/F + 1} p\phi_e = \frac{1}{G/F + 1} \phi f_e = \frac{1}{(G/F + 1)^2} f \tag{3.32}$$

This means that the effective InIm system is composed of an elemental image with a pixel pitch, which is the fundamental source of the 3D image quality, reduced by the factor of $(G/F + g/F + 1)$. As discussed in the previous section, the effective system is capable of displaying a more distant 3D image because the upper limit of the location of the central depth plane can be increased according to the ratio G/F.

The effective InIm system can be designed to have a viewing angle parameter Ω and a lenslet pitch ϕ_o by adopting a lenslet array with the following parameters:

$$\phi = (G/F + 1)\, \phi_o f = (G/F + 1)^2\, f_e \simeq (G/F + 1)^2\, \frac{\phi_o}{\Omega} \tag{3.33}$$

where the approximation holds for the sufficiently far location of the central depth plane. Hence, for the case where the integrated image is displayed at a far distance, the viewing angle of the lenslet array adopted for the system can be estimated as

$$\Omega_o \simeq \frac{\phi}{f} = \frac{1}{(G/F + 1)} \frac{\phi_e}{f_e} \simeq \frac{1}{(G/F + 1)} \Omega \tag{3.34}$$

Equation (3.34) shows that the appropriate lenslet array for the system should have a much narrower viewing angle than the required value. The lenslet array

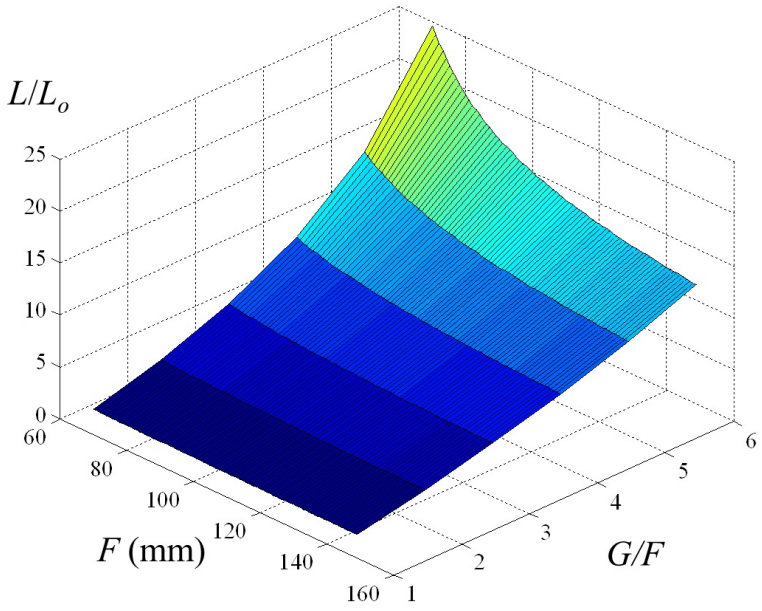

Figure 3.22 Simulation result showing the extended upper bound of L according to G and F.

that can be used for the system is generally useless by itself because of the narrow viewing angle. Hence, it is usually not commercially available and customization is needed. Nonetheless, the physical implementation of our system is guaranteed because the narrow viewing angle corresponds to a larger radius of curvature of each lenslet.

Figure 3.22 shows how much the proposed system can enhance the upper bound of the central depth plane according to the adopted concave lens. The pixel pitch of the display device is set to 0.1 mm for the simulation. The effective lenslet pitch and the viewing angle parameter Ω must be 2 mm and 0.33, respectively. L is the upper bound of the proposed system and L_o is the upper bound of the ordinary InIm system satisfying the same lenslet pitch and

viewing angle. As G becomes larger, the upper bound of L is further extended because of the increased reduction factor of the pixel pitch of the display device. However, a larger G means that the adopted display device has a larger lateral size for displaying images of the same size. Hence, the ratio between G and F should be determined by considering the volume of the implemented system and the system becomes more efficient as F becomes smaller. However, the smaller F value usually causes lens distortion and severely affects the quality of the displayed image. Hence, the values of F and G should be carefully designed by considering various factors.

The proposed integral floating system should have the ability to mix a real world scene with a displayed 3D image in order to be used as an AR system. The easiest way to achieve such a mixture is to adopt a half mirror between the observer and the proposed system. However, an optical system adopting a half mirror always suffers from a large implementation volume, which makes it inadequate for HMD application. Instead of using the simple flat half mirror, the volume of the system can be reduced by applying the concept of a HMLF that combines the functions of a convex mirror and a half mirror. Considering the implementation, the HMLF should have a structure whose external shape is a transparent plate with a thin convex mirror embedded, as shown in Fig. 3.14, which depicts the concept of the HMD system based on the integral floating scheme implemented by a HMLF.

3.3.4 Experimental results

A preliminary experiment was performed to show the feasibility of our proposed scheme, which uses a concave lens for an integral floating system to display 3D images that are located a great distance from the observer. As stated in the previous subsection, a lenslet array adequate for the proposed scheme is

Table 3.2 System specifications of experimental setup for integral floating display using concave lens.

Parameters	
Pixel pitch of display device, p	124.5 μm $\times$ 124.5 μm
Focal length of lens let array, f	30 mm
Pitch of each lens let, ϕ	5 mm $\times$ 5 mm
Focal length of concave lens, $-F$	- 100 mm
Gap between lens let array and concave lens, G	100 mm
Effective focal length of lens let array, f_e	7.5 mm
Effectvie pitch of lens let array, ϕ_e	2.5 mm $\times$ 2.5 mm

generally not available as a readymade product because of an extremely small viewing angle. Instead, an experiment was performed with an ordinary lenslet array to prove the validity of our method for interpreting the proposed system as an effective InIm system. The system was configured as shown in Fig. 3.14. The detailed system specifications are listed in Table 3.2.

Figure 3.23 shows a series of camera-captured integrated images displayed by the proposed integral floating system with a concave lens. The considerably enhanced fundamental capability gained by the effectively reduced pixel pitch is used for enlarging the viewing angle because an ordinary lenslet array was adopted. As shown in Table 3.2, the upper bound of L calculated by Eq. (3.31) is around 40 mm. However, the range in which voxels exist extends to around 300 mm, according to Eq. (3.30). InIm images with L varying from 40 mm to 300 mm were displayed. For comparison with the theoretical values, L and θ were experimentally calculated by measuring the disparity value with a ruler located in front of the concave lens. Table 3.3 presents the comparison results,

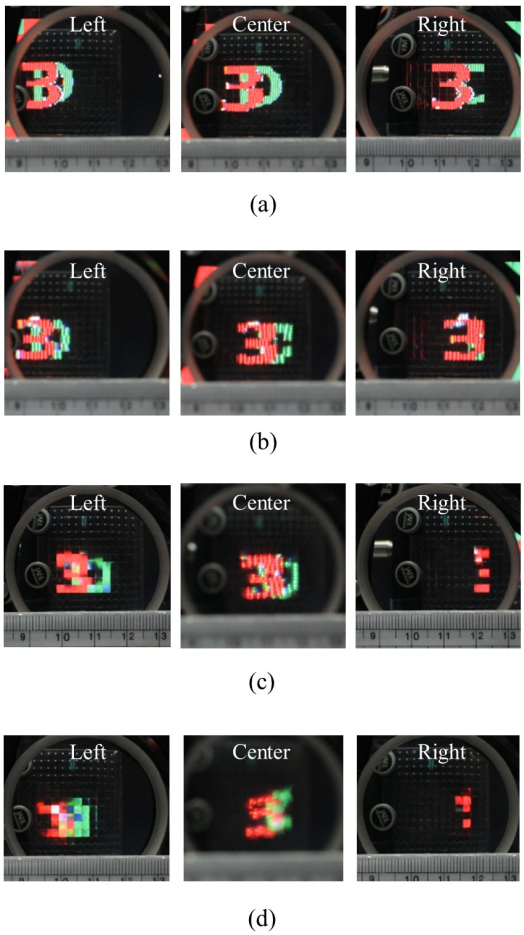

Figure 3.23 Camera-captured images showing the disparity in integrated images displayed by an integral floating system with a concave lens for various values of L: (a) $L = 40$ mm; (b) $L = 70$ mm; (c) $L = 149$ mm; (d) $L = 300$ mm. For each L, "3" and "D" are located 10 mm in front of and behind the central depth plane. For (c) and (d), the camera focus could not cover both the ruler and the integrated image. The center images of (c) and (d) are focused at integrated images.

Table 3.3 Comparison of theoretical and experimental values of L and θ using interpretation of proposed system as effective InIm system

Fig. 3.23	Target L	Theoretical θ	Measured L	Measured θ
(a)	40 mm	22.4°	38 mm	20.1°
(b)	70 mm	20.9°	62 mm	18.0°
(c)	149 mm	19.9°	132 mm	15.3°
(d)	300 mm	19.4°	315 mm	16.0°

in which the experimentally obtained characteristic values are a good match to those of the effective InIm theoretical model system. Hence, we can conclude that the fundamental capability of the InIm scheme has been enhanced by the proposed scheme.

The series of camera-captured images shown in Fig. 3.23 show that the central depth plane located near the upper bound, 40 mm, provides acceptable integrated image visual quality. However, the visual quality degrades as the central depth plane grows farther from 40 mm. When $L = 300$ mm, the quality of the displayed integrated image is degraded to a level where the shape is not easily recognized, although the voxel still exists at that distance, because the angular resolution of the displayed image reaches the limit determined by human visual acuity. The distortion of the lenslet of the lenslet array is another reason for the degraded image quality. Hence, the experimental results reveal the following: 1) the upper bound of L determined by Eq. (3.31) provides a good guideline for displaying an integrated image with an acceptable visual quality, 2) the interpretation of our proposed method, which considers the system to be an effective InIm system, explains well the investigated experimental results.

The adoption of a HMLF for HMD application was proposed in the previ-

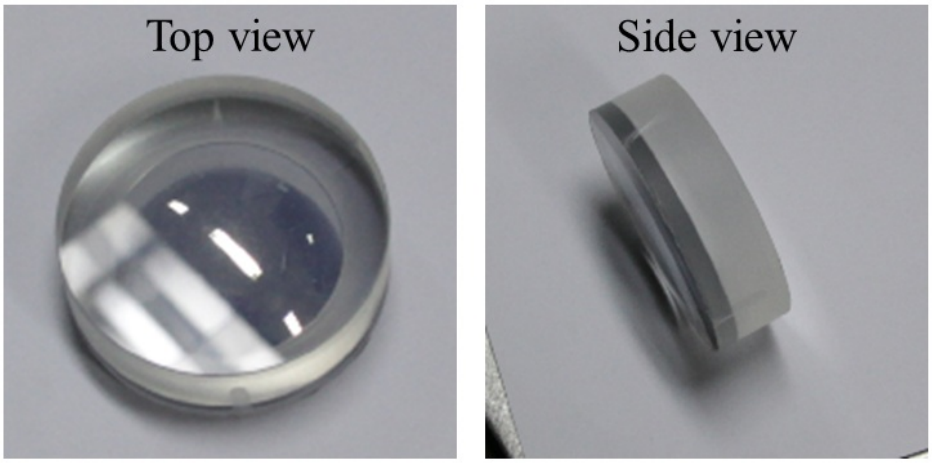

Figure 3.24 Implemented prototype of HMLF.

ous subsection. A prototype HMLF was implemented using the negative mask method because the target structure includes only one convex mirror. The convex lens used for the prototype has a focal length of 100 mm and a pitch of 50 mm. The transreflective layer was formed by Al deposition and the thickness was controlled to make the reflectance 50%. The focal length is shortened to about -25 mm when the optical concave lens function is provided by the transreflective convex mirror [33]. It is difficult to secure a sufficient optical path length when implementing the system, because of the short focal length. Hence, a convex lens with a much larger focal length is required for the base structure when fabricating a HMLF for the actual product. The see-through characteristic of the HMLF and the feasibility of an integral floating scheme that adopts a convex side of HMLF instead of a concave lens are shown in experiments using the prototype.

Figure 3.25 shows the camera-captured images of experimental results with the lenslet array and display device listed in Table 3.2. The real object that is

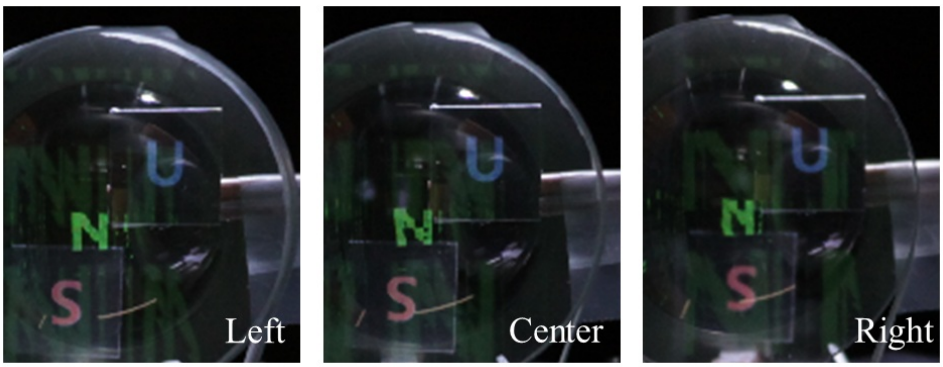

Figure 3.25 Camera-captured images of integrated image "N" displayed by the integral floating system adopting a convex side of HMLF. L was set to 30 mm. Real objects "S" and "U," which are printed on pieces of paper, were located for disparity comparison. "U" is located at the same distance as "N," while "S" is 30 mm behind "N" and "U."

located behind the HMLF is shown directly to the observer because of the see-through characteristic of the HMLF. The HMLF also displays the integrated image according to the principle of the integral floating system with a concave lens. A ghost artifact appears because of reflection at the HMLF surface. It might be possible to avoid such artifacts by using an antireflective coating on the surface. The proposed system cannot implement real world scene occlusions, unlike many other see-through displays. The real world scene will dominate over the integrated image when the brightness of the real world scene is significant compared to the integrated image. Hence, the brightness of the integrated image should be sufficiently high to suppress perception of the overlapped real world scene.

3.4 Summary and conclusion

In this chapter, it was verified that the adoption of HMLF or its array can inspire to spawn new ideas by providing two new types of 3D display systems.

In Sec. 3.2, the novel method to implement the see-through and bidirectional InIm system has been proposed. For the implementation, HMLF array was fabricated by the fluid filling method which can realize the perfect index matching between the base and cover layer. And the characteristics of the reflection type InIm for the design of the system was analyzed. However there was tradeoff relationship between quality factors, so they should be balanced according to the application. The experimental results using the prototype of HMLF array fabricated by the fluid filling method show that the proposed system can realize the seamless overlay of 3D virtual image onto the real world. Moreover, the bidirectional imaging functionality makes it possible to do collaborative work for the group of people. It is expected that the proposed system can be a new standard for AR display because it satisfies all of 4 requirements listed in Sec. 3.2.

Though the feasibility of the proposed system was verified, there are still problems to be solved for the practical use of the proposed system. At first, the projector optic should be redesigned for InIm. The pixel pitch of projected image should be much smaller with a sufficiently long operating distance. It is expected that the projector with such specification will be developed as the needs for 3D display increases. The other problem is that the reflection at the surface of HMLF array results in the halo effect as discussed before. To enhance the quality of the virtual 3D image, the method to reduce the reflection should be investigated and it is remained as a future work.

In Sec. 3.3, a novel integral floating scheme, that adopts a concave lens in-

stead of a convex lens, has been proposed. As discussed, the proposed system can be interpreted as an effective InIm system in which all of the system specifications have been changed. The pixel pitch of the display panel is reduced and is helpful in extending the upper bound of the location of the central depth plane, as explained in Sec. 3.3. However, a lenslet array with an extraordinarily small viewing angle should be adopted in order to obtain a meaningful viewing angle and lenslet pitch when it is transformed to an effective InIm system. Such a lenslet array is usually not commercially available because, by itself, it is useless. Fortunately, a lenslet array with a smaller viewing angle is physically realizable. Hence, it is possible to customize the lenslet array for the intended specifications. It was also demonstrated that the optical see-through HMD, which is capable of displaying a 3D image with a proper accommodation cue, can be implemented by adopting a HMLF for the proposed integral floating scheme. Actually, the focal length of the convex lens prepared for the base structure of the HMLF must be sufficiently long to secure a sufficient optical path length. The feasibility of the proposed system was verified with a prototype implemented using the commercially available lenslet array, convex lens, and concave lens. An actual system capable of providing 3D images with a see-through property at far distances is expected to be implemented using the customized optical components.

Chapter 4

3D/2D convertible integral imaging systems using half mirror with lens function

4.1 Introduction

One of the important issues in the 3D display technique is that the industry requires a new 3D display device to be compatible with the huge amount of 2D contents accumulated so far; i.e., 3D display device should operate as the 2D display while displaying 2D contents. Because of a lack of 3D contents in the early market of 3D display, 3D/2D convertible feature is essential for the fast penetration of 3D display into the display market. Stereoscopic display, which is now commercially available, is readily 3D/2D convertible for the device itself, though the standards for sharing the compatible contents are still in progress. However the autostereoscopic display demands special techniques to be implemented to provide 3D/2D convertible feature because a some kind of optical component is usually attached in front of the display panel.

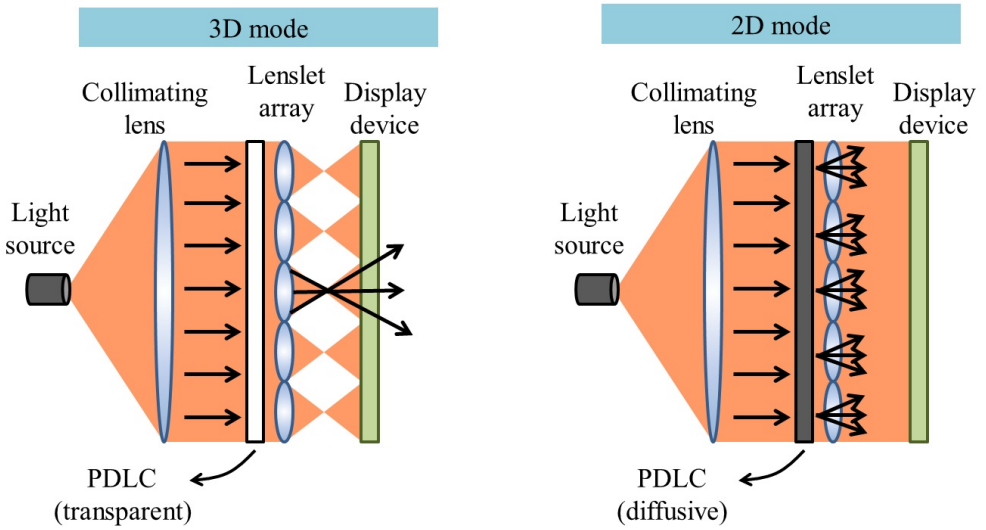

Figure 4.1 3D/2D convertible InIm scheme using PDLC and the collimated light source.

The 3D/2D convertible feature for the autostereoscopic displays which provide only the horizontal parallax, such as the parallax barrier and the lenticular lens, already had been investigated in various ways. Actually, the parallax barrier can easily utilize the 3D/2D convertible feature by implementing barriers using active mask such as LC panels. Providing 3D/2D convertible feature for lenticular lens display is relatively much difficult because the switching between different refractive optical functions - transparent plate and lens - should be implemented. Though various types of LC lens has been developed to support the electronic switching between lens and transparent plate [55–58], the investigations are still in progress to resolve practical issues such as long focal length.

3D/2D convertible feature of InIm has been extensively investigated after the research conducted by J.-H. Park *et al.* (to my knowledge, this is the first

work implementing 3D/2D convertible feature in InIm) [59]. The 3D information of integrated image by InIm system in *focused mode* is basically given by the directionality of rays emitted from each pixel of display device (each lenslet is perceived as a pixel in the *focused mode* of InIm scheme) unlike 2D display which emits conceptually ambient light from each pixel; i.e., the InIm of *focused mode* can provide different color information from each pixel when the observer is located at different position. The objective of early works related to the implementation of 3D/2D convertible feature of InIm was to make it possible to alternate the status of backlight of display between the directional light and the ambient light.

Figure 4.1 shows the configuration of InIm system which can provide the 3D/2D convertible feature by the method proposed in Ref. [59]. The source light is provided as a parallel light by the combination of the point light source and the collimating lens. When this parallel light passes through the following lenslet array, each lenslet creates the directional light by focusing the incident parallel light at the focal length. By locating the polymer-dispersed liquid-crystal (PDLC), which can be electronically controlled to be transparent or diffusive, behind the lenslet array, the status of backlight can be alternated. When the PDLC is transparent, the backlight is directional as described. However, when the PDLC becomes diffusive, the parallel light becomes the ambient light before entering to the lenslet array. And, after passing through the lenslet array, the ambient light source again becomes an ambient backlight. By electronically changing the status of PDLC, the backlight becomes directional or ambient, and the image information on the display device (usually transparent LC) creates 3D or 2D images.

Though the implementation in Fig. 4.1 successfully implements the 3D/2D convertible feature of InIm, the entire system configuration suffers from the

bulky structure which comes from the preparation of the parallel light. Noticing that the directional backlight of Fig. 4.1 is prepared as an array of point light sources, the following researches had focused on creating an array of point light sources maintaining the flat-panel-type configuration.

Figure 4.2 shows the configurations of some representative researches that can provide 3D/2D convertible feature of InIm in flat-panel-type implementation. Especially, the methods presented in Fig. 4.2(a) and (b) are practically useful because they are based on the commercially available flat-panel display devices, LCD and OLED.

Recently, the scheme of Fig. 4.2(a) had been developed to more effective form with the aid of the light field representation which has been richly investigated in the computer science society. Instead of using the fixed pinhole array pattern for the frontal layer, the researchers developed the algorithm to find the optimal combination of images to be displayed on the frontal and back display layer [64]. It is surprising that such optimization technique has been developed just a few years ago in spite of long history of parallax barrier or pinhole array type 3D display. The researchers argued that their method shows effectiveness in the brightness of the displayed 3D image because the optimally designed front layer does not unnecessarily cut the illumination from the back layer. And, based on the similar idea, they also proposed the method to optimize the multiple layers of display to reproduce proper light field [65]. Though the topic has been extensively investigated recently, there still remain issues to be resolved.

In this chapter, some applications of HMLF for resolving the issues related to the 3D/2D convertible InIm system are presented. One of them is implementation of the 3D/2D convertible projection-type InIm. In spite of the importance of the projection-type implementation, there was no method so far to realize

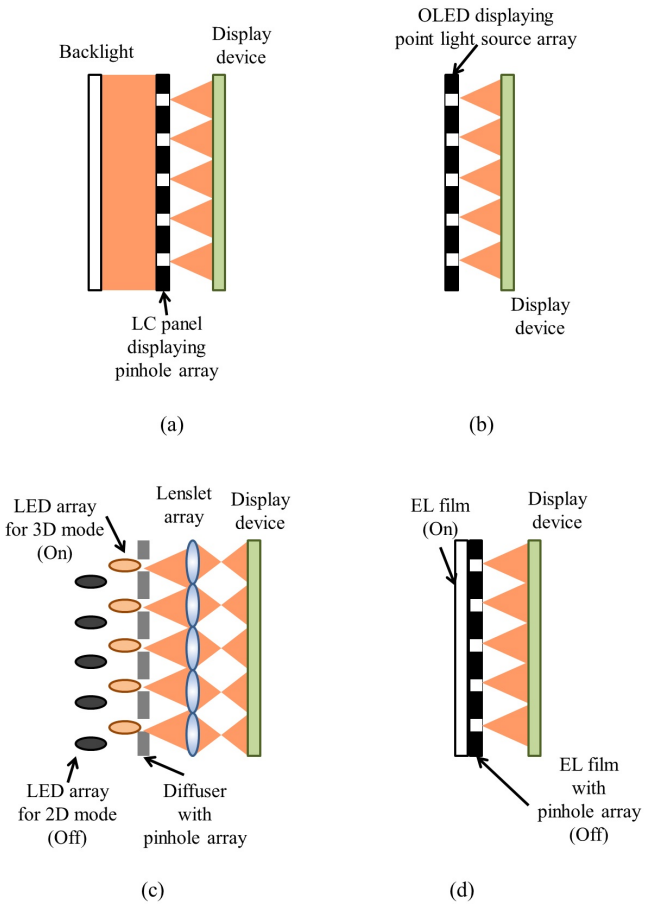

Figure 4.2 3D/2D convertible InIm schemes utilizing an array of point light sources. All figures depict the 3D mode state of their corresponding schemes. (a) Scheme using LC panel. For 2D mode, LC panel displaying pinhole array changes to be transparent (by displaying white image) [60]. (b) Scheme using organic light emitting diode (OLED). For 2D mode, OLED displays white image [61]. (c) Scheme using light emitting diode (LED) array. For 2D mode, LED array for 2D mode becomes "on" instead of LED array for 3D mode [62]. (d) Scheme using electroluminescent (EL) film. For 2D mode, EL film with pinhole array becomes "on." [63]

the 3D/2D convertible feature to the projection-type InIm. Because the theater, which will be the most appropriate application of projection-type InIm, occupies the considerably large space, the 3D/2D convertible feature would be especially important feature for the projection-type InIm. In Sec. 4.2, the scheme to provide 3D/2D convertible feature to projection-type InIm using the HMLF array is discussed.

The other issue is that the most of the developed 3D/2D convertible InIm schemes only support the *focused mode* of InIm which gives priority to the longitudinal expressible range of 3D image. However, sometimes the *real/virtual mode* of InIm is required when the resolution of displayed 3D image is considered to be more important. Hence, the 3D/2D convertible feature that supports the *real/virtual mode* of InIm is necessary for the wide adoption of InIm in commercial market. In Sec. 4.3, the 3D/2D convertible InIm configured in *real/virtual mode* is implemented using the HMLF array. Two proposed schemes adopting the HMLF array demonstrate that the HMLF is an useful optical component that can be adopted to various applications.

4.2 3D/2D convertible projection-type integral imaging

4.2.1 Introduction

Now the 3D theaters where we can see the stereoscopic 3D movie wearing special glasses are easily available everywhere. However, it is still far from widespread of 3D theaters based on autostereoscopy because of largely 3 unresolved issues. One is that it is difficult to provide 3D movies of the similar visual quality to a large number of the audiences because it will require outrageous resolution of display device. The other one is that the frontal projection, where the projection occurs from the backside of audience, is preferred to reduce the room space. Considering this issue, the projection-type InIm is usually implemented as a reflection-type using an array of concave mirror. Recently, the frontal projection-type implementation of multiview display based on the parallax barrier or pinhole array also has been demonstrated using the combination of polarizer and quarter-wave retarding film [66].

Another issue is that the screen should be capable of displaying 3D and 2D images simultaneously in one scene to provide 2D image without any loss of visual quality. By doing so, 3D/2D convertible feature is readily available. However, most of 3D/2D convertible methods developed for various multi-view display are not acceptable for the projection-type implementation because they are usually rely on the active devices with size comparable to the screen. To prepare the active device of such large size is economically inefficient and often impossible. Hence, the scheme to provide 3D/2D convertible feature using the passive optical element is indispensable for the application of projection-type

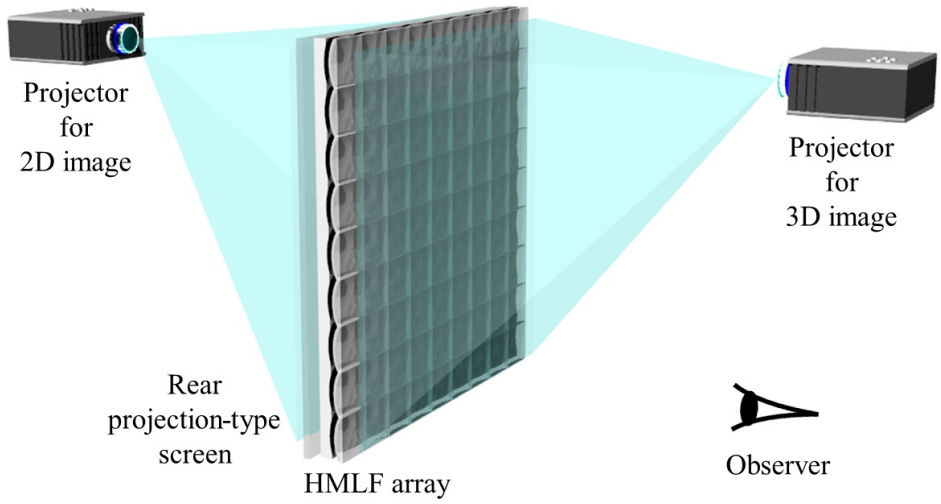

Figure 4.3 System configuration of the proposed method.

implementation.

In this section, the scheme to provide 3D/2D convertible feature to projection-type InIm is developed using the passive optical element based on the HMLF array.

4.2.2 Principle of the proposed scheme

To achieve 3D/2D convertible feature in the projection-type InIm, the novel optical structure HMLF array is used for the implementation. Figure 4.3 shows the system configuration that achieves the 3D/2D convertible feature for the projection-type InIm by adopting HMLF array described in previous chapter. For the proposed system, two projectors are used – one is for the 3D integrated

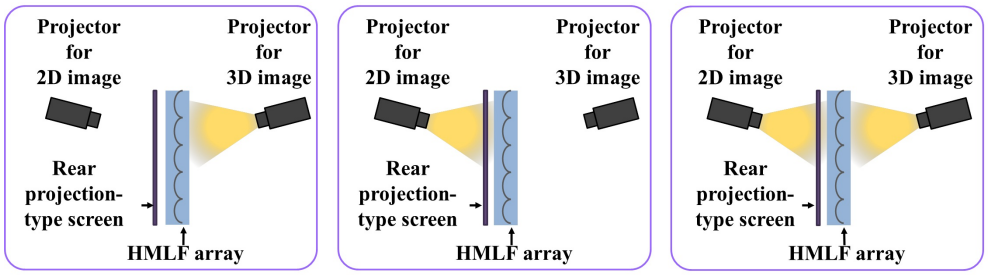

Figure 4.4 Operation of the proposed system. (a) 3D mode. (b) 2D mode. (c) 3D on 2D mode.

image and the other is for the 2D image. In the proposed system, HMLF array acts as the screen that shows the 3D integrated image.

As shown in Fig. 4.3, HMLF array is located in front of the observer and the projector for 3D integrated image projects image from the direction of observer. As mentioned in previous chapter, both concave and convex mirror arrays can be used for the projection-type InIm, so there is no preference in determining which side of HMLF array will be the frontal side. In Fig. 4.3, the concave mirror side was determined as the frontal side as an example. The rear projection-type screen is located behind HMLF array for the display of 2D image. Then the projector for 2D image is located behind the screen to project 2D image from the back side.

Figure 4.4 describes the operation of the proposed system depicted in Fig. 4.3. To show the 3D integrated image to the observer, only the projector for 3D image is activated as shown in Fig. 4.4(a). Then the projected image is separated by HMLF array into reflected and transmitted light components as discussed before, and the reflected part is shown to the observer. Because the reflected part is modulated by the concave mirror array structure, the 3D integrated

image is shown to the observer if the proper elemental image is projected. In generating the proper elemental image, the refraction on the surface of HMLF array should be considered. The refraction affects the optical path of both the projection and integration. Hence the compensation of such refraction should be incorporated in the elemental image, and it can be easily done by using simple geometrical optics.

Part of the transmitted term can be backscattered on the rear projection-type screen. Such backscattering can cause the emergence of halo or decrease the contrast of 3D image. The way to avoid such effect is to reduce the luminance of the backscattered light. The luminance of backscattering is reduced by the ratio of $t^2\epsilon$, where t is the transmittance of HMLF array and ϵ is the scattering efficiency of the rear projection-type screen. Therefore, if t or ϵ is lowered, the backscattering can be reduced. The holographic diffuser with transmittance over 90% is now available from several companies. When such diffuser is used for the rear projection-type screen, the backscattering effect can be sufficiently eliminated with low ϵ.

The mode change can be easily done by alternating activated projectors. By activating the projector for 2D image with the projector for 3D image inactivated, 2D image projected on the rear projection-type screen will be shown to the observer as the transmitted light as shown in Fig. 4.4(b). Moreover, if we activate both projectors, it is possible to display 3D integrated image and 2D image in one scene together as shown in Fig. 4.4(c). This will be called '3D on 2D mode.'

4.2.3 Experimental results

For the verification of the proposed method, a prototype of HMLF array was fabricated for the several preliminary experiments by the soft lithography

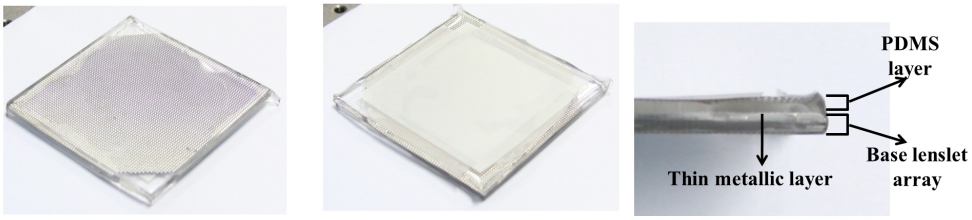

(a) (b) (c)

Figure 4.5 Camera captured image of the prototype. (a) Frontal side of the prototype. The concave mirror side is used as the frontal side for this prototype. (b) Rear side of the prototype. On the rear side, the rear projection-type screen is attached. (c) Cross sectional view of the prototype. Three layers – the base, metallic and cover layers - can be investigated.

method using PDMS as an elastomeric material. Figure 4.5 shows the camera captured image of the fabricated prototype. We can see that the external shape of the prototype is the plate. In this prototype, the concave mirror side was determined as the frontal surface. On the backside of the prototype, the rear-projection-type screen was attached for the display of the 2D image in 2D mode.

For the cover layer, Sylgard 184 base and curing agents was used in the soft lithography process. Then they were mixed by the ratio of 10:1 for 10 minutes. As shown in Table 1, the 2D lenslet array used as the base layer was made of polymethyl methacrylate (PMMA) whose refractive index is about 1.49. But the cover layer is made of PDMS and its refractive index is about 1.43. Because of such slight mismatch in refractive index, the prototype HMLF array is not a perfectly transparent plate for the transmitted light.

If the lenslet array made of PDMS is used as the base layer, the problem of index mismatching would be resolved. But the PDMS lenslet array cannot be

Table 4.1 Specifications of the implemented prototype system.

	Two-dimensional lenslet array	
Base lenslet array	Lenslet pitch	1 mm
	Focal length	3.3 mm
	Refractive index	1.4917 (PMMA)
	Total size	50 mm × 50 mm
Metallic layer	Material	Al
	Thickness	150 nm
Cover layer	Refractive index	1.43 (PDMS)
	Thickness	2 mm

used because of the thermal evaporation which is the first step of the process. To obtain the high surface uniformity of the mirror layer, the hardness of the base layer should be more than certain level. The base layer made of PMMA guarantees the uniform mirror surface, while the metallic layer evaporated on PDMS does not show the mirror characteristic because PDMS is damaged during thermal evaporation.

Though the lens effect is not perfectly canceled because of the slight mismatch in refractive index, the proposed fabrication is still valid for the purpose of implementing proposed scheme. The effective focal length of the prototype is sufficiently larger than the focal length of the base lenslet array, so the quality of 2D image is significantly enhanced by the existence of the cover layer. The effective focal length of each lenslet can be estimated as 26.95 mm by using the formula $f = R/\Delta n$ where R is the radius of curvature of the lenslet and Δn is the difference of the refractive index across the lenslet surface.

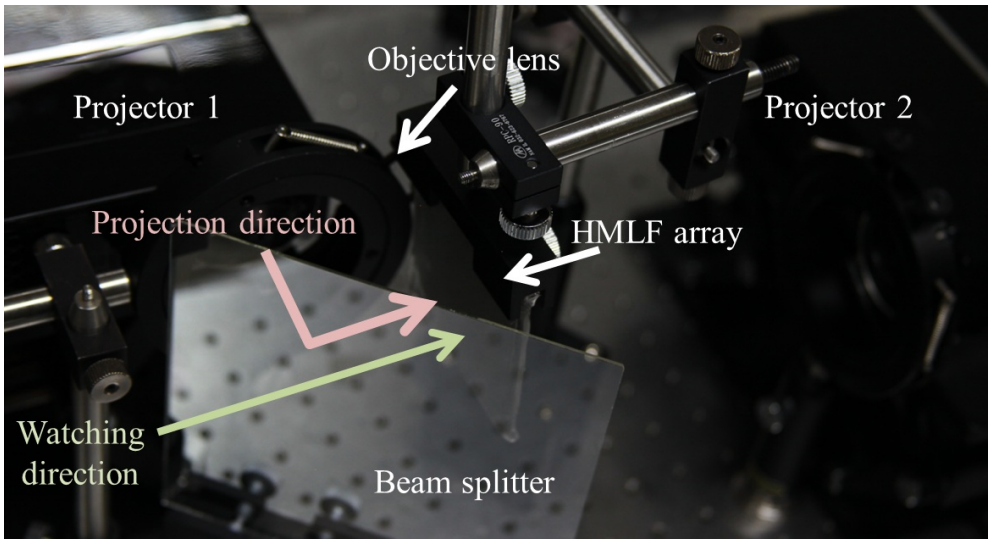

Figure 4.6 System configuration of the experimental setup.

For the thin metallic layer, aluminum was evaporated with thickness about 150 nm. We can estimate the transmittance of the mirror array as 30% approximately [33]. Then the reflectance of the prototype is about 70%. As a result, the luminance of the 2D image will be reduced to 30% as it is shown by the transmission.

Figure 4.6 shows the configuration of the experimental setup to implement the system described in the previous subsection. The configuration comprises two projectors, an objective lens, a beam splitter and a HMLF array prototype. HS102 of LG Electronics, whose resolution is 800 $\times$ 600, was used for the both projectors. The elemental image is projected onto the concave mirror-side of HMLF array by the projector 1. To enhance the performance of the integration, the pixel pitch of the projected elemental image should be much smaller than the pitch of one concave mirror of HMLF array.

Because the commercial projector used in the experiment is not designed

for the intention of InIm, it is needed to reduce the size of the projected image by using the objective lens as shown in Fig. 4.6. As a result, the pixel pitch of the projected elemental image was reduced to 88 μm. As the side effect of using the objective lens, the operating distance where the projected image is well focused was shortened to 60 mm.

To secure the enough watching distance, the beam splitter was located crossing the optical path of the projection to separate the watching direction from the projecting direction. In Fig. 4.6, the optical paths of the projection and watching in 3D mode are depicted. The projector 2 used for 2D mode is located behind the HMLF array and the pixel pitch of the projected image is 133 μm.

A preliminary experiment was performed to verify the proposed method as shown in Fig. 4.7. In the 3D mode, two letters 'S' and 'U' are located at 7 mm front of and 7 mm behind of the HMLF array. 'N' is located on the surface of HMLF array. The elemental image was generated to display these integrated images by the computer aided calculation. Therefore the real image 'S', the surface image 'N' and the virtual image 'U' can be easily displayed together. In Fig. 4.7, the horizontal and vertical parallaxes are well expressed in the 3D image displayed by reflection-type InIm.

Though the ordinary diffuser was used for the rear projection-type screen, the backscattering effect discussed in the previous subsection is hardly noticed as image. In the experiment, t is about 0.3 and ϵ of the ordinary diffuser is generally under 0.5. Hence the luminance of backscattering is reduced below 5% of the projected image. It means that this level of reduction is enough to avoid backscattering effect in the experimental setup. Additionally, the fact that the projected image is focused near the surface of the concave mirror layer was also helpful in reducing backscattering effect.

As described in the previous subsection, the proposed system is also able

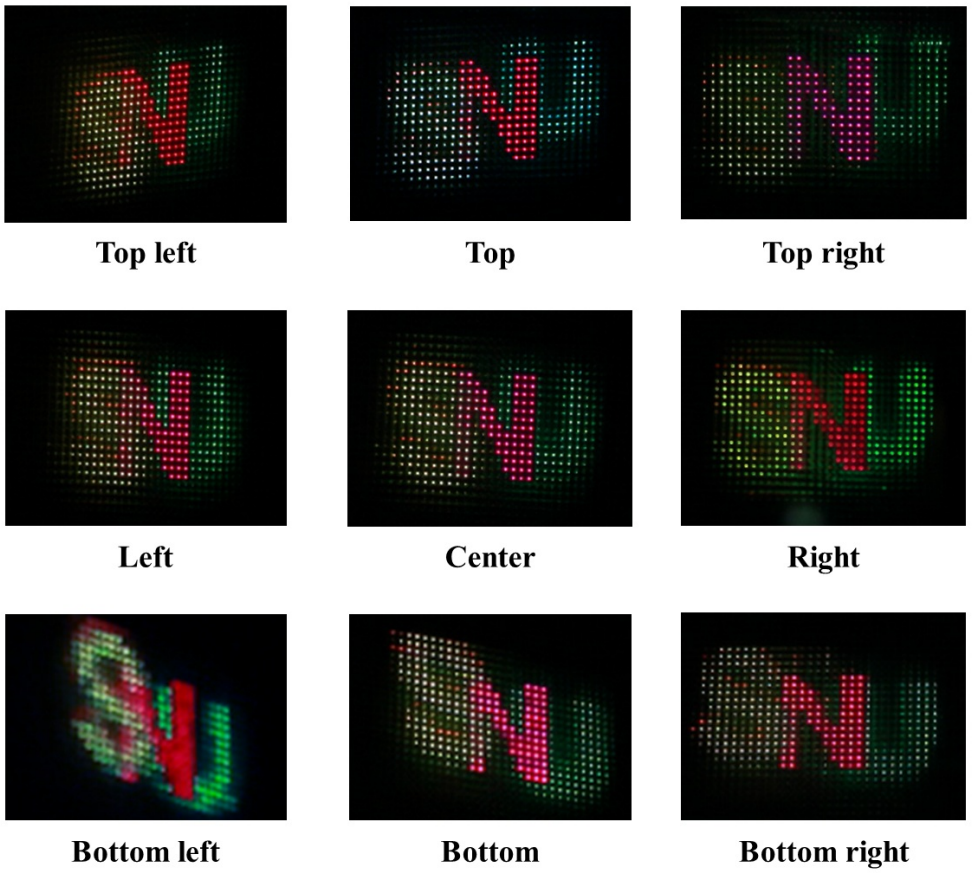

Figure 4.7 Camera captured images of the integrated images displayed by the 3D mode of our proposed system.

to display 3D integrated image and 2D image in one scene together. The experimental results shown in Fig. 4.8 illustrate this functionality. 3D integrated images were the same as the experiment in Fig. 4.7. For the 2D image, the image indicated as 'Image used for 2D image' was displayed in Fig. 4.8. The 2D image is displayed with the pixel pitch of 133 μm as described before, and there is no noticeable artifacts caused by index mismatch of the HMLF array prototype as discussed. However the luminance of the 2D image is reduced to 30% of the original image by the transmittance of the metallic layer. As we can see from Fig. 4.8, 3D integrated image and 2D image were successfully displayed in one scene. The luminance of the 2D image varies as the watching direction changes because the rear projection-type screen used in the experiment has directionally non-uniform diffusing characteristic.

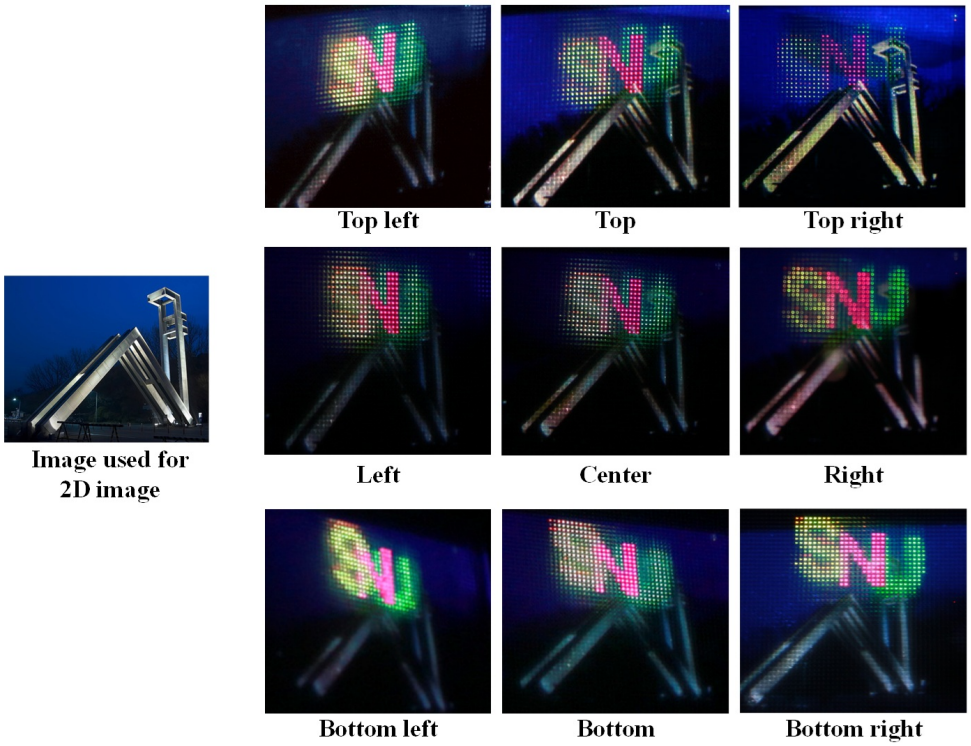

Figure 4.8 Camera captured image of the displayed images in '3D on 2D mode' of the prototype. Original image used for 2D image is shown in the left side of the figure; the main gate of Seoul National University.

4.3 3D/2D convertible integral imaging using dual depth configuration

4.3.1 Introduction

Recently, a number of investigations have been conducted to make InIm providing a 3D/2D convertible feature to meet a demand from commercial market as introduced in Sec. 4.1. Most of them implement 3D/2D convertible feature by generating an array of point light sources with active devices [50]. However the implementation of an InIm system based on an array of point light sources cannot retrieve full functionality of the InIm scheme. As discussed, InIm has two options, *real/virtual mode* and *focused mode* in displaying a 3D image. And which display mode will be enabled should be determined considering a usage scenario. Although a 3D/2D convertible InIm scheme that can utilize the *real/virtual mode* is also necessary, when implementing a 3D/2D convertible feature with an array of point light sources, only the *focused mode* can be utilized. To date, only one method has been reported to implement a 3D/2D convertible InIm that can operate as a *real/virtual mode* [70].

Figure 4.9 shows the system configuration that can provide a 3D/2D convertible feature in the *real/virtual mode* InIm developed by H. Choi *et al.* [70]. In this scheme, two LC panels, which can act as active masks, are adopted in front and behind of the lenslet array where each lenslet has pitch adequate for the *real/virtual mode*. The 3D/2D conversion is easily implementable by operating one of LC panel to be active and the other to be transparent. In 3D mode, the LC panel behind the lenslet array becomes active and the LC panel in front of the lenslet array becomes transparent. Illuminated by the backlight,

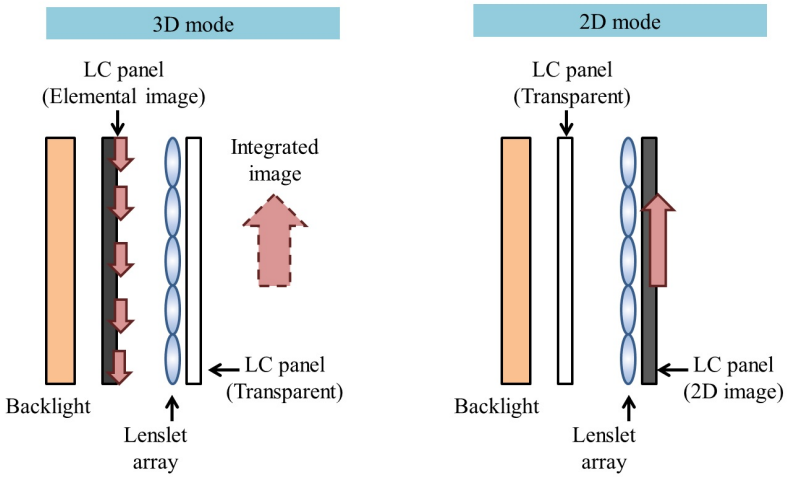

Figure 4.9 3D/2D convertible scheme for *real/virtual mode* InIm using two LC panels.

the activated LC panel can display the elemental image and it is integrated by the lenslet array to provide 3D image. Because the LC panel in front of the lenslet array is set to be transparent, the displayed 3D image is delivered to the observer as it is.

On the other hand, the LC panel in front of the lenslet array becomes active in 2D mode. The illumination from the backlight is altered by the lenslet array however the ambient light becomes the ambient light again after passing through the lenslet array. The light reaching at the LC panel in front of the lenslet array can be considered as a normal illumination from backlight in the conventional 2D displays. Hence, by displaying intended 2D image on the LC panel in front of the lenslet array, the configuration perfectly acts as a 2D display device. Though the scheme described in Fig. 4.9 successfully implements the 3D/2D convertible feature for the *real/virtual mode* configuration of InIm,

further study on finding another way to resolve this issue is still needed.

In this section, a novel scheme that can realize a 2D/3D convertible InIm system utilizing a *real/virtual mode* is proposed based on a dual depth configuration. The feasibility of the proposed scheme is verified by experimental results obtained from an implemented prototype. For the implementation of the prototype, the fluid filling method has been used for fabricating a HMLF array. The proposed system implements an InIm scheme with a 2D array of concave mirrors instead of convex lenses. In general, the focal length of a concave mirror is shorter than that of the convex lens if the radius of curvature is the same. It will be discussed that such a short focal length can provide advantageous features for integrated images.

4.3.2 Principle of the proposed scheme

Figure 4.10 shows the configuration of the proposed 2D/3D convertible InIm system using a combination of dual depth configuration and HMLF array. HMLF array is an optical component which is a transparent plate to transmitted rays, whereas the optical paths of reflected rays are modulated by the embedded half mirror structure, i.e., a 2D array of concave mirrors [41]. Because a concave mirror is a direct alternative to a convex lens, if a properly generated elemental image is provided, the reflected image can be used to generate 3D images based on the InIm scheme [16, 35]. A transmitted light can provide a clear 2D image, which is not altered by the embedded half mirror structure of HMLF array. However, HMLF array cannot provide a 2D/3D convertible feature solely as the reflected and transmitted rays come out together. By adopting a dual depth configuration, HMLF array can provide a 2D/3D convertible feature without such a problem.

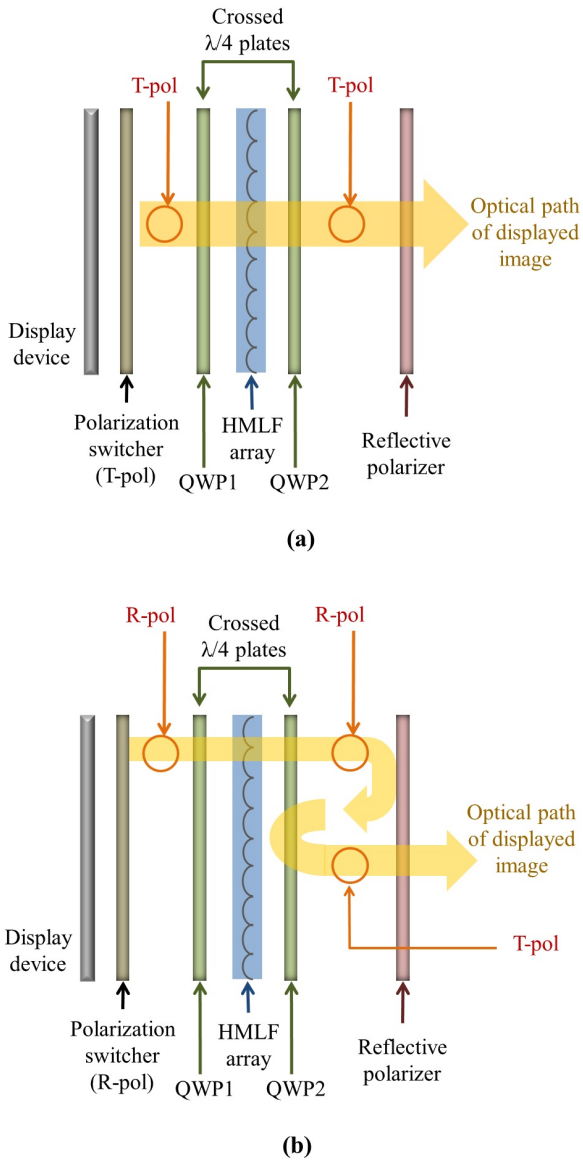

Figure 4.10 System configuration of the proposed scheme. (a) 2D mode and (b) 3D mode.

A dual depth configuration is a display scheme that changes the optical path length from observer to display by a polarization-based multiplexing method [71]. It can be applied to HMLF array to separate reflected and transmitted terms and selectively show one of them to an observer. As shown in Fig. 4.10, HMLF array replaces a half mirror of the conventional dual depth configuration. A polarization state of the polarization shutter in Fig. 4.10 determines whether the final image shown to the observer will be a 2D or 3D image by changing the optical path of the displayed image. The optical path of each mode is described in Fig. 4.10.

In 2D mode, the polarization state of the polarization shutter is the same as the transmission polarization of the reflective polarizer, and this polarization will be named T-pol. After passing through two crossed $\lambda/4$ plates, QWP1 and QWP2, the polarization state of the 2D image is maintained as T-pol. Hence, in 2D mode of the proposed system, a 2D image is directly delivered to an observer through the reflective polarizer.

In 3D mode, the polarization state of the polarization shutter is the same as the reflection polarization of the reflective polarizer, which will be named R-pol. In this case, as the polarization state of the displayed image is R-pol after passing through QWP1 and QWP2, it is reflected back by a reflective polarizer. The reflected image reaches the HMLF array again passing through QWP2. Among the reflection and transmission of HMLF array, reflection has a valid direction for delivering an image to an observer. By reflection of HMLF array, the displayed image is integrated by a 2D array of a concave mirror structure following the InIm principle. During this round-trip between the reflective polarizer and HMLF array, the displayed image meets QWP2, HMLF array, and QWP2 in sequence. As a result of the round-trip, the polarization state of the displayed image is changed to T-pol. Hence, the displayed image is transmitted

through the reflective polarizer and the 3D integrated image is delivered to the observer.

Besides achieving a 2D/3D convertible feature, the proposed system can also take advantage of using a concave mirror instead of a convex lens to implement the InIm scheme. Under the same radius of curvature, a concave mirror has shorter focal length than a convex lens. If the focal length of the convex lens is f_0, the focal length of the concave mirror of the same shape is approximately

$$f = \frac{n-1}{2} f_0 = \frac{f_0}{s}, \tag{4.1}$$

where n is the refractive index of the reference convex lens and s is a scaling factor. The refractive index of a convex lens is usually around 1.5; hence, the focal length can be reduced to nearly a quarter with the concave mirror. A shorter focal length brings a wider viewing angle of an integrated 3D image. The viewing angle θ of the InIm system implemented by a concave mirror is

$$\theta = 2\tan^{-1}\left[\frac{\phi}{2}\left(\frac{s}{f_0} - \frac{1}{l}\right)\right], \tag{4.2}$$

where ϕ is the pitch of the convex lens or concave mirror and l is the distance from the convex lens or concave mirror array to the central depth plane where image planes of the convex lenses or concave mirrors are superposed. Hence, the viewing angle becomes wider as s increases.

Another advantage of adopting a concave mirror is that its short focal length can also be helpful in overcoming a severe limitation in depth expression of the InIm system utilizing a real/virtual display mode. To enhance the expressible depth range of the InIm system with a real/virtual display mode, a number of methods have been developed to make multiple central depth planes by changing the gap between the lens array and the display panel mechanically or electronically [50, 72]. However, as the varied gap distance becomes larger,

it becomes problematic because it can induce a vibration or time delay in mechanical implementation. It also gives a limitation in designing a system for electronic implementation, as various system parameters are closely related to the gap value.

A shorter focal length enables the generation of multiple central depth planes at the same locations with a smaller change in the gap value. A change in the gap affects the change in the location of the central depth plane by the relationship

$$\Delta l \simeq \left|\frac{\partial l}{\partial g}\right| \Delta g = \left(\frac{sl}{f_0} - 1\right)^2 \Delta g. \tag{4.3}$$

Hence, a change in the gap can move the location of the central depth plane more with s larger than one. Moreover, the proposed system configuration enforces rays to have round-trips between HMLF array and the reflective polarizer when the 3D mode is enabled. By changing the distance between HMLF array and the reflective polarizer, the varied distance of the effective gap value is amplified to be three times larger. As a result, the required distance in moving some part of the system is reduced by a ratio of

$$\frac{(1 - f_0/l)^2}{3(s - f_0/l)^2}. \tag{4.4}$$

4.3.3 Experimental results

A prototype system was implemented to verify the feasibility of the proposed scheme. In constructing the HMLF array structure, the fluid filling method was used for the fabrication. And the transreflective layer was formed by the thin metallic layer. Aluminum was deposited by thermal evaporation and the thickness was determined to make the reflectance 50% for the highest brightness in the 3D mode. With this value of reflectance, the brightness of the 2D mode is ideally two times larger than that of the 3D mode considering the leakage

Table 4.2 Specifications of the implemented prototype system.

Display device	Resolution	800×600
	Pixel pitch	$200\ \mu\text{m} \times 200\ \mu\text{m}$
Reference lens array	Lens pitch	5.4 mm (H) $\times$ 7 mm (V)
	Focal length	41.9 mm
	Material	Glass

caused by HMLF array. Hence, the brightness of the image on the display panel should be adjusted to balance the brightness of the image between the 2D and 3D modes. Moreover a leakage occurred by HMLF array incurs a reduction in contrast ratio and it is required to use a brighter light source to enhance the contrast ratio. A commercial twisted nematic (TN) LC panel was adopted for the polarization switcher. The type of LC panel should be carefully determined because it can affect the performance of polarization switching. For the usage as a polarization switcher, polarizers attached to the LC panel were removed. Detailed system specifications of the implemented prototype are listed in Table 4.2.

Figure 4.11 shows the camera-captured images of experimental results for the verification of the 2D/3D convertible feature of the proposed system. As the polarization switcher was implemented using an LC panel in the prototype system, the polarization state of the switcher is addressable pixel by pixel. Hence, it is possible to display 2D and 3D images in one scene simultaneously, as shown in Fig. 4.11(a). A conversion to 2D mode can be done by simply changing the polarization state of the polarization switcher to T-pol. The InIm principle does not work in the 2D mode of the proposed system; hence, the elemental image used to show an integrated image in 3D mode is explicitly

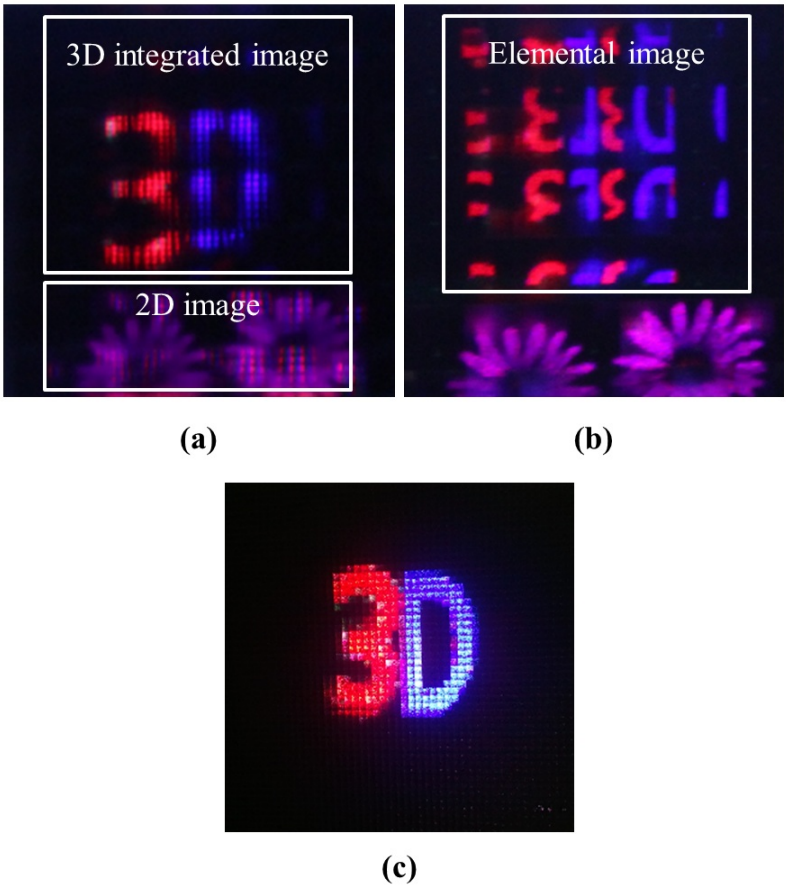

Figure 4.11 Images displayed by prototype system operating on (a) 3D and 2D display mode and (b) 2D display mode. (c) 3D image displayed by a focused mode for the comparison of image resolution. Lens pitch of the lens array was determined to be 1 mm to guarantee enough viewing angle and depth expression.

shown in Fig. 4.11(b).

In the real implementation, the characteristics of LC panel and reflective polarizer are not ideal. Hence the ghost images can appear as observed in Fig. 4.11. The performance of each component in the implemented system should be improved to reduce such artifacts. Figure 4.11(c) shows the 3D image reconstructed by the focal mode of the InIm scheme. As shown in Fig. 4.11, image resolution is much higher in *real/virtual mode*.

Figure 4.12 shows the experimental result, comparing the viewing angle between the conventional and proposed InIm systems. The central depth plane of the prototype system was located 31 mm in front of the system. Referring to Table 4.2, the theoretical viewing angle of the prototype system is around 19.5°. As shown in Fig. 4.12(a), an integrated image is well displayed inside the viewing angle nearly up to the theoretical value. In this large viewing angle, lens grid of the lens array becomes noticeable as vertical dark lines. However, a conventional InIm system, which is implemented using a 2D convex lens array that has the same radius of curvature as the concave mirror used for the prototype of the proposed scheme, cannot support such a viewing angle, as shown in Fig. 4.12(b). Though a viewing angle can be enhanced by reducing the f number of lens array, it is difficult to make a diffraction-limited (or aberration-free) structure compared with concave mirror [16].

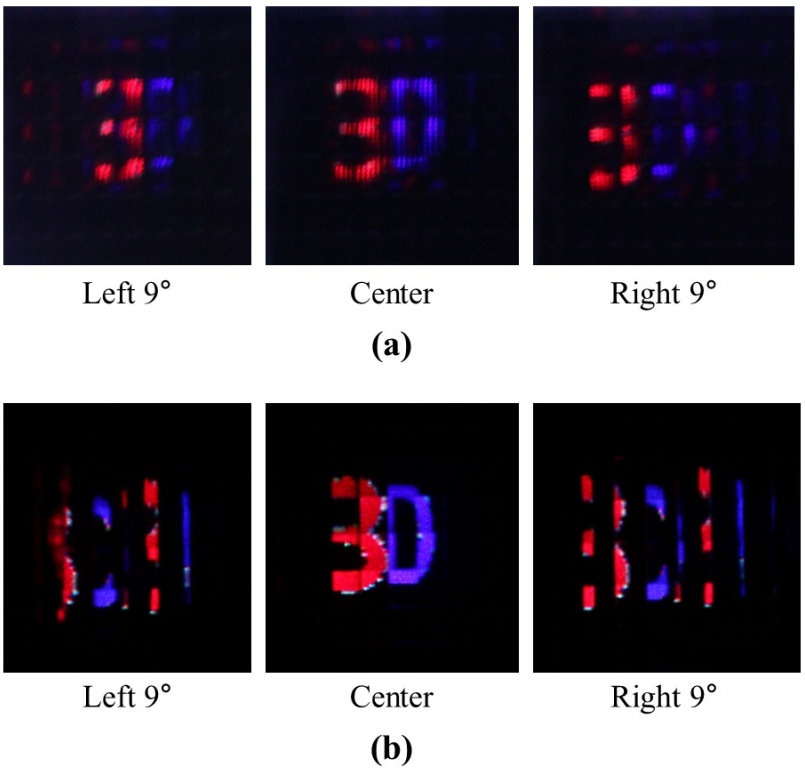

Figure 4.12 Comparison of a viewing angle between systems implemented by proposed and conventional schemes. For both cases, '3' is located 5 mm in front of the central depth plane and 'D' is located 5 mm behind the central depth plane. Integrated image displayed by the (a) proposed scheme and (b) conventional scheme. A flipping problem is apparent in the integrated image displayed by the conventional scheme.

4.4 Summary and conclusion

In this chapter, it was verified that the HMLF is also useful for resolving existing problems as well as inspiring new ideas by applying the HMLF to implementing 3D/2D convertible feature which is a long known issue of InIm. It was presented that 3D/2D convertible feature for the projection-type InIm and *real/virtual mode* InIm could be implemented by adopting the HMLF array. Especially, the 3D/2D convertible feature for the projection-type InIm has remained as an unresolved issue before this study is conducted.

In Sec. 4.2, the novel method to provide 3D/2D convertible feature to the projection-type InIm has been proposed. To my knowledge, this is the first proposal that makes it possible for the projection-type InIm to provide 3D/2D convertible feature with the passive optical components. In fact, it is also the first proposal for the autostereoscopic 3D display implemented as projection-type to have 3D/2D convertible feature.

As discussed, the prototype has the slight mismatch in the refractive index between the base and cover layers, but it is enough for our application as verified before. Moreover the soft lithography process has advantage in that it is facile and inexpensive. Hence our fabrication method will be acceptable in most cases.

This study will be useful for the 3D industry because the 3D theaters will require autostereoscopic display as the next step. The advantage of adopting the proposed system is not only the saving in space of the theater. It will give a higher degree of freedom to 3D movie makers in doing their work because it is easy to mix up 3D images and 2D images with the proposed system. The proposed method will contribute to the widespread of autostereoscopic 3D display in 3D theaters.

In Sec. 4.3, a new method to implement a 2D/3D convertible InIm sys-

tem operating as a *real/virtual display mode* has been provided. The proposed method can be used for an application where the resolution of the reconstructed 3D image is highly important. As discussed, the proposed scheme shows a wide viewing angle characteristic. However, the viewing angle is in a tradeoff relationship with the depth expression of the integrated image [39], and it means that the proposed scheme is disadvantageous in the depth expression. Compared with the scheme in ref. [70], which is based on a convex lens, the proposed scheme here is expected to be used for cases where a wide viewing angle is required.

Chapter 5

Conclusion

We all know what the ultimate 3D display should look like, however we all do not know how to realize it. We have just faced to see the opening of 3D industry based on the stereoscopy which is the oldest technique in the history of development of 3D display. Despite of tens of years of researches, we are still far from the satisfactory solution to the goal because of large gap between the present status of related technologies and the required level. This dissertation has shown that the introduction of new optical element can be helpful for making a breakthrough by presenting a new optical component, HMLF, and implementing 3D display systems based on it.

Investigation on AR displays had shown different aspect in approaching to the development of 3D display though the final goal is eventually the same. By adopting the HMLF, new 3D display systems, that consider the requirements induced from AR display, could be established. In Sec. 3.2, the see-through and bidirectional 3D display system, which nearly satisfies the requirements, has been demonstrated. Recalling the requirements of interpreted version in the

viewpoint of 3D display, it satisfies:

(1) Free space imaging without any noticeable frame; (2) Supporting interaction with 3D image; (3) Autostereoscopic 3D image.

However, it only partially satisfies the condition:

(4) Volumetric 360-degree viewable 3D image of high visual quality. It cannot fully cover 360 degrees and the visual quality is significantly lower than the acceptable quality. However, it is meaningful that the proposed display system can provide 3D image around the system without any mechanical motion. For the development of the method to increase the coverage to 360 degrees without any mechanical motion, further study is required. The limitation to the visual quality requires development of the projector and it can be relieved by multiplexing techniques.

HMD is still popular in the field of AR, though it is very old-fashioned technique, because it is the easiest way to implement AR functionality. The adoption of the HMLF has provided the way to realize HMD displaying 3D image in the strict sense. The HMD system developed in Sec. 3.3 is capable of displaying 3D display which addresses a correct accommodation cue. Hence, the accommodation-vergence mismatch, which can be a reason of nausea in using HMD system, was resolved by adopting the HMLF.

Along with inspiring the totally new types of display devices, it was also shown that the adoption of new optical element can be helpful in resolving the existing issues. Chapter 4 has shown the usages of the HMLF array for resolving the famous issues related to 3D/2D conversion. In Sec. 4.2, the 3D/2D convertible feature of InIm has been developed without the large-sized active device by adopting the HMLF array. Hence, the proposed system could firstly provide the 3D/2D convertible feature for the projection-type InIm system. In Sec. 4.3, the 3D/2D convertible feature for *real/virtual mode* InIm, which has

only one related study unlike *focused mode*, was implemented using the HMLF array. Hence, it has been shown that the new optical component can provide a solution to the unresolved issues of 3D display system.

Though this dissertation has only focused on the applications for the 3D display system, it is expected that the HMLF can be adopted for various optical systems. As discussed so far, the HMLF can inspire the new concept of optical system as well as providing new methods to resolve the existing problems. To support various optical applications, the fabrication method of the HMLF should be developed further. Among the proposed fabrication methods, it seems that the fluid filling method is generally the best method because it provides the perfect index matching even for the complicated structure. As investigated, the methods proposed in Sec. 2.2 is generally only acceptable for the imaging purpose especially because of the additional transparent plate structure. For more general usage, the pellicle-type implementation is required, and the fabrication method to realize such structure is remained as a future work.

Bibliography

[1] C. Wheatstone, "Contributions to the physiology of vision. Part the first. On some remarkable, and hitherto unobserved, phenomena of binocular vision," Phil. Trans. R. Soc. Lond. **128**, 371-394 (1838).

[2] B. Lee, "3D Display - Where We Are and Where to Go," in *Biomedical Optics, OSA Technical Digest* (Optical Society of America, 2012), paper JM1A.2.

[3] J. Hong, Y. Kim, H.-J. Choi, J. Hahn, J.-H. Park, H. Kim, S.-W. Min, N. Chen, and B. Lee, "Three-dimensional display technologies of recent interest: principles, status, and issues," Appl. Opt. **50**, H87–H115 (2011).

[4] P. Benzie, J. Watson, P. Surman, I. Rakkolainen, K. Hopf, H. Urey, V. Sainov, and C. von Kopylow, "A survey of 3DTV displays: techniques and technologies," IEEE Trans. Circuits Syst. Video Technol. **17**, 1647-1658 (2007).

[5] F. E. Ives, "Parallax stereogram and process of making same," U.S. Patent 725,567 (14 Apr. 1903).

[6] G. Lippmann, "La photographie integrale," C. R. Acad. Sci. **146**, 446–451 (1908).

[7] W. Hess, U.S. Patent 1,128,979 (16 Feb. 1915).

[8] D. Gabor, "A new microscopic principle," Nature **161**, 777-778 (1948).

[9] J. Upatnieks and E. N. Leith, "Lensless, three-dimensional photography by wavefront reconstruction," J. Opt. Soc. Am. 54A, 579-580 (1964).

[10] Ultimate Holography. http://www.ultimate-holography.com

[11] T. Nagoya, T. Kozakai, T. Suzuki, M. Furuya, and K. Iwase, "The D-ILA device for the world's highest definition (8K4K) projection systems," in *Proceedings of International Display Workshop* (Society for Information Display, 2008), pp. 203–206.

[12] D. Armitage, I. Underwood, and S.-T. Wu, *Introduction to Microdisplays* (Wiley, New York, 2006).

[13] H. Sakai, M. Yamasaki, T. Koike, M. Oikawa, and M. Kobayashi, "Autostereoscopic display based on enhanced integral photography using overlaid multiple projectors," in *SID Sym. Dig.* **40**, 611–614 (2009).

[14] S. Tay, P.-A. Blanche, R. Voorakaranam, A. V. Tunç, W. Lin, S. Rokutanda, T. Gu, D. Flores, P. Wang, G. Li, P. St Hilaire, J. Thomas, R. A. Norwood, M. Yamamoto, and N. Peyghambarian, "An updatable holographic three-dimensional display," Nature **451**, 694-698 (2008).

[15] J. Hong, K. Hong, Y. Kim, and B. Lee, "Analysis of projection-type integral imaging by using convex mirror array," in *SNU-UT Joint Seminar* (2010).

[16] J.-S. Jang and B. Javidi, "Three-dimensional projection integral imaging using micro-convex-mirror arrays," Opt. Express **12**, 1077-1083 (2004).

[17] Cargille Laboratories. http://www.cargille.com/

[18] F. Zhou, H.B.-L. Duh, and M. Billinghurst, "Trends in augmented reality tracking, interaction and display: A review of ten years of ISMAR," in *Proceedings of 7th IEEE/ACM International Symposium* (IEEE, 2008), pp. 193-202.

[19] S. Eitoku, T. Tanikawa, and Y. Suzuki, "Display Composed of Water Drops for Filling Space with Materialized Virtual Three-dimensional Objects," in *IEEE Virtual Reality Conference (VR 2006)* (IEEE, 2006), pp. 159-166.

[20] K. Kiyokawa, M. Billinghurst, B. Campbell, and E. Woods, "Occlusion-capable optical seethrough head mount display for supporting co-located collaboration," in *Proceedings of 2nd IEEE/ACM International Symposium* (IEEE, 2003), pp. 133-141.

[21] D. Cheng, Y. Wang, H. Hua, and M. Talha, "Design of an optical see-through head-mounted display with a low f-number and large field of view using a freeform prism," Appl. Opt. **48**, 2655-2668 (2009).

[22] D. Schmalstieg and D. Wagner, "Experiences with handheld augmented reality," in *Proceedings of 6th IEEE/ACM International Symposium* (IEEE, 2007), pp. 3-18.

[23] D. Wagner and I. Barakonyi, "Augmented reality Kanji learning," in *Proceedings of 2nd IEEE/ACM International Symposium* (IEEE, 2003), pp. 335-336.

[24] O. Bimber, L. M. Encarnação, and D. Schmalstieg, "Augmented reality with back-projection systems using transflective surfaces," in *Proceedings of Eurographics* (2000), pp. 161-168.

[25] Y. Takaki, Y. Urano, S. Kashiwada, H. Ando, and K. Nakamura, "Super multi-view windshield display for long-distance image information presentation," Opt. Express **19**, 704–716 (2011).

[26] A. Jones, I. McDowall, H. Yamada, M. Bolas, and P. Debevec, "Rendering for an interactive 360-degree light field display," ACM Trans. Graph. **26**, Article 40, (2007).

[27] A. Olwal, C. Lindfors, J. Gustafsson, T. Kjellberg, and L. Mattsson, "ASTOR: An auto-stereoscopic optical see-through augmented reality system," in *Proceedings of 4th IEEE/ACM International Symposium* (IEEE, 2005), pp. 24-27.

[28] Y. Kim, J. Kim, K. Hong, H. K. Yang, J.-H. Jung, H. Choi, S.-W. Min, J.-M. Seo, J.-M. Hwang, and B. Lee, "Accommodative response of integral imaging in near distance," J. Disp. Technol. **8**, 70–78 (2012).

[29] J.-H. Park, H. Choi, Y. Kim, J. Kim, and B. Lee, "Scaling of three-dimensional integral imaging," Jpn. J. Appl. Phys. **44**, 216-224 (2005).

[30] J.-H. Jung, K. Hong, G. Park, I. Chung, J.-H. Park, and B. Lee, "Reconstruction of three-dimensional occluded object using optical flow and triangular mesh reconstruction in integral imaging," Opt. Express **18**, 26373-26387 (2010).

[31] S.-W. Min, S. Jung, J.-H. Park, and B. Lee, "Study for wide-viewing integral photography using an aspheric Fresnel-lens array," Opt. Eng. **41**, 2572-2576 (2002).

[32] J. Jang, F. Jin, and B. Javidi, "Three-dimensional integral imaging with large depth of focus by use of real and virtual image fields," Opt. Lett. **28**, 1421-1423 (2003).

[33] Y. Kim, S. Park, S.-W. Min, and B. Lee, "Integral imaging system using a dual-mode technique," Appl. Opt. **48**, H71-76 (2009).

[34] J.-H. Park, S.-W. Min, S. Jung, and B. Lee, "Analysis of viewing parameters for two display methods based on integral photography," Appl. Opt. **40**, 5217–5232 (2001).

[35] Y. Jeong, S. Jung, J.-H. Park, and B. Lee, "Reflection-type integral imaging scheme for displaying three-dimensional images," Opt. Lett. **27**, 704-706 (2002).

[36] S. Park, B. Song, and S. Min, "Analysis of Image Visibility in Projection-type Integral Imaging System without Diffuser," J. Opt. Soc. Korea **14**, 121-126 (2010).

[37] S.-W. Min, J. Hong, and B. Lee, "Analysis of an optical depth converter used in a three-dimensional integral imaging system," Appl. Opt. **43**, 4539-4549 (2004).

[38] F. Okano and J. Arai, "Optical shifter for a three-dimensional image by use of a gradient-index lens array," Appl. Opt. **41**, 4140-4147 (2002).

[39] S.-W. Min, J. Kim, and B. Lee, "New Characteristic Equation of Three-Dimensional Integral Imaging System and its Applications," Jpn. J. Appl. Phys. **44**, L71-L74 (2005).

[40] H. Stolle, J.-C. Olaya, S. Buschbeck, H. Sahm, and A. Schwerdtner, "Technical solutions for a full resolution autostereoscopic 2D/3D display technology," in *Proc. SPIE* **6803**, 1-12 (2008).

[41] J. Hong, Y. Kim, S. Park, J.-H. Hong, S.-W. Min, S.-D. Lee, and B. Lee, "3D/2D convertible projection-type integral imaging using concave half mirror array," Opt. Express **18**, 20628-20637 (2010).

[42] O. Cakmakci and J. Rolland, "Head-worn displays: a review," J. Disp. Technol. **2**, 199–216 (2006).

[43] S. Liu, H. Hua, and D. Cheng, "A novel prototype for an optical see-through head-mounted display with addressable focus cues," IEEE Trans. Vis. Comput. Graph. **16**, 381–393 (2010).

[44] Y. Takaki and N. Nago, "Multi-projection of lenticular displays to construct a 256-view super multi-view display," Opt. Express **18**, 8824–8835 (2010).

[45] S.-W. Min, M. Hahn, J. Kim, and B. Lee, "Three-dimensional electro-floating display system using an integral imaging method," Opt. Express **13**, 4358–4369 (2005).

[46] J. Kim, S.-W. Min, and B. Lee, "Viewing region maximization of an integral floating display through location adjustment of viewing window," Opt. Express **15**, 13023–13034 (2007).

[47] J. Kim, S.-W. Min, Y. Kim, and B. Lee, "Analysis on viewing characteristics of integral floating system," Appl. Opt. **47**, D80–D86 (2008).

[48] J. Kim, S.-W. Min, Y. Kim, and B. Lee, "Floated image mapping for integral floating display," Opt. Express **16**, 8549–8556 (2008).

[49] J. Kim, G. Park, Y. Kim, S.-W. Min, and B. Lee, "Elimination of image discontinuity in integral floating display by using adaptive image mapping," Appl. Opt. **48**, H176-H185 (2009).

[50] J.-H. Park, K. Hong, and B. Lee, "Recent progress in three-dimensional information processing based on integral imaging," Appl. Opt. **48**, H77-H94 (2009).

[51] G. Park, J.-H. Jung, K. Hong, Y. Kim, Y.-H. Kim, S.-W. Min, and B. Lee, "Multi-viewer tracking integral imaging system and its viewing zone analysis," Opt. Express **17**, 17895–17908 (2009).

[52] F. Jin, J. Jang, and B. Javidi, "Effects of device resolution on three-dimensional integral imaging," Opt. Lett. **29**, 1345–1347 (2004).

[53] F. W. Campbell and D. G. Green, "Optical and retinal factors affecting visual resolution," J. Physiol. **181**, 576–593 (1965).

[54] K. Hong, J. Hong, J.-H. Jung, J.-H. Park, and B. Lee, "Rectification of elemental image set and extraction of lens lattice by projective image transformation in integral imaging," Opt. Express **18**, 12002–12016 (2010).

[55] S. T. deZwart, W. L. IJzerman, T. Dekker, and W. A. M. Wolter, "A 20" switchable auto-stereoscopic 2D/3D display," in *Proceedings of In-*

ternational Display Workshop (Society for Information Display, 2004), pp. 1459-1460.

[56] J. Harrold, D. J. Wilkes, and G. J. Woodgate, "Switchable 2D/3D display - solid phase liquid crystal microlens array," in *Proceedings of International Display Workshop* (Society for Information Display, 2004), pp. 1495-1496.

[57] O. Pishnyak, S. Sato, O. D. Lavrentovich, "Electrically tunable lens based on a dual-frequency nematic liquid crystal," Appl. Opt. **45**, 4576-4582 (2006).

[58] H.-C. Lin and Y.-H. Lin, "An electrically tunable-focusing liquid crystal lens with a low voltage and simple electrodes," Opt. Express **20**, 2045-2052 (2012).

[59] J.-H. Park, H.-R. Kim, Y. Kim, J. Kim, J. Hong, S.-D. Lee, and B. Lee, "Depth-enhanced three-dimensional-two-dimensional convertible display based on modified integral imaging," Opt. Lett. **29**, 2734-2736 (2004).

[60] H. Choi, J. Kim, S.-W. Cho, Y. Kim, J. B. Park, and B. Lee, "Three-dimensional-two-dimensional mixed display system using integral imaging with an active pinhole array on a liquid crystal panel," Appl. Opt. **47**, 2207-2214 (2008).

[61] Y. Kim, J. Kim, Y. Kim, H. Choi, J.-H. Jung, and B. Lee, "Thin-type integral imaging method with an organic light emitting diode panel," Appl. Opt. **47**, 4927-4934 (2008).

[62] S.-W. Cho, J.-H. Park, Y. Kim, H. Choi, J. Kim, and B. Lee, "Convertible two-dimensional-three-dimensional display using an LED array based on modified integral imaging," Opt. Lett. **31**, 2852-2854 (2006).

[63] J.-H. Jung, Y. Kim, Y. Kim, J. Kim, K. Hong, and B. Lee, "Integral imaging system using an electroluminescent film backlight for three-dimensional-two-dimensional convertibility and a curved structure," Appl. Opt. **48**, 998-1007 (2009).

[64] D. Lanman, M. Hirsch, Y. Kim, and R. Raskar, "Content-adaptive parallax barriers: optimizing dual-layer 3D displays using low-rank light field factorization," ACM Trans. Graph. **29**, Article 163 (2010).

[65] G. Wetzstein, D. Lanman, W. Heidrich, and R. Raskar, "Layered 3D: tomographic image synthesis for attenuation-based light field and high dynamic range displays,"ACM Trans. Graph. **30**, Article 95 (2011).

[66] Y. Kim, K. Hong, J. Yeom, J. Hong, and B. Lee, "Optical block module for autostereoscopic three-dimensional display," in *Digital Holography and Three-Dimensional Imaging, OSA Technical Digest* (Optical Society of America, 2012), paper DSu1C.4.

[67] G. J. Woodgate, J. Harrold, A. M. S. Jacobs, R. R. Moseley, and D. Ezra, "Flat-panel autostereoscopic displays: Characterization and enhancement," in *Proc. SPIE* **3957**, 153 -164 (2000).

[68] J.-G. Lu, X.-F. Sun, Y. Song, and H.-P. D. Shieh, "2-D/3-D switchable display by Fresnel-type LC lens," J. Display Technol. **7**, 215–219 (2011).

[69] J. Arai, M. Okui, T. Yamashita, and F. Okano, "Integral three-dimensional television using a 2000-scanning video system," Appl. Opt. **45**, 1704-1712 (2006).

[70] H. Choi, J.-H. Park, J. Kim, S.-W. Cho, and B. Lee, "Wide-viewing-angle 3D/2D convertible display system uing two display devices and a lens array," Opt. Express **13**, 8424-8432 (2005).

[71] E. Walton, A. Evans, G. Gay, A. Jacobs, T. Wynne-Powell, G. Bourhill, P. Gass, and H. Walton, "Seeing Depth from a Single LCD," in *SID Sym. Dig.* **40**, 1395-1398 (2009).

[72] J. Hong, J.-H. Park, S. Jung and B. Lee, "Depth-enhanced integral imaging by use of optical path control," Opt. Lett. **29**, 1790-1792 (2004).

Appendix

Portions of the work discussed in each chapter of this dissertation are also presented in the following publications:

[Chapter. 1] J. Hong, Y. Kim, H.-J. Choi, J. Hahn, J.-H. Park, H. Kim, S.-W. Min, N. Chen, and B. Lee, "Three-dimensional display technologies of recent interest: principles, status, and issues," Appl. Opt. **50**, H87–H115 (2011).

[Chapter. 3.3] J. Hong, S.-W. Min, and B. Lee, "Integral floating display systems for augmented reality," Appl. Opt. **51**, 4201-4209 (2012).

[Chapter. 4.2] J. Hong, Y. Kim, S. Park, J.-H. Hong, S.-W. Min, S.-D. Lee, and B. Lee, "3D/2D convertible projection-type integral imaging using concave half mirror array," Opt. Express **18**, 20628-20637 (2010).

[Chapter. 4.3] J. Hong, J. Kim, and B. Lee, "Two-dimensional/three-dimensional convertible integral imaging using dual depth configuration," Appl. Phys. Express **5**, article 012501 (2012).

초록

본 논문에서는 새로운 광학 소자로써 렌즈 기능의 반거울을 제안하고, 이를 이용한 3차원 디스플레이 시스템들에 대하여 논한다. 렌즈 기능의 반거울은 반사형 광학 구조를 통해 렌즈의 광학적 기능을 구현하는 반거울이다. 광 결합기로써 렌즈 기능의 반거울은 see-through 이미징 특성을 가지며 광학 시스템의 정렬에 있어서 장점을 가진다. 본 논문은 렌즈 기능의 반거울을 실제로 구현할 수 있는 세 가지 공정 방법을 제안한다. 각각의 공정 방법은 서로 다른 장단점을 가지고 있기 때문에 응용처에 따라서 적절한 공정 방법을 택할 수 있도록 각 공정 방법에 의해 원형들을 제작하고 그 특성을 비교 및 분석한다.

본 논문에서는 두 가지 측면에서 렌즈 기능의 반거울의 유용성을 살펴본다. 첫째로 렌즈 기능의 반거울이라는 새로운 광학 소자의 도입을 통해서 새로운 개념의 3차원 디스플레이 시스템을 제안할 수 있는 기반을 제공한다는 측면, 두번째로는 기존의 3차원 디스플레이에 존재하였던 문제점들을 해결할 수 있는 새로운 방법들을 제공한다는 측면을 살펴본다. 본 논문에서는 집적 영상 방법에 기반한 다양한 3차원 디스플레이들을 구현함으로써 이와 같은 연구를 수행한다.

먼저 렌즈 기능의 반거울의 도입으로 증강 현실에 적용 가능한 새로운 2가지의 3차원 디스플레이시스템을 제안할 수 있음을 제시한다. See-through 및 양방향 이미징 집적 영상 시스템은 어떠한 기계적 움직임 없이도 시스템 주변으로 무안경식 3차원 이미지를 보여줄 수 있는 새로운 개념으로써 제안된다. 이는 렌즈 기능의 반거울을 어레이로 이용하여 구현할 수 있으며, 이때 렌즈 기능의 반거울 어레이는 결국 오목 거울 어레이의 기능을 갖게 된다. 프로젝션형 집적 영상의 이미징 원리의 분석을 통해 10%의 반사율을 갖는 렌즈 기능의 반거울을 사용하여 실세계에 3차원 영상을 자연스럽게 겹쳐 보여줄 수 있음을

보인다.

렌즈 기능의 반거울의 볼록 거울 방향에 집적 부유형 디스플레이의 원리를 적용하여 정확한 초점 조절을 유발할 수 있는 see-through head mounted display의 개념을 제시한다. 디스플레이 장치의 픽셀 크기가 집적 영상의 원거리 이미징을 제한하는 원인임을 밝히고, 볼록 거울의 사용이 어떠한 물리적 개선 없이 효과적으로 디스플레이 장치의 픽셀 크기를 줄여 결과적으로 집적 영상의 원거리 이미징이 가능토록 함을 보인다.

또한 렌즈 기능의 반거울은 기존의 집적 영상에 알려진 문제였던 2차원/3차원 변환 기능의 구현에도 유용하게 사용될 수 있다. 특히, 프로젝션형 집적 영상의 경우, 기존의 방법들은 스크린 크기에 대응하는 크기의 능동 소자를 사용하여야 하기 때문에, 지금까지는 2차원/3차원 변환을 구현할 수 있는 적절한 방법이 존재하지 않았다. 반면 렌즈 기능의 반거울을 적용하면 2차원/3차원 변환 기능을 수동 소자를 이용하여 구현할 수 있는 방법을 제시할 수 있다. 따라서 본 논문에서는 렌즈 기능의 반거울을 적용하여 2차원/3차원 변환 기능을 구현한 프로젝션형 집적 영상 시스템을 최초로 제안한다.

기존에는 focused mode의 집적 영상 구조에 대한 2차원/3차원 변환 기능을 구현하기 위한 연구가 다수 이루어져 왔으나 real/virtual mode 집적 영상에 대해서는 오직 한가지 방법만이 제안된 바 있다. 본 논문에서는 렌즈 기능의 반거울을 이용하여 real/virtual mode 집적 영상의 2차원/3차원 변환 기능을 구현하기 위한 새로운 방법을 제안한다. 제안된 시스템은 또한 넓은 시야각과 깊이감 향상을 위한 다층 중심 깊이 평면 생성에 있어 광경로 단축과 같은 여러 가지 장점들을 보여준다.

비록 본 논문에서는 렌즈 기능의 반거울의 유용성을 3차원 디스플레이 시스템에 한정하여 살펴보았으나, 그 외의 다양한 광학적 응용에 대해서도 렌즈 기능의 반거울이 유용하게 사용될 것으로 기대된다.